

AN ABSTRACT OF THE DISSERTATION OF

Jan-Shiang Taur for the degree of Doctor of Philosophy in Pharmacy presented on July 23, 2003.

Title: Alterations in the Permeability of Cimetidine by Dietary Flavonoids Using An *In Vitro* Transport Model, Caco-2 Cells

Abstract approved:

Redacted for privacy

Rosita J. Rodriguez

The goal of this dissertation is to investigate the interaction between cimetidine and dietary flavonoids using the Caco-2 cell transport model. It has been shown that flavonoids can change the bioavailability of pharmaceuticals, either by inhibiting metabolizing enzymes or inhibiting the drug efflux transporters. However, the effect of dietary flavonoids in the absorption of cimetidine has not been investigated. Therefore, the hypothesis of this study is that the absorption of cimetidine is mediated by a drug efflux pump, P-glycoprotein, of which dietary flavonoids can enhance the permeability of cimetidine by reducing P-glycoprotein function. The increase in permeability of cimetidine can increase the bioavailability of cimetidine. To test the hypothesis, three objectives were proposed. The first

objective was to validate the Caco-2 transport model in our laboratory. The validation was performed by measuring the electrical resistance of the monolayer and determining the transport of paracellular marker. Also P-glycoprotein function was determined using rhodamine 123.

The second objective was to describe the transport characteristics of cimetidine in the Caco-2 cell monolayers. The permeability of cimetidine was determined at different pH environments. When the permeability of cimetidine from apical to basolateral and basolateral to apical was compared, there appeared to be an efflux mechanism involved transport of cimetidine. The permeability of cimetidine in the presence of verapamil, a P-glycoprotein competitive inhibitor, suggested that P-glycoprotein was involved in the efflux.

The third objective was to study the effect of dietary flavonoids on the permeability of cimetidine in the Caco-2 cell model. In the present study, four different flavonoids, quercetin, genistein, naringenin, and xanthohumol were selected. When co-treated with flavonoid aglycones, the permeability of cimetidine was significantly reduced in the basolateral to apical direction. However, only genistin, a glycoside of genistein, significantly reduced the efflux of cimetidine.

The present studies demonstrate that some dietary flavonoids, especially aglycones, can significantly reduce the efflux of cimetidine in the Caco-2 cell monolayers. Therefore, the flavonoids consumed in a normal diet have the potential to enhance the bioavailability of cimetidine and possibly other P-glycoprotein substrates by altering their permeability.

©Copyright by Jan-Shiang Taur

July 23, 2003

All Rights Reserved

Alterations in the Permeability of Cimetidine by Dietary Flavonoids Using An *In Vitro* Transport Model, Caco-2 Cells

**by
Jan-Shiang Taur**

A DISSERTATION

submitted to

Oregon State University

**in partial fulfillment of
the requirements for the
degree of**

Doctor of Philosophy

**Presented July 23, 2003
Commencement June 2004**

Doctor of Philosophy dissertation of Jan-Shiang Taur presented on July 23, 2003.

APPROVED:

Redacted for privacy

Major Professor, representing Pharmacy

Redacted for privacy

Dean of the College of Pharmacy

Redacted for privacy

Dean of the Graduate School

I understand that my dissertation will become part of the permanent collection of Oregon State University libraries. My signature below authorizes release of my dissertation to any reader upon request.

Redacted for privacy

Jan-Shiang Taur, Author

ACKNOWLEDGMENTS

I sincerely appreciate my major professor, Dr. Rosita Rodriguez, for her guidance, encouragement and financial support throughout my program. She provided me a great opportunity to expand my knowledge and inspired my enthusiasm for research. I also appreciate my other committee members, Dr. James Ayres, Dr. Mark Christiansen, Dr. David Birkes, and Dr. David Williams, for their precious suggestion in completing my thesis.

I greatly appreciate the many others who contributed to this project, Dr. John Mata for technical discussion; Dr. Cristobal Miranda for providing xanthohumol; Dr. Mark Zabriskie for discussing enzyme kinetics. I am grateful for my colleagues, Dr. Iman Ahmed, Dr. Manshiu Leung, Dr. Vipaporn Rakkanka, Dr. Angkana Tantituvanont, Propoch Watanalumlerd, Samar Farid, Sahar Fahmy, and Valerie Stanik, for their wonderful friendship.

Finally, I give my special thanks to all the staff in the College of Pharmacy and Oregon State University, for providing me an excellent learning and working environment during my studies.

TABLE OF CONTENTS

	<u>Page</u>
1. INTRODUCTION.....	1
2. LITERATURE REVIEW.....	4
2.1 Grapefruit Juice-drug Interaction.....	4
2.2 Flavonoids.....	6
2.3 Caco-2 Cells.....	23
2.4 Cimetidine.....	32
2.5 P-glycoprotein (P-gp).....	39
3. MATERIALS AND METHODS.....	49
3.1 Materials	49
3.2 Cell Culture of Caco-2 Cells.....	50
3.2.1 Preparation of Culture Medium.....	50
3.2.2 Procedures for Growing Caco-2 Cells in 162 cm ² Flasks.....	50
3.2.3 Subculturing Caco-2 Cells in 162 cm ² Flasks.....	51
3.2.4 Plating and Maintaining Caco-2 Cells in Transwell® Plates.....	52
3.3 Lactate Dehydrogenase (LDH) Assay.....	52
3.4 Caco-2 Cell Monolayer Integrity	56
3.4.1 Mannitol Transport.....	56
3.4.2 Measurement of Transepithelial Electrical Resistance (TEER).....	57

TABLE OF CONTENTS (Continued)

	<u>Page</u>
3.5 Transport Experiments of Cimetidine.....	59
3.6 Rhodamine 123 Transport Experiments	61
3.7 Uptake Experiments of Cimetidine.....	61
3.8 Data Analysis.....	63
3.8.1 Calculation of the Apparent Permeability Coefficient (Pe).....	63
3.8.2 Determination of the Michaelis-Menton Constant (K_m)...	65
3.8.3 Inhibitory Concentration 50% (IC_{50}) Determination of Flavonoids	66
3.8.4 Statistical Analysis.....	67
4. RESULTS.....	68
4.1 Cytotoxicity of the Flavonoids in Caco-2 Cells.....	68
4.2 Integrity of the Caco-2 Cell Monolayers.....	71
4.3 Transport of Rhodamine 123.....	74
4.4 Transport of Cimetidine.....	74
4.5 Effect of Flavonoids on the Transport of Cimetidine.....	88
4.6 Effect of Quercetin on the Uptake of Cimetidine.....	101
5. DISCUSSION.....	106

TABLE OF CONTENTS (Continued)

	<u>Page</u>
BIBLIOGRAPHY.....	117
APPENDICES.....	144

LIST OF FIGURES

<u>Figure</u>	<u>Page</u>
2.1 The basic structure of flavonoids.	8
2.2 Chemical structure of quercetin and its glycosides.....	11
2.3 Chemical structure of genistein and its glycoside, genistin.....	16
2.4 Chemical structure of naringenin and its glycoside, naringin.....	19
2.5 Chemical structure of xanthohumol.....	22
2.6 Cross-section of Caco-2 cells.....	26
2.7 Proposed metabolic pathways of cimetidine.....	38
2.8 Proposed 2D structural model of human P-glycoprotein.....	41
3.1 The Transwell® plate with inserts.....	53
3.2 Cross-sectional diagram of a Transwell® insert with Caco-2 cells ..	54
3.3 A diagram representing the resistance measurement of the Caco-2 cell monolayer using a voltohmmeter with a STX-2 chopstick electrode.....	58
4.1 Two-hour lactate dehydrogenase (LDH) release pattern of various drug/flavonoids in 7-day-old Caco-2 cell monolayers.....	69
4.2 Four-hour lactate dehydrogenase (LDH) release pattern of various drug/flavonoids in 7-day-old Caco-2 cell monolayers.....	70

LIST OF FIGURES (Continued)

<u>Figure</u>	<u>Page</u>
4.3 The apical-to-basolateral permeability coefficient of ^3H -mannitol as a function of days in culture in Caco-2 cell monolayers.....	72
4.4 Percent transport of ^3H -mannitol in 21 day old Caco-2 cell Monolayers.....	72
4.5 Transepithelial electrical resistance (TEER) readings of Caco-2 cell monolayers as a function of days in culture.....	73
4.6 Permeability coefficient of rhodamine 123 (2.5 μM) with various conditions in Caco-2 cell monolayers.....	75
4.7 Basolateral-to-apical permeability coefficient of 20 μM cimetidine under different pH environments in Caco-2 cell monolayers.....	77
4.8 Basolateral-to-apical permeability coefficient of 20 μM cimetidine with or without co-treatment of 0.5%(v/v) ethanol or 0.2% (v/v) DMSO in Caco-2 cell monolayers.....	78
4.9 Permeability coefficient of 20 μM cimetidine in different directions in Caco-2 cell monolayers.....	80
4.10 Permeability coefficient of 20 μM cimetidine with or without co-treatment of 100 μM verapamil in Caco-2 cell monolayers.....	81
4.11 Scatter plot of basolateral-to-apical permeability coefficient versus the concentration of cimetidine with or without the co-treatment of 100 μM verapamil... ..	83
4.12 Scatter plot of efflux rate versus the concentration of cimetidine with or without the co-treatment of 100 μM verapamil.....	84

LIST OF FIGURES (Continued)

<u>Figure</u>	<u>Page</u>
4.13 Scatter plot of P-gp efflux rate versus the concentration of cimetidine	86
4.14 Basolateral-to-apical permeability coefficient of 20 μ M cimetidine with or without co-treatment of 100 μ M bumetanide or 100 μ M diisothiocyanatostilbene-disulfonic acid in Caco-2 cell monolayers...	87
4.15 Basolateral-to-apical permeability coefficient of 20 μ M cimetidine with or without co-treatment of 100 μ M flavonoid aglycones in Caco-2 cell monolayers.....	89
4.16 Basolateral-to-apical permeability coefficient of 20 μ M cimetidine with or without co-treatment of 100 μ M flavonoid glycosides in Caco-2 cell monolayers.....	91
4.17 Basolateral-to-apical permeability coefficient of 20 μ M cimetidine with or without co-treatment of 100 μ M flavonoid aglycones in Caco-2 cell monolayers.....	92
4.18 Basolateral-to-apical permeability coefficient of 20 μ M cimetidine with or without co-treatment of 100 μ M flavonoid glycosides in Caco-2 cell monolayers.....	94
4.19 Basolateral-to-apical permeability coefficient of 20 μ M cimetidine versus various concentrations of quercetin.....	95
4.20 Basolateral-to-apical permeability coefficient of 20 μ M cimetidine versus various concentrations of naringenin.....	97
4.21 Basolateral-to-apical permeability coefficient of 20 μ M cimetidine versus various concentrations of xanthohumol.....	98

LIST OF FIGURES (Continued)

<u>Figure</u>	<u>Page</u>
4.22 Basolateral-to-apical permeability coefficient of 20 μ M cimetidine versus various concentrations of genistein.....	99
4.23 Basolateral-to-apical permeability coefficient of 20 μ M cimetidine versus various concentrations of genistin.....	100
4.24 Uptake of 20 μ M cimetidine with or without co-treatment of 100 μ M quercetin in Caco-2 cell monolayers.....	103
4.25 Uptake of 20 μ M cimetidine at pH 5.5 and pH 7.4 with or without co-treatment of 100 μ M quercetin in Caco-2 cell monolayers.....	105

LIST OF TABLES

<u>Table</u>	<u>Page</u>
2.1 The pharmacokinetic parameters of oral naringenin in healthy subjects.....	20
2.2 Enzymes found in Caco-2 cells.....	27
2.3 Transporters found in Caco-2 cells.....	29
2.4 Physicochemical characteristics of cimetidine.....	34
2.5 Pharmacokinetic characteristics of cimetidine resulting from I.V. injections.....	35
2.6 Absorption and bioavailability of cimetidine of various formulations in healthy subjects.....	36
2.7 Substrates and inhibitors of P-glycoprotein.....	44
4.1 The inhibitory concentration 50% (IC ₅₀) and 95% confidence interval of the effective flavonoids on the permeability of cimetidine.....	102

DEDICATION

This thesis is dedicated to my family:

My grandparents, Jin-Yu Tao, Tien-Su-Lan Tao

My parents, Yu-Chi Tao, Jin-Yuan Cheng

My wife, Mei-Chuan Wang

My daughter, Sophia, and the oncoming baby

Alterations in the Permeability of Cimetidine by Dietary Flavonoids Using An *In Vitro* Transport Model, Caco-2 Cells

1. INTRODUCTION

Flavonoids are polyphenolic compounds only found in green plants. There are over 6,000 different flavonoids been identified. In nature, flavonoids usually occur as sugar conjugates called flavonoid glycosides. Flavonoids are abundant in our daily diet. It has been estimated that one person can consume approximately 1 gram of various flavonoids per day based on a typical western diet [1]. This is very likely to cause some physiological effects or significant drug-diet interaction in such high amount.

There are many *in vitro* and *in vivo* studies [2-5] demonstrating that flavonoids can cause various biochemical and pharmacological effects, which includes inhibiting the activity of P-glycoprotein (P-gp), an efflux pump that expels various structure-unrelated compounds back to the intestinal lumen or extracellular medium. These alterations in P-gp activity may provide an alternative method to improve the therapeutic effect of drugs that have low bioavailability due to P-gp related drug resistance. This thesis evaluates four flavonoids commonly found in

our diet which are quercetin, naringenin, genistein, and xanthohumol, to investigate if they can enhance the bioavailability of our model drug, cimetidine.

Cimetidine is an oral histamine H₂-receptor antagonist used to treat duodenal and gastric ulcers, systemic mastocytosis, and upper gastrointestinal bleeding. The oral bioavailability of a cimetidine tablet is approximately 60% with high variation seen in healthy subjects. Previous *in vitro* studies suggested that cimetidine is a substrate of P-gp which may be a reason for the variability in the bioavailability of cimetidine [6].

It was demonstrated that the secretion of cimetidine was reduced when co-treated with P-gp substrates verapamil and cyclosporine *in vitro* [6]. It has also been reported that some flavonoids such as genistein and quercetin could inhibit the activity of P-gp [5, 7]. Thus, one can speculate that flavonoids can reduce the efflux phenomena of cimetidine by inhibiting P-gp function. Therefore, flavonoids such as genistein and quercetin may have the potential to increase the bioavailability of cimetidine *in vivo*. Once this relationship has been established, one can use the flavonoids to enhance the absorption of drugs that are substrates for P-gp.

The model that was selected to evaluate the hypothesis was the Caco-2 cell *in vitro* transport model. Caco-2 cells are a cell line derived from human colon adenocarcinoma. As the Caco-2 cell culture matures and differentiates, the cells are very similar to the human intestinal epithelial cells, which are the major barrier for oral drug absorption. Cell culture studies only requires relatively small amount of test compounds compared to *in vivo* studies. Also, an advantage of cell culture is

that one can screen lots of compounds for permeability, metabolism and transport studies in a short period of time. The permeability studies obtained to date from Caco-2 cell monolayers have been investigated extensively [8] and had good association with *in vivo* absorption [9]. These advantages have made Caco-2 cells become the most popular cell culture model to study the drug transport during the early stage of drug development process in pharmaceutical research.

The focus of this dissertation is to investigate how flavonoids alter the permeability of cimetidine using the Caco-2 cell monolayers. First, several validation assays were performed to check the integrity and cytotoxicity studies of the various drug compounds/flavonoids prior to performing the transport studies. The function of P-gp in Caco-2 cells was also determined using known substrate and competitive inhibitor of P-gp. Next, the transport of cimetidine under various treatment conditions was characterized. Then, the effects of flavonoids (quercetin, naringenin, genistein, and xanthohumol) on either absorption or efflux of cimetidine were investigated and the inhibition potency, IC_{50} , of effective flavonoids on efflux of cimetidine was calculated. The results of these studies will provide not only an alternative approach to enhance drug bioavailability but also valuable information on drug-diet interactions.

2. LITERATURE REVIEW

2.1 Grapefruit Juice-drug Interaction

It is not surprising that the occurrence of drug-diet interaction is a frequent event. The interaction can be important if the absorption of drug is altered. It has been recognized that concomitant administration of drug with food can change the rate and extent of drug absorption. Those alterations may arise from an effect of dietary substance on physiologic factors such as gastric pH as seen with Coca-Cola and ketoconazole [10]. The alteration may also come from the direct physiochemical interactions with dietary constituents such as partitioning or solubilization of the drug in dietary fat. One example is that a high-fat meal can significantly reduce the peak concentration and the ratio of peak concentration to the area under plasma concentration-time curve of oral sirolimus nonaqueous solution [11].

In some cases, dietary components can alter the expression and activity of hepatic metabolizing enzymes. The alteration can lead to changes in the systemic elimination of drugs. Increased intake of charcoal-broiled meat for four days, the average plasma peak concentration of phenacetin was reduced to 352 ng/ml compared with 1,628 ng/ml for the control diet. The charcoal-broiled meat diet can also significantly increase the ratio of N-acetyl-p-aminophenol to its parent drug, phenacetin [12].

In 1991, Baily et al [13] demonstrated that a single glass of grapefruit juice caused a two- to three-fold increase in the plasma concentrations of felodipine after oral intake of a 5 mg tablet. However, a similar amount of orange juice did not change the pharmacokinetic profile of the drug in the same study. In the recent years, various research groups have investigated the effect of grapefruit juice on the pharmacokinetics of different drugs. It has been found that calcium channel blockers such as felodipine, nisoldipine, nimodipine, and nifedipine [13-15] underwent a significant increase in area under the plasma concentration-time curve. Also, other drugs have been shown to have an increase in bioavailability after concurrent administration with grapefruit juice in clinical studies, such as midazolam [16], triazolam [17], terfenadine [18], 17 alpha-ethinylestradiol [19], saquinavir [20], lovastatin [21], cyclosporine [22], buspirone [23], cisapride [24], artemether [25], atorvastatin [26], scopolamine [27], sildenafil [28], and halofantrine [29].

When one investigates these grapefruit juice interaction studies closely, the one commonality of these drugs is that they are substrates of cytochrome P-450 3A4 (CYP3A4). Moreover, they all undergo presystemic metabolism. Using halofantrine as an example, when halofantrine is taken orally with 250 mL grapefruit juice, the area under the plasma concentration-time curve (AUC) and peak plasma concentration increase by 2.8-fold and 3.2-fold compared to control, with a concomitant 2.4-fold decrease in N-debutyl-halofantrine AUC [29]. Thus, the most likely mechanism of this grapefruit juice interaction is that grapefruit juice

inhibits the function of intestinal CYP3A4 thereby impairing the metabolism of drugs resulting in enhanced bioavailability. This suggested mechanism was supported by the study of Lown *et al.* [30]. In their study, ten healthy subjects consumed 8 oz grapefruit juice three times a day for six days. After chronic grapefruit juice administration, the concentration of CYP3A4 protein in small bowel epithelia (enterocytes) fell 62% with no corresponding change in CYP3A4 mRNA levels while hepatic CYP3A4 mRNA was not altered [30]. Lown *et al.* proposed that some components in grapefruit juice damages the enzyme (suicide inhibition) resulting in its accelerated degradation. Because grapefruit juice consists of a number of flavonoids such as naringenin, quercetin, and kaempferol, and some of them exist in relative high amount [31], it is possible that some flavonoids may be responsible for the CYP3A4 inhibition.

2.2 Flavonoids

Flavonoids are polyphenolic compounds that are only found in green plants. They are one of the largest groups of natural products. According to *The Handbook of Natural Flavonoids*, there have been 6,467 flavonoids identified [32]. Flavonoids have various functions in plants. Quercetin and kaempferol produced by soybean can protect plants from ultraviolet-B radiation [33]. The flavonoids isolated from cudweed *Gnaphalium affine* D. Don have been shown insect antifeedant activity against the common cutworm (*Spodoptera litura* F.) [34]. Quercetagenin-7-arabinosyl-galactoside, a flavonoid glycoside extracted from leaves of *Tagetes*

minuta, showed antimicrobial activity against Gram positive and Gram negative microorganisms [35].

Flavonoids are formed in plants from the aromatic amino acid phenylalanine and tyrosine, and malonate via the general phenylpropanoid biosynthetic pathway [36]. The basic structure of flavonoids is shown in Figure 2.1, which consists of fifteen carbon atoms arranged within three rings ($C_6-C_3-C_6$). The various subclasses of flavonoids express different oxidation levels and pattern of substitution of the C ring. Flavonoid subclasses are flavonols, anthocyanidines, isoflavonols, flavones, isoflavones, flavanones, isoflavanones, flavanols, isoflavanols, flavanes, isoflavanes, aurones, and coumarins. Flavonoids usually occur in plants as glycosylated derivatives, which are called glycosides, or more specifically glucosides, rutinosides, or xylosides depending on their sugar moiety.

Because flavonoids are widespread and abundant in nature, it is not surprising that one can find substantial amount of flavonoids in the human daily diet. In the United States, the daily dietary intake of mixed flavonoids is estimated to be in the range of 500 to 1000 mg [1], but it can be as high as several grams in people who supplement their diet with flavonoid- containing herb preparation such as ginkgo biloba, or grape seed extract. Such intake can create concentrations in the micromolar range in the intestinal lumen and produce pharmacologically effective serum concentrations in humans if absorption is efficient.

In nature, flavonoids conjugate with sugar as beta-glycosides, which cannot be hydrolyzed by human digestive enzymes. Nevertheless, microorganisms such as

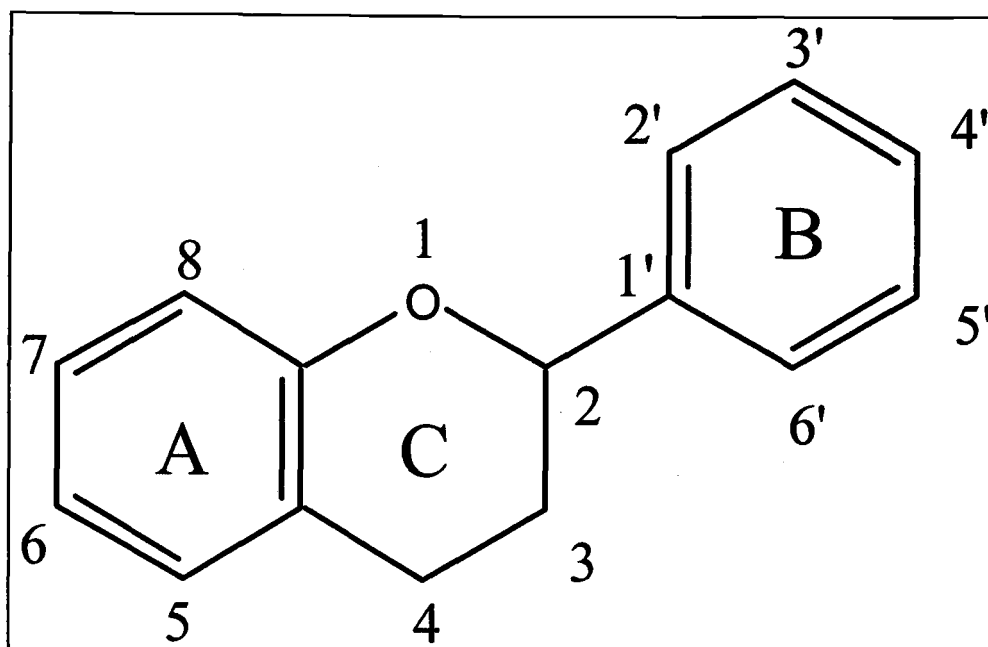


Fig 2.1 The basic structure of flavonoids.

Bacteroides uniformis and *Bacteroides ovatus* [37] in human intestine can hydrolyze them into free aglycones that are expected to pass through the gut wall. For instance, rutin and quercitrin are hydrolyzed to quercetin, and robinin is hydrolyzed to kaempferol by alpha-rhamnosidase and beta-galactosidase, respectively. These two enzymes were produced by some strains of *Bacteroides distasonis* which can be found in the faecal flora from healthy humans [37]. The intestinal microflora also metabolize flavonoids into phenolic acids. Because only free aglycones that escape from the metabolism of intestinal microflora will have chance to be absorbed, the bioavailability of flavonoids in general is considered to be low. However, a glycoside of quercetin from onion showed better absorption compared to aglycone [38]. This suggests that at least some flavonoids can utilize an alternative pathway to pass through the intestine wall and exhibit enhanced bioavailability.

There are two major sites of flavonoid metabolism: the intestinal microflora and the liver. Studies have shown that the majority of enzymes responsible for the initial ring fission of flavonoids, or demethylation and dehydroxylation of the resulting phenolic acid are enzymes of intestinal microorganisms [39, 40]. A study using rat liver microsomes demonstrated that the B-ring of the flavonoid structure is key for metabolism [41]. Flavonoids without hydroxyl groups in the B-ring or with one hydroxyl group in 4'-position were hydroxylated by microsomal CYP1A, and flavonoids with a methoxy group in the 4'-position were demethylated by other CYP isozymes. Other than hydroxylation and demethylation, two animal

studies showed flavonoids such as quercetin and phloretin were metabolized through glucuronic and/or sulfuric conjugation [42, 43]. One study indicated that those conjugation reactions appears to occur in the intestinal wall [42].

Flavonoids can exert a wide range of biochemical and pharmacological effects *in vitro* as well as *in vivo*. Flavonoids such as epicatechin and catechin have antioxidant properties [44], as well as cytostatic effects as seen with biochanin A and genistein in tumorigenesis [45]. Flavonoids have the ability to inhibit a broad spectrum of enzymes, such as protein kinase C [46], tyrosine protein kinase [47], and topoisomerase II [3]. These results have led scientists to consider flavonoids as anticarcinogens and cardioprotective agents. Moreover, in several *in vitro* studies, some flavonoids such as quercetin, kaempferol, and genistein can significantly influence the pharmacological potency of drugs like dihydropyridine, adriamycin, and azidopine by inhibiting CYP 3A4 or blocking P-glycoprotein (P-gp) [5, 31, 48]. This interaction provides another alternative to improve the therapeutic effect of the drugs that have low bioavailability due to extensive CYP metabolism or multiple drug resistance phenomena. In our present studies, four flavonoids quercetin, genistein, naringenin, and xanthohumol along with their glycosides were investigated. Each flavonoid will be discussed separately in the following paragraphs.

Quercetin, 3,3',4',5,7-pentahydroxyflavone (Figure 2.2), is a flavonoid present in vegetables particularly in onion, fruits, and red wines. It is the major bioflavonoid in the human diet. The estimated average daily dietary intake of

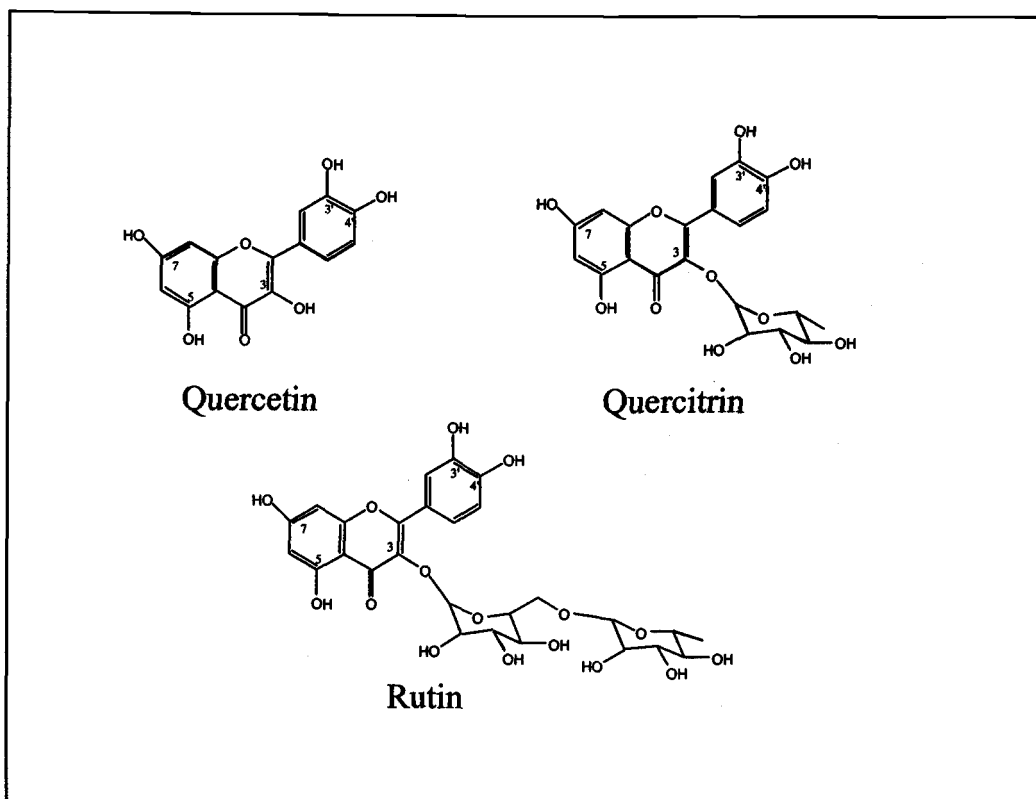


Figure 2.2 The chemical structures of quercetin and its glycosides.

quercetin by an individual in the United States is 25 mg [49]. The oral absorption of quercetin is thought to be poor (approximate 20%). This was based on a 1975 study that showed a 4-gram oral dose of quercetin aglycone led to no measurable quercetin in either the plasma or urine of six healthy volunteers [50]. However, the sensitivity of the plasma assay may have been inappropriately poor (0.1 mcg/ml). Also urinary output was used as a primary measure of absorption. Another clinical trial found that intact quercetin urinary excretion was insignificant [51]. One study from the Netherlands found that two subjects fed fried onions, containing quercetin glucosides equivalent to 64 mg of the aglycone, reached maximum serum concentration of 196 ng/ml (0.6 μ M) at 2.9 hr after ingestion [52]. The half-life of quercetin in this study was 16.8 hr where significant serum levels were seen up to 48 hr after ingestion. Later on, the same investigators fed nine healthy subjects onions and apples that contain different quercetin glycosides [38]. The peak plasma concentration of quercetin was 224 ng/mL and 92 ng/mL, respectively after subjects consumed onions and apples. It can be determined that oral absorption of dietary quercetin is reasonably high.

The absorption of dietary quercetin in pharmacological doses has not been determined. The serum concentration of quercetin required for achieving pharmacological effects (\sim 10 μ M) are much higher than those concentrations achieved with an oral dose (100 mg or less) in human studies (serum concentrations up to 0.8 μ M). Considering the relatively long elimination half-life (16.8 hr) of

quercetin, one can extrapolate that a 1,500 mg daily dose may reach 10 μ M. In a study done with rats demonstrated that 10 μ M quercetin in serum was feasible with a semipurified diet supplemented with 0.2% quercetin [53]. Twelve micromolar quercetin serum concentration can be reached by a single 100 mg intravenous dose in human [50].

When taken by oral administration, the majority of quercetin is degraded by intestinal microflora [50]. The conjugation of quercetin with glucuronic and sulfuric acid was observed in intestinal wall in the pig model [42]. In rat model, the major metabolites found in plasma are glucurono and sulfo conjugates of isorhamnetin (3'-O-methyl quercetin) and quercetin [53]. The elimination half-life of quercetin and its glycosides ranged from 11 to 28 hours among different studies[38, 54].

The safety of quercetin was also investigated. A single oral dose of up to 4 grams of quercetin was not associated with any significant side effect in humans [50]. A single intravenous bolus doses of 100 mg were tolerated well [50]. When quercetin was administrated by a short intravenous infusion of 1400 mg/m² once weekly for three weeks, 2 out of 10 subjects had renal toxicity [55]. The mutagenicity of quercetin has been well studied in the Ames test [56, 57]. It is among the most mutagenic flavonoids. Nevertheless, mutagenicity is not equivalent to carcinogenicity. Most *in vivo* studies have shown that quercetin, along with its rutinoid, were not carcinogens [58-60]. However, in Dunnick and Hailey's study, feeding up to 40,000 ppm quercetin for two years can cause benign tumors of the

renal tubular epithelium in male F344/N rats [61]. More effort is still needed to distinguish the controversy between the different experimental models.

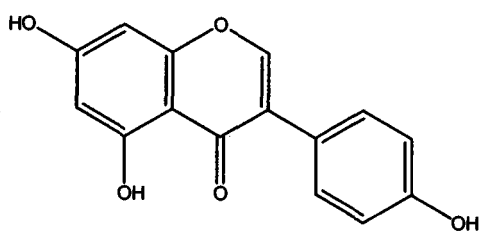
It has been shown that quercetin and its glycosides can generate various biological responses with both *in vitro* and *in vivo* studies. It has been well established that quercetin is a powerful antioxidant. *In vitro* studies have also shown that quercetin can prevent the oxidation of low density lipoproteins (LDL) [62]. Because oxidized LDL is associated with atherosclerosis, quercetin may potentially prevent atherosclerosis by protecting LDL from becoming oxidized. Other studies have demonstrated that quercetin can down regulate the expression of mutant p53 protein [63]. Also quercetin can inhibit both *in vitro* and *in vivo* tyrosine kinase activity [55, 64]. Moreover, quercetin inhibits the expression of the p21-ras oncogene in colon cancer cell lines [65] as well as inhibits and/or down regulates the growth of several tumor cell lines such as human breast carcinoma MDA-MB-435, Human colon carcinoma HT29 and Caco-2, and human melanoma MNT1 [66-69]. These findings suggest a possible chemopreventive role for quercetin in carcinogenesis. Beside acting as a chemopreventive agent, quercetin was found to inhibit the activity of angiotensin-converting enzyme [70]; thereby giving quercetin another role for reducing the risk of cardiovascular disease. In fact, some epidemiological prospective studies found a positive association between flavone intake and reduced the risk of coronary heart disease and stroke [71, 72].

It was demonstrated that quercetin can inhibit the activity of CYP1A and P-gp [7, 73]. CYPs are heme-containing mixed-function oxidases that are responsible

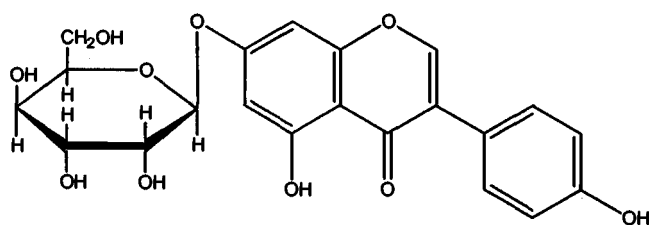
for metabolism of many therapeutic agents. P-gp is an efflux transporter that causes multidrug resistance. Interaction between quercetin and CYPs and/or P-gp may provide an alternative strategy to improve the bioavailability of drugs.

Genistein, 4',5,7-trihydroxyisoflavone (Figure 2.3), is a member of the isoflavone subfamily. It is mainly found in legumes such as lentils chickpeas, soybeans, and soy-based products like tofu, miso, soymilk, and tempeh. The concentration of genistein in most soy products range from 1-2 mg/g [74]. Daily dietary intake of soy protein in heavy soy consumers such as in Asian populations has been estimated to be 20 g to 80 g; whereas, the average Western dietary intake is approximately 1 to 3 g [74]. In one study, seven healthy male volunteers were fed 60 g baked soybean powder that contained 112 micromoles genistein [75]. The peak plasma concentration of genistein was $0.44 \mu\text{M} \pm 0.65 \mu\text{M}$ at 6 hr after ingestion. Genistein excretion in urine at 6 hr was approximately $1.1 \mu\text{M}/\text{h}$. The percent genistein recovered in the feces was 20.1%. The elimination half-life of plasma genistein was 8.36 hr. An other study showed that genistein bioavailability depends upon the relative ability of gut microflora to degrade these compounds[76].

In the last decade, there have been over 3,600 published studies that investigated the biological activities of genistein. Most of these studies focused on the phytoestrogen activity of genistein. The pharmacological activities of genistein have demonstrated inhibition of tyrosine kinase activity as well as chemoprotectant



Genistein



Genistin

Figure 2.3 The chemical structures of genistein and its glucoside, genistin.

activities against cancers and cardiovascular disease. Thus, genistein has become a major subject of discussion in the context of nutraceutical and functional foods.

Isoflavones are also called 'phytoestrogens' because they share structural features with the potent estrogen estradiol-17 β . These features give genistein the ability to bind estrogen receptors and sex hormone binding proteins such as sex steroid-binding globulin. Thus, isoflavones can exert both estrogenic and antiestrogenic activity. The binding affinity of genistein to estrogen receptor has been shown to be several-fold weaker than that of estradiol [77]. The estrogenic characteristic of genistein was thought to be the main reason of reducing the risk of mammary cancer [78]. Other factors that could contribute to the anticancer characteristics of genistein are inhibition of topoisomerase I and II activities [79], inhibition of tyrosine kinase phosphorylation [80], and induction of differentiation of cancer cell lines [81, 82]. Some epidemiological results have shown that the risk of American women developing breast cancer was seven times higher than that of Asian women [83]. Despite inherited factors, most of the breast cancer cases may be caused by unspecified factors related to lifestyle, such as the difference in daily intake of isoflavones between the Western and Asian women.

Genistein can inhibit the activities of CYP1A and CYP2E1 in mice liver microsomes [84]. Thus, genistein may enhance the therapeutic effect of some drugs which are metabolized by CYP1A or CYP2E1. On the other hand, genistein could also inhibit the activity of multidrug resistance-associated protein (MRP) by

decreasing the cellular concentration of ATP, offering an alternative mechanism for increasing bioavailability of drugs that are substrates of MRP such as daunorubicin [85].

Naringenin, 5,7,4'-trihydroxyflavanone (Figure 2.4), is a member of the flavanone subfamily. The main sources of naringenin are citrus fruits such as grapefruits and tomatoes. In citrus fruits, naringenin is predominantly present as the glycosidic forms such as naringenin-7-neohesperidoside (naringin) (Figure 2.4), and naringenin-7-rutinoside (narirutin). Naringenin exists as aglycone in the skin of tomatoes. The concentration of naringenin ranges from 0 up to and exceeding 500 mg/L in grapefruits and sour oranges [86], and 0.8 to 4.2 mg/100 g in whole red tomato [87].

The bioavailability of naringenin from a variety of sources has been investigated in human subjects (Table 2.1). The cleavage of sugar moiety is the first metabolic step of the naringenin glycoside as it enters the human intestinal tract [88]. This cleavage has been assumed to be done by the intestinal bacteria. Most of absorbed naringenin has been shown to be in the conjugated form, either as the naringenin sulfate or the naringenin glucuronide [89].

Like other bioflavonoids, naringenin exhibits various physiological effects *in vitro*. Naringenin is similar to phytoestrogens in exhibiting antiestrogenic activity in female rat uterus and MCF-7 human breast cancer cells [90]. Furthermore, naringenin also possesses anticarcinogenic activity in the human

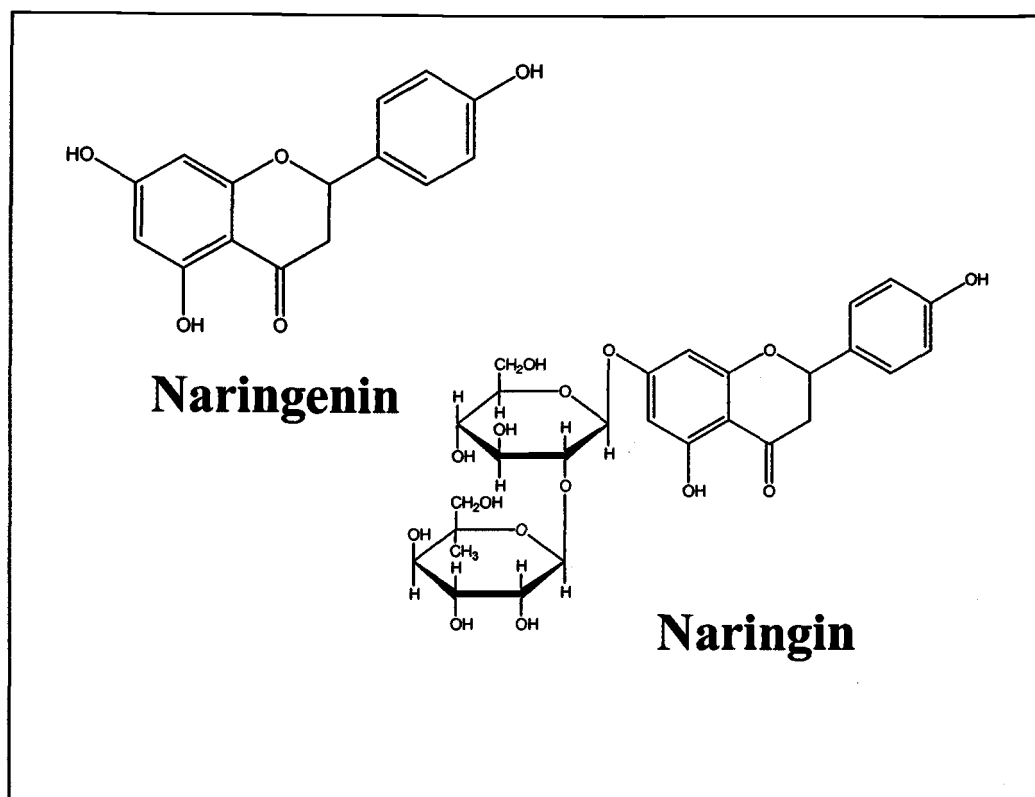


Figure 2.4. The chemical structures of naringenin and its glycoside, naringin.

Table 2.1 The pharmacokinetic parameters of oral naringenin in healthy subjects.

	Erlund <i>et al.</i> [91]	Erlund <i>et al.</i> [91]	Bugianesi <i>et al.</i> [89]
Subject number	8	5	5
Sources	orange juice	grapefruit juice	cooked tomato
Serving size	8 mL/Kg	8 mL/Kg	150 g
Naringenin amount	218 mg/L	349 mg/L	3.8 mg/150 g
T _{max}	5.5 ± 2.9 hr	4.8 ± 1.1 hr	2 hr
Cp _{max}	0.6 ± 0.4 µM	6 ± 5.4 µM	0.12 ± 0.03 µM
t _{1/2}	1.3 hr	2.2 hr	nd
fe	30.3 ± 25.5 %	1.1 ± 0.8 %	nd

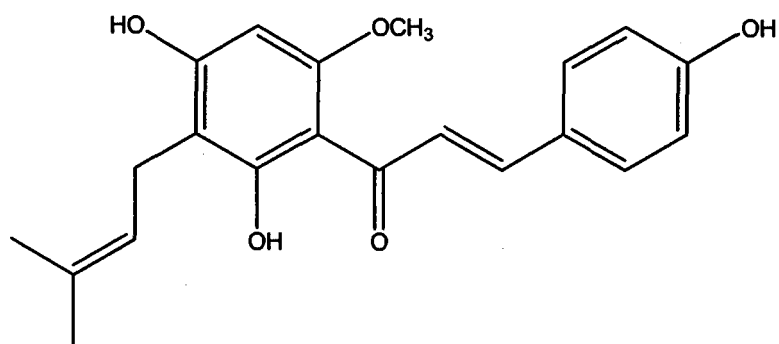
T_{max}: Time of maximum plasma concentration. Cp_{max}: Maximum plasma concentration. fe: Fraction of dose excreted unchanged in urine. t_{1/2}: elimination half-life. nd: not determined.

breast cell line [92], antioxidant activity in rat liver microsomes [93], and lipid-lowering effect in rats [94].

Because naringenin exists in high amounts in grapefruit, many scientists believe that naringenin is the primary cause of the well-documented grapefruit juice interaction with drugs. However, there have been conflicting studies that did not support this hypothesis [95, 96]. For instance, in Edwards and Bernier's study, naringenin and naringin could not significantly inhibit the CYP3A activity in rat liver microsomes [96]. However, Ghosal *et al* showed that naringenin inhibited the metabolism of midazolam in human liver microsomes, which is a substrate of CYP3A [97]. Thus, more studies are needed to clarify the primary mechanism of action of grapefruit juice interaction.

In spite of an arguable role in CYP3A inhibition, naringenin has been shown to inhibit CYP1A2 using methoxyresorufin as a substrate [98]. Naringenin has been shown to significantly reduce the activity of P-gp in the Caco-2 cell model using vinblastine as a substrate of P-gp [99]. Therefore, enhancing bioavailability of P-gp substrate by co-administration of naringenin is probable.

Xanthohumol, 2',4',6',4-tetrahydroxy-3'-prenylchalcone (Figure 2.5), belongs to the subfamily of chalcones. Unlike the other flavonoids, chalcones do not have the heterocyclic C ring. Xanthohumol is the major flavonoid in hop cones which are widely used by the brewing industry to add bitterness and aroma to beer. The estimated concentration of xanthohumol ranges from 0.5 µg to 690 µg per liter among the various U.S. brands of beer [100]. Unlike the aforementioned flavonoids



Xanthohumol

Figure 2.5. The chemical structure of xanthohumol.

selected in our studies, xanthohumol has not been extensively studied. Thus, there are no published bioavailability studies performed in human or in animals.

Briefly, xanthohumol is a very potent antioxidant which prevents the oxidation of human LDL when compared to alpha-tocopherol, vitamin E [101]. Xanthohumol also inhibits the activity of diacylglycerol acyltransferase with an IC_{50} of 50.3 μ M in rat liver microsomes [102]. This characteristic gives xanthohumol the potential to prevent obesity and related diseases such as diabetes. Also, xanthohumol has been shown to have antiproliferative and cytotoxic effects *in vitro* with the human breast cancer MCF-7 cells, the human colon cancer, HT-29 cells, and the human ovarian cancer, A2780 cell [103].

The interaction between xanthohumol and drug-metabolizing enzymes has been studied *in vitro*. Xanthohumol can inhibit the *in vitro* catalytic activity of recombinant human CYP1A1, CYP1B1, but not CYP2E1 or CYP3A4 [104]. It has also been shown to induce quinone reductase in the mouse hepatoma Hepa 1c1c7 cell line used for studying the Ah receptor and CYP1A1 regulation [105]. However, there has been no study investigating the interaction between xanthohumol and the drug efflux transporters such as P-gp. This thesis will evaluate the effect of xanthohumol on the efflux of cimetidine in Caco-2 cells.

2.3 Caco-2 Cells

Because oral dosage formulations are the most preferred route of drug administration due to the patient compliance, pharmaceutical industries have placed

a lot of effort in the development of investigating new models to screen the oral possibility of drug candidates. This evaluation considers the physiochemical factors such as the pKa, lipophilicity, and solubility and how these parameters can influence intestinal absorption. Moreover, the capability of the drug candidate to pass through the intestinal epithelia, the major biological barrier to oral absorption, is also under investigation during the drug discovery process. There are several experimental designs and animal models that are commonly used for the investigation of oral drug absorption. Because of increasing concern to decrease the use of animals in experiments, an *in vitro* cell culture model, such as the Caco-2 cells, has become an attractive alternate for the study of drug absorption.

The Caco-2 cell line was derived from a human colo-rectal adenocarcinoma [106]. When the cells are grown in a tissue culture treated flask or semipermeable membrane, the Caco-2 cells can differentiate spontaneously and exhibit many characteristics of the human small intestinal epithelium. Among the 20 human colon cell lines available, the Caco-2 cells are the only ones that can differentiate spontaneously under standard culture conditions [107]. The Caco-2 model has been well characterized and is the most common model used for the prediction of oral bioavailability. When grown in a flask, the Caco-2 cells start to proliferate after a lag time of 48 hours. Confluency is often reached 5 days after seeding [108]. Caco-2 cells starts to differentiate after reaching confluency. However, when the Caco-2 cells are seeded on semipermeable membrane such as the Transwell® inserts, it takes longer for the Caco-2 cells to reach confluency. Vachon and

Beaulieu determined that the three states for Caco-2 cells in culture were: (i) homogeneously undifferentiated (subconfluent); (ii) heterogeneously polarized and differentiated (0-20 days after confluence); and (iii) homogeneously polarized and differentiated (> 30 days after confluence) [109].

After differentiation, the Caco-2 cells share many morphological characteristics with the human small intestinal epithelium. Both are highly polarized and have tall columnar cells that are sealed with tight junctions which can regulate solute movement [110]. The formation of the brush boarder with microvilli in the apical surface of Caco-2 cells has also been observed (Figure 2.6) [8]. The microvilli greatly increase the apical surface area such that it enhances nutrition absorption. Terminal webs are formed underneath the microvilli to provide structural support and organization of the various transporters and/or ion channels on the apical side.

In addition to the morphology similar to human intestine, Caco-2 cells also express many enzymes found in the intestinal epithelium. Table 2.2 lists some enzymes that are present in Caco-2 cells. Caco-2 cells do not express the activity of CYP 3A4 [111], which is involved in the metabolism of many pharmaceuticals. However, there have been several Caco-2 clones such as TC7 that have CYP3A4 activity [112].

Intestinal epithelial cells also have various transporters to facilitate the uptake of poorly absorbed compounds. Pharmaceutical industries are interested in many of these transporters because drugs may utilize these transporters to enhance

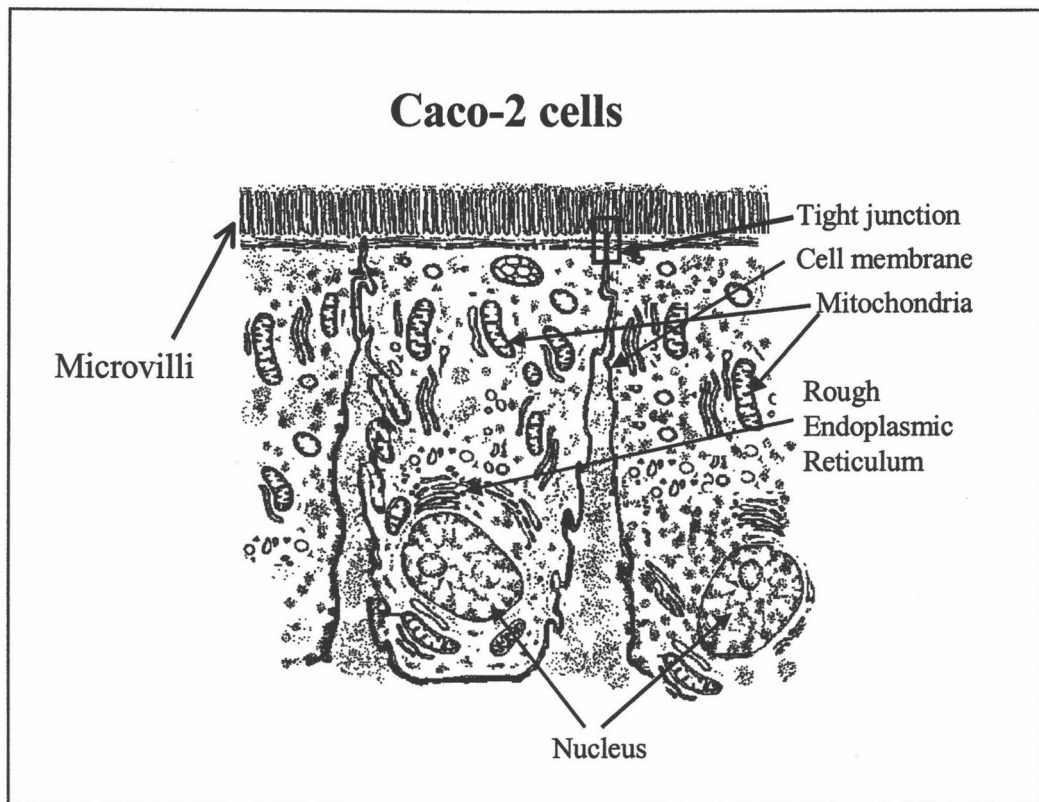


Figure 2.6 Cross-section of Caco-2 cells.

Table 2.2 Enzymes found in Caco-2 cells

Enzyme	Reference
Antioxidant enzymes	
Catalase	[113]
Glutathione peroxidase	[113]
Glutathione reductase	[113]
Superoxide dismutase	[113]
Digestive enzymes	
Alkaline phosphatase	[114]
Glycosidases	
Lactase	[115]
Sucrase-isomaltase	[114]
Peptidase	
Aminopeptidase N	[116]
Aminopeptidase P	[116]
Aminopeptidase W	[116]
Dipeptidyl peptidase IV	[116, 117]
Endopeptidase-24.11	[116]
Gamma-glutamyl transpeptidase	[116]
Membrane dipeptidase	[116]
Peptidyl dipeptidase A	[116]
Metabolic enzymes	
17-beta-hydroxysteroid dehydrogenase	[118]
Cyclooxygenase	[119]
Cytochrome P450 1A1(CYP1A1)	[120]
Diamine oxidase	[121]
Flavin-containing monooxygenase (FMO)	[122]
Glutathione-S-transferase	[123]
Ornithine decarboxylase	[121]
Phenol sulfotransferase	[124]

their absorption. The Caco-2 cells are also suitable model for screening drug transporter interaction because they express many of transporters that are found in small intestine epithelial cells. Table 2.3 lists the transporters that are found in Caco-2 cells. Caution is warranted when the passage number becomes too high for the cell line because the expression of transporters may be diminished due to mutations [125]. The characteristics of Caco-2 cells vary from passage to passage, especially at high passage number. Lu *et al.* compared the difference between early passage (35-47: Caco-2E) and late passage (87-112: Caco-2L) Caco-2 cells in morphology, cell proliferation, permeability, and electrophysiology [126]. The Caco-2L cells developed multiple layers while Caco-2E cells formed a monolayer under identical culture conditions [126]. Caco-2L cells also had higher transepithelial electrical resistance (TEER) (1,100 to 1,500 $\text{ohm}\cdot\text{cm}^2$) compared with Caco-2E cells (475 to 700 $\text{ohm}\cdot\text{cm}^2$). Moreover, Caco-2L cells had higher proliferation rates determined by the incorporation rate of thymidine. Besides the morphological and physiological differences, the Caco-2L and Caco-2E cells did not have significant differences with respect to the apparent permeability coefficient (P_e) of D-mannitol, hydrocortisone, or dipeptide glycylsarcosine. Briske-Anderson *et al.* [127] also reported that their TEER values increased as the passage number increased from 20 to 36, with a decline after passage 60. However, the sucrase-isomaltase activity increased as the passage number increased, until it reached a plateau at passage 36. Mesonero *et al.* [128] demonstrated that there were different levels of expression with the apical sodium-dependent glucose transporter

Table 2.3 Transporters found in Caco-2 cells

Name	Reference
Acid-base transporters	
Monocarboxylic acid transporter	[129] [130]
Na^+H^+ antiporter (NHE1 and NHE3)	[131] [132]
$\text{Na}^+\text{HCO}_3^-$ cotransporter	[131]
Amino acid transporters	
Acidic amino acids transport system X_{AG}^-	[133]
Gamma-glutamyl transpeptidase (γ -GT)	[134]
Na^+ -independent systems y^+ (L-cationic amino acids)	[135]
Bile acid transporters	
Na^+ -dependent bile acid transporter	[136]
Efflux pumps	
Multidrug associated proteins (MRP1, 2, 5)	[137]
P-glycoprotein (P-gp)	[138, 139]
Nucleoside transporters	
Na^+ -independent nucleoside transporters (ENT1, ENT2)	[140]
Peptide transporters	
Basolateral dipeptide transporter	[141]
H^+ -coupled dipeptide transporter (Pep T1)	[142]
H^+ -independent peptide transporter	[143]
Receptor- and carrier-mediated transporters	
Biotin transporter	[144]
Folate transporter	[145] [146]
Na^+ independent glucose transporters (GLUT1, 2, 3, 5)	[147]
Na^+ /glucose cotransporter (SGLT1)	[148]
Riboflavin transporter	[149]
Vitamin B_{12} transporter	[150]

(SGLT1), sodium-independent glucose transporters GLUT1 and GLUT3, and GLUT5 mRNA levels in the Caco-2 cells. These studies indicate that Caco-2 cells function differently at various passage numbers, therefore, one must take this into consideration when reviewing the literature and designing their own experiments.

The measurement of TEER values provides a good marker to evaluate the integrity of the Caco-2 cell monolayer. In the Caco-2 cell monolayer, the electrical conductivity is restricted to the ion flux in the paracellular pathway that is gated by the tight junctions [151]. Tight junction development is an important indicator of monolayer integrity. The commercially available “chop-stick” electrodes, such as STX-2 designed by World Precision Instruments, Inc., can determine TEER readings easily without damaging the monolayer. TEER reading values vary among laboratory with the range from 377 to 2,400 $\text{ohm}\cdot\text{cm}^2$ [139, 152]. Several factors can result in this variability: passage number, cell density, conditions at the time of measurement such as pH and temperature. Although it is difficult to set a standardized criterion for the TEER value, it is recommended to measure it before and after each experiment to make sure the Caco-2 cells monolayer is undamaged during the experiment.

During oral drug absorption, drug transport may be reduced because of the existence of the aqueous boundary of barrier, also called the “unstirred water layer” [153]. Because of this barrier, the drug concentration decreases when it contacts the surface of absorptive cells, compared to when it is in the intestinal lumen. The thickness of the unstirred water layer in human small intestine lumen is about 600

μm [154], which is thinner compared to the Caco-2 cell monolayer of 1,966 μm [155]. To reduce the thickness of the unstirred water layer *in vitro*, the water can be stirred. The mounting of the inserts in a plate shaker will help reduce the thickness of the unstirred water layer effectively [156]. However, the integrity of the monolayer may be compromised during agitation.

The primary value of the Caco-2 cell model is due to its prediction of *in vivo* oral drug absorption. There are numerous publications associating drug permeability of the Caco-2 cells and *in vivo* drug absorption [9, 152, 157-159]. For example, Pade and Stavchansky established a relationship between drug permeability and drug solubility using the Caco-2 *in vitro* model and the extent of drug absorption in human [9]. Their results showed that there was a significant association between the permeability measured in the Caco-2 cells, the solubility of the drugs, and the fraction of drug absorbed in humans. The primary goal for the use of the Caco-2 cell model is to predict the *in vivo* absorption of an unknown compound based on the data obtained from the *in vitro* model as well as other physical-chemical information. In fact, the Food and Drug Administration (FDA) has recently accepted that, when the appropriate conditions are met, Caco-2 permeability data can be used instead of *in vivo* data to claim a waiver of bioavailability or bioequivalence studies [160]. It is foretelling that pharmaceutical industries would prefer to use the Caco-2 model to obtain permeability information rather than performing *in vivo* experiments that are more labor intensive and costly.

Thus, the Caco-2 cells express much similarity with intestinal epithelial absorptive cells in both morphology and function. The association between Caco-2 permeability data and *in vivo* absorption data has also been well studied. The Caco-2 cells offer an excellent *in vitro* model to study the drug transport because of its relatively low cost, ease of obtaining data, and minute quantities of compound required.

2.4 Cimetidine

Cimetidine, N-cyano-N'-methyl-N''-[2-[(5-methyl-1H-imidazol-4-yl)methyl]thio]ethyl]guanidine, is a substituted imidazole [161]. Cimetidine is a histamine H₂-receptor antagonist which inhibits basal and nocturnal gastric acid secretion by competitive inhibition at the histamine H₂-receptors of the parietal cells. It also inhibits gastric acid secretion that is stimulated by food [162]. There are other histamine H₂-receptor antagonists in the market such as famotidine, nizatidine, and ranitidine. Cimetidine was the first histamine antagonist with wide clinical application. The brand name of cimetidine is Tagamet® by SmithKline Beecham. There are also generic products of cimetidine made by Sanofi Pharmaceuticals Inc. and Sidmak Laboratories Inc. Cimetidine can be used for treating duodenal and gastric ulcers, systemic mastocytosis, and upper gastrointestinal bleeding [163]. Currently, there are three dosage forms commercially available: tablet, oral solution, and solution for IV injection [163]. It is recommended that an adult take 300 mg cimetidine four times a day orally, with

meals and at bedtime or 400 or 600 mg twice a day, in the morning and bedtime or 800 mg at bedtime to treat duodenal ulcer. Because cimetidine can raise gastric pH, it has the potential to change the bioavailability of drugs which absorption is pH-dependent such as ketoconazole. Table 2.4 lists some of the physicochemical characteristics of cimetidine.

The pharmacokinetic characteristics of cimetidine have been studied in healthy subjects as well as ulcer patients. In a study by Walkenstein *et al.*, subjects were given either 300 mg oral solution formulation or a 300 mg oral tablet. The peak blood levels, C_{\max} , were 1.53 and 1.44 $\mu\text{g/ml}$ for oral solution and tablet, respectively [164]. The time for blood level to reach concentrations above 0.5 $\mu\text{g/ml}$ was 4.23 hrs for oral solution and 4.35 hrs for the tablet. Table 2.5 and Table 2.6 list some pharmacokinetic parameters of cimetidine for intravascular and extravascular administrations, respectively. For the I.V. injection, there was no obvious difference in elimination half-life, $t_{1/2}$, and total clearance, Cl_p , compared to the ulcer patients [164]. However, the renal clearance, Cl_R , and fraction of dose excreted unchanged in urine, f_e , are lower in ulcer patients compared with healthy subjects. Intramuscular absorption was relatively rapid and complete compared to both oral administrations [164]. The oral solution and tablet administration have a bioavailability about 70% and 58%, respectively. The bioavailability for the oral tablet varied from 58% to 70% among different studies [164, 165].

Table 2.4 The physicochemical characteristics of cimetidine [166]

Molecular formula:	$C_{10}H_{16}N_6S$
Molecular weight:	252.34
Appearance:	Colorless crystalline with bitter taste
Melting point:	141-143 °C
pKa:	6.8
Octanol/water partition coefficient:	2.5 at pH 9.2
Solubility:	1.14% in water at 37 °C, pH 9.3
	14.1% in methanol at 24 °C
	0.27% in acetonitrile at 24 °C
	14.9% at 25 °C in water for hydrochloride salt

Table 2.5 The pharmacokinetic characteristics of cimetidine resulting from an I.V. injection.

Parameters	Walkensgtein <i>et al.</i> [164]	Somogyi <i>et al.</i> [167]	Bodemar <i>et al.</i> [168]
Subject group	Healthy	Gastric/duodenal ulcer	Peptic ulcer
Number	12	6/6	10
Age (yr)	26 ± 3	28 - 64	19 - 71
Vd _{ss} (L/kg)	1.0 ± 0.2	nd	nd
Vd _β (L/kg)	0.8 ± 0.2	1.2 ± 0.4	nd
t _{1/2β} (h)	1.9 ± 0.3	2.0	1.8 ± 0.8
Cl _p (ml/min)	583 ± 140	495 ± 190	655 ± 173
Cl _r (ml/min)	451 ± 123	293 ± 166	375 ± 106
Cl _{nr} (ml/min)	nd	191 ± 46	280 ± 112
fe (%)	77 ± 6	57 ± 12	58 ± 11

Vd_{ss}: Volume of distribution at steady-state. Vd_β: Apparent volume of distribution. t_{1/2β}: Half-life of the terminal exponential phase. Cl_p: Total systemic plasma clearance. Cl_r: Renal clearance. Cl_{nr}: Non-renal clearance. fe: Fraction of dose excreted unchanged in urine. nd: not determined.

Table 2.6 The absorption and bioavailability of cimetidine from various formulations in healthy subjects.

Parameters	Intramuscular [164]	Oral solution [164]	Tablet [165]
Dose (mg)	300	300	200
No. of subjects	12	12	6
C _p _{max} (µg/ml)	4.57 ± 0.71	1.59 ± 0.43	0.86 ± 0.31
T _{max} (h)	0.25	1.0 ± 0.08	nd
AUC (mg/ml*h/100mg)	2.86 ± 0.4	1.69 ± 0.29	1.40 ± 0.60
fe	0.73 ± 0.04	0.48 ± 0.06	nd
F (from AUC data)	1.04	0.68 ± 0.12	0.58
F (from urine data)	0.95 ± 0.06	0.62 ± 0.06	nd

C_p_{max}: Maximum plasma concentration. T_{max}: Time of maximum plasma concentration. AUC: Area under the plasma concentration-time curve. fe: Fraction of dose excreted unchanged in urine. F: Bioavailability. nd: not determined.

Cimetidine is mainly excreted by renal elimination as unchanged drug, the metabolism consists of a minor portion of its total elimination [169]. Taylor *et al.* showed that cimetidine is metabolized to three metabolites: cimetidine sulfoxide, hydroxymethyl cimetidine, and guanylurea cimetidine [169] (Figure 2.7). Of these three metabolites, cimetidine sulfoxide is the major metabolite. Lu *et al.* demonstrated that both flavin-containing monooxygenases (FMO) and CYP located in mammalian intestine were involved in cimetidine sulfoxidation [170]. In addition, Mitchell *et al.* detected another new metabolite, cimetidine-N'-glucuronide, which is the major urinary metabolite of cimetidine [171].

The drug interactions associated with cimetidine have been studied extensively. Several *in vivo* and *in vitro* studies in the rat model revealed that cimetidine inhibits the activity of CYP2C6 and CYP2C11, but not CYP2A1, CYP2B1, or CYP3A1 [172-174]. Levine and Bellward demonstrated that forming a metabolite/intermediate complex with CYP2C11 was the proposed inhibition mechanism in rat microsomes [174].

Because cimetidine is a weak base with pKa of 6.8, it exists in the cationic form under physiological pH condition (pH 7.4). Several *in vivo* and *in vitro* studies have shown that the organic cation transporter and sodium-dependent facilitated diffusion were involved in the elimination of cimetidine in the kidney [175, 176]. Moreover, other studies have shown that cimetidine is a substrate of P-gp, an efflux pump that exists in various tissues, which serves as a defense system to remove

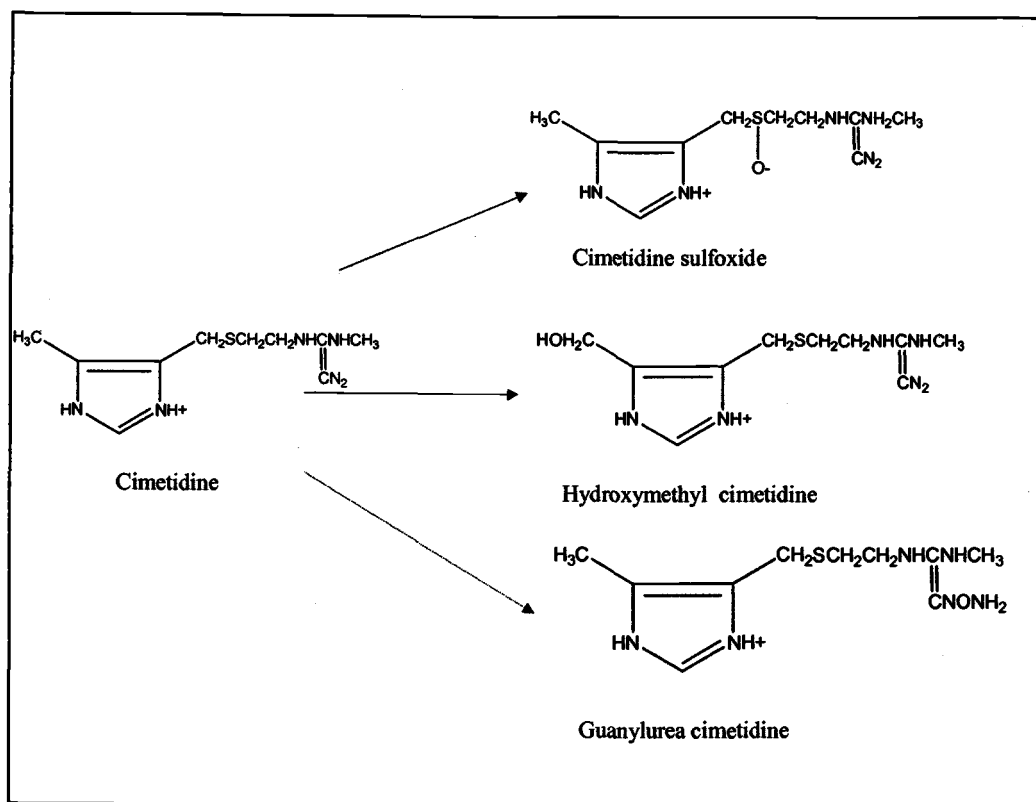


Figure 2.7 Proposed metabolic pathways of cimetidine.

xenobiotics [177]. The efflux phenomenon may be a possible mechanism for the variability of the bioavailability seen with cimetidine.

Because of the aforementioned facts, cimetidine was chosen as the model drug to evaluate the effect of flavonoids on the permeability of cimetidine in the Caco-2 transport model. Because cimetidine has been shown to be a substrate of P-gp and some flavonoids can inhibit the activity of P-gp as well as other efflux transporters, one can speculate that certain flavonoids can reduce the efflux phenomena of cimetidine by inhibiting P-gp function. Therefore, flavonoids may have the potential to increase the bioavailability of cimetidine *in vivo*. Once this relationship has been established, one can utilize specific flavonoids to enhance the absorption of drugs which are substrates of P-gp.

2.5 P-glycoprotein (P-gp)

Resistance to chemotherapy is a major problem to the treatment of human cancers. Many factors can contribute to the resistance of which one of them is the efflux transporters. This mechanism of resistance is referred to as multidrug resistance (MDR) because it occurs with a broad spectrum of unrelated anticancer drugs. This MDR phenomenon was first described in the early 1970s [178]. MDR is usually associated with an over expression of P-gp. Inhibiting the function of P-gp becomes a potential strategy in a successful treatment of chemotherapeutic drugs in the cure for various human cancers.

Tumor cell lines, selected with an anticancer drug, have been shown to display resistance to other compounds with different mechanisms of cytotoxicity, such as anthracycline, vinblastine, and actinomycin D [179, 180]. Most of these compounds are natural products of which close examination of their structures reveals no common chemical characteristics. Studies has been shown MDR was associated with an increased expression of a 170 kDa plasma membrane glycoprotein, P-gp, by Juliano and Ling [181]. In the 1980s, the MDR genes were identified in both human and rodent [182, 183]. Subsequently, MDR gene sequence was shown to match one of the P-gp cDNA clones which indicated that P-gp was a product of the MDR genes [184].

In past decade, the physical properties of P-gp have been extensively studied. The two dimensional structure P-gp model is shown in Figure 2.8. P-gp contains 1,280 amino acids consisting of two halves that are similar in structure. Each half has six transmembrane domains plus a relatively hydrophilic intracytoplasmic loop that has ATPase activity. Those characteristics place P-gp into the category of the ATP-binding cassette (ABC) superfamily. ABC transporters utilize the energy of ATP hydrolysis to transport substrate across membranes against a concentration gradient. In addition, there are several sites in the extracellular space for glycosidation. The function of glycosidation still needs investigation. Rosenberg *et al.* used electron microscopy and image analysis to investigate the possible three dimension structure of the purified P-gp [185]. They

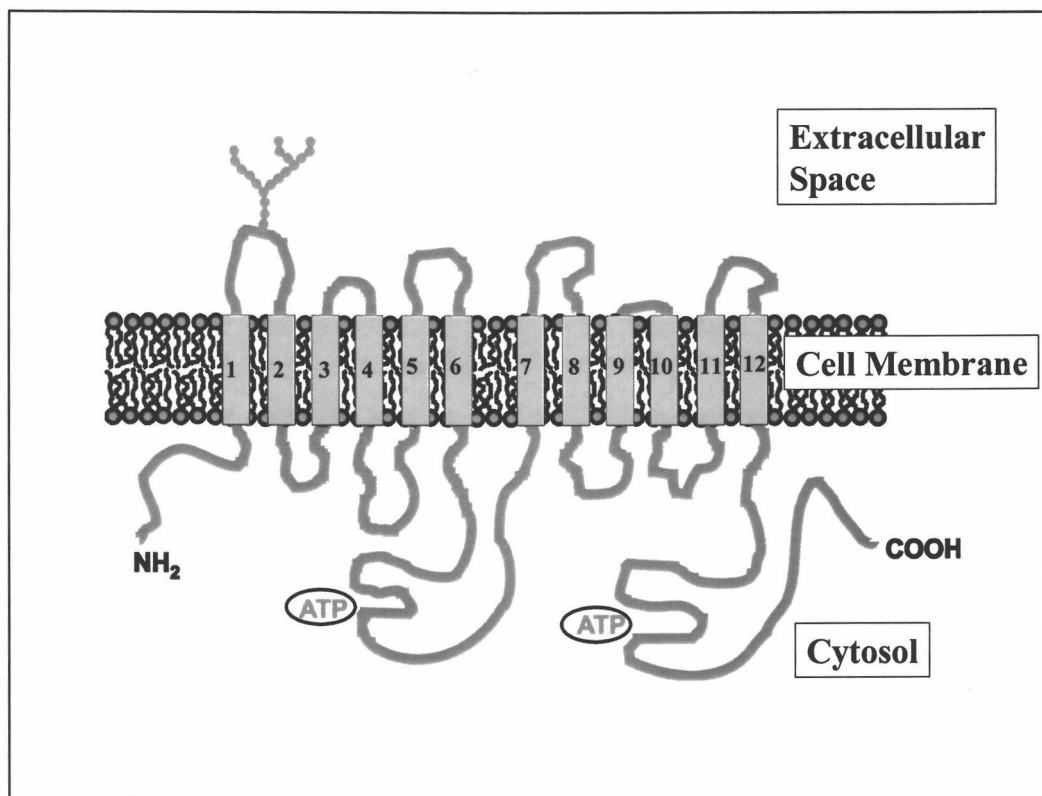


Figure 2.8 Proposed two dimension structural model of human P-glycoprotein.

found that the central aqueous channel has an opening into the lipid phase of cell membrane and that P-gp formed a monomer, in contrast with the symmetrical dimer proposed by amino acid sequence analysis.

There have been many studies evaluating the expression of P-gp in various cancers. P-gp expression is usually high and constitutive in tumors that arise from tissue known to physiologically express P-gp such as carcinoma of the colon, kidney, adrenal gland, pancreas, and liver [186]. An intermediate level of P-gp expression was found in neuroblastomas [187] and soft tissue carcinomas and in some hematological malignancies, including CD34+ acute myeloid leukemias [188], acute lymphoblastic leukemias [189], and chronic myeloid leukemias in blast crisis [189]. By contrast, tumors of lung, esophagus, stomach, ovary and breast, melanomas, and lymphomas expressed low level of P-gp [186]. However, some of these cancers may have elevated P-gp expression after chemotherapy. A higher incidence of P-gp expression after treatment has been demonstrated for human breast cancer [190], human lymphomas [191], and human myelomas [192].

Not only expressed in cancers, P-gp is also expressed in humans in a tissue-specific pattern. The human MDR1 gene has been found in liver, kidney, pancreas, and small and large intestine [193]. In all of these organs, P-gp is localized at the luminal surface of epithelial cells which suggests that P-gp physiologically plays a role in the elimination of xenobiotics. P-gp has also been shown to be expressed in endothelial cells at blood-tissue barrier sites in both human and rat such as the

blood-brain barrier [194] which offers protective effects of the brain from circulating xenobiotics and anticancer drugs such as vinblastine.

P-gp has been shown to transport various compounds such as listed in Table 2.7 back into the extracellular space. The spectrum of P-gp substrates covers both endogenous and exogenous compounds. P-gp has a high affinity for transporting compounds that are relatively hydrophobic and carry positive charge at physiological pH environments. The compounds pumped by P-gp are structurally unrelated to each other.

P-gp appears to be the main transporter of anticancer drugs involved in the MDR phenomenon. Several mechanisms have been proposed to explain how P-gp performs this function. The classic model describes P-gp as a transmembrane pore-forming protein that interacts with its substrates in the cytoplasm and pumps substrates directly into the extracellular medium [195]. According to the model, P-gp binds directly with substrates in the cytosol side of the plasma membrane and uses ATP hydrolysis as energy to pump substrates out of the cell. This mechanism has been supported by the Horio *et al.* study which demonstrated that the plasma membrane vesicles from MDR cell lines can accumulate ^3H -vinblastine in an ATP dependent pattern [196]. Higgins and Gottesman proposed that P-gp was a flippase [197]. In the flippase model, P-gp encounters substrates in the inner leaflet of the plasma membrane and flips them to the outer leaflet from which they diffuse into the extracellular medium [197]. Roepe *et al* demonstrated an alternative mechanism

Table 2.7 The substrates and inhibitors of P-glycoprotein.

Substrates		Inhibitors	
<u>Anticancer drugs</u>		<u>Tricyclic ring structures</u>	
Actinomycin D	Daunorubicin	Phenoxazine	Phenothiazine
Daunorubicin	Etoposide	Phenoxazone	Resurfin acetate
Mitomycin C	Paclitaxel	Xanthene carboxylic acid	Xanthene
Tamoxifen	Vinblastine	Acridine	Acridine orange
Vincristine		Quinacrine	
<u>Anti-allergics</u>		<u>Alkaloids</u>	
Terfenidine		Colchicine	Reserpine
<u>Antibiotics</u>		Staurosporine	
Cefazolin	Cefoperazon	<u>Antimalaria drugs</u>	
<u>Immunosuppressants</u>		Primaquine	Chloroquine
Cyclosporin A	Tacrolimus	<u>Neuroleptics</u>	
<u>Calcium channel blockers</u>		Phenothiazines	Thioxanthene
Diltiazem	Nicardipine	Flupentixol	
Verapamil		<u>Peptides</u>	
<u>Cardiacs</u>		Prenylcysteines	
Propafenone	Amiodarone		
Quinidine	Digoxin		
<u>CNS drugs</u>			
Domperidone	Fluphenazine		
Ondansetron	Perphenazine		
Phenoxazine	Phenytoin		
<u>HIV protease inhibitors</u>			
Indinavir	Ritonavir		
Saquinavir			
<u>Morphins</u>			
Morphine	Loperamide		
Morphine 6-glucuronide			
<u>Peptides</u>			
Gramicidin D	Valinomycin		
N-acetyl-leucyl-leucyl-norleucinal			
<u>Steroids</u>			
Aldosterone	Dexamethasone		
Hydrocortisone			
<u>Others</u>			
Rhodamine 123	Hoechst 33342		
Triton X-100			

Modified from Kerb *et al.* [198]

for P-gp [199]. Instead of binding compounds directly, they assumed that P-gp affects the intracellular pH and/or the plasma membrane electric potential of the cell by acting as a proton pump or a chloride channel; thereby, indirectly reducing the intracellular accumulation of compounds which are weakly basic, cationic and lipophilic. However, this model was challenged by Shapiro and Ling whom demonstrated that Hoechst 33342, a fluorescent substrate of P-gp, was expelled directly by purified P-gp [200]. More studies are needed in order to clarify the precise mechanism of P-gp transport with a variety of drug molecules which display a diverse range of physicochemical properties.

In the past ten years, the regulation of P-gp has been extensively studied. A point mutation was found in the first cytoplasmic loop, Gly 185 → Val 185 substitution which causes an increase in the resistance to colchicines, an inhibitor of P-gp, and decrease the resistance to vinblastine, a substrate of P-gp [201]. Acute anticancer drug treatment can upregulate the P-gp levels in human leukemia cancer cell line [202]. This induction may be dependent on transcriptional mechanisms because the MDR1 promoter responds directly to cytotoxic agents such as vincristine, daunomycin, adriamycin and colchicine [203]. Environmental stress such as heat shock, arsenite, and cadmium chloride treatments can enhance *in vitro* P-gp expression in the human renal adenocarcinoma cell line HTB-46 [204]. Osmotic shock and a low external pH environment can upregulate MDR1 mRNA in human colon and kidney cell lines [205]. This may explain why many solid

tumors develop multidrug resistance because they usually grow under acidic environmental conditions. There are other compounds found to regulate the expression of P-gp mRNA or protein, such as sodium butyrate, dimethyl sulfoxide, dimethylformamide, estradiol, and dexamethasone [206-208].

Since the initial study by Tsuruo *et al.* [209] demonstrated that verapamil can down regulate MDR, many compounds were found to inhibit P-gp-mediated transport thereby reversing the resistance of anticancer drugs shown in Table 2.7. These compounds are called P-gp inhibitors, modulators, chemosensitizers, or reversing agents. Most of these inhibitors can inhibit the radiolabeling of P-gp by a photoaffinity substrate such as ^3H -azidopine [210]. Therefore, the proposed mechanism of P-gp inhibitors is competition with the anticancer drugs for binding sites on P-gp. It has been shown that some of these P-gp inhibitors such as verapamil are also the substrates for P-gp [211]. Based on the study by Shapiro and Ling, P-gp has at least two drug binding sites positioned in a positively cooperative manner [212]. This may explain why some P-gp inhibitors are only effective on certain P-gp substrates.

Because P-gp is the major cause of MDR, many studies have been conducted with these P-gp inhibitors to reverse MDR thereby enhancing the success rate of cancer chemotherapy. Some P-gp inhibitors such cyclosporine have recently entered clinical trials [213]. At this time, the major limitation for these P-gp inhibitors in clinical applications appears to be undesirable side effects at *in vivo*

concentrations required to inhibit P-gp function. One solution to avoid side effects is to develop agents that specifically inhibit P-gp function without causing the undesirable pharmacological effect. One example is the non-immunosuppressive cyclosporine A analog PSC-833 [214]. Another alternative approach to minimize side effects is to find P-gp inhibitors that have low toxicity. Because some flavonoids have been demonstrated to inhibit P-gp function and flavonoids are found in high amounts in our daily diet, certain these could be good candidates to reverse the MDR *in vivo* without toxic side effects.

It has been well established that MDR is one of the main causes for low or variable bioavailability of certain drugs, especially the anticancer drugs. In the last decade, scientists tried to find compounds to block MDR while producing minimal side effects. Dietary supplements such as grape seed extract and their individual components such as flavonoids have begun to draw growing attention on their potential medical applications. The work presented in this dissertation is based on the evidence of previous *in vitro* studies which has demonstrated that flavonoids can inhibit the activity of efflux transporters such as P-gp. According to this rationale, an inhibitory effect on the efflux of P-gp substrates is predicted with co-treatment of these flavonoids and P-gp substrates *in vitro*. This work is part of an effort to understand the mechanism of drug-dietary interaction of orally administered drugs. Most of the studies presented herein use the Caco-2 cell transport model to investigate the permeability of cimetidine. An understanding of

how flavonoids reduce the efflux of cimetidine in the Caco-2 cell model will provide valuable information about the interactions between flavonoids and efflux substrates. It also offers a foundation for future *in vivo* or clinical studies about drug-diet interactions.

3. MATERIALS AND METHODS

3.1 Materials

Caco-2 (HTB-37) cells were purchased from American Type Culture Collection, ATCC, (Rockville, MD). [^3H]-mannitol (specific activity, 20 Ci/mmol) was purchased from American Radiolabeled Chemical, Inc. (St. Louis, MO). [^3H]-cimetidine (specific activity, 19.4 Ci/mmol) was purchased from Amersham Pharmacia Biotech, Inc. (Piscataway, NJ). Potassium phosphate monobasic, sodium hydroxide, calcium chloride hexahydrate, magnesium chloride hexahydrate, sodium chloride, and sodium bicarbonate were obtained from Fisher Scientific Company (Pittsburg, PA). Cimetidine, quercetin, quercitrin, rutin, naringenin, naringin, genistein, genistin, potassium chloride, magnesium sulfate heptahydrate, sodium phosphate dibasic, D- (+)-glucose, (N-[2-Hydroxyethyl]piperazine-N'-[2-ethanesulfonic acid]) (HEPES), hydrochloric acid, reduced β -nicotinamide adenine dinucleotide (NADH), sodium pyruvate, dimethyl sulphoxide (DMSO), ethylenediaminetetraacetic acid (EDTA), antibiotic and antimycotic solution, diisothiocyanatostilbene-disulfonic acid (DIDS), verapamil, and bumetanide were purchased from Sigma Chemical Company (St. Louis, MO). Trypsin, non-essential amino acids, and Dulbecco's Modified Eagle's Medium (DMEM) were from GIBCO, Life Technologies, Inc. (Grand Island, NY). Liquid scintillation cocktail was purchased from ICN Pharmaceutical, Inc. (Costa Mesa,

CA). Fetal bovine serum (FBS) was obtained from HyClone, Inc. (Logan, UT).

Lastly, rhodamine 123 was purchased from Molecular Probes Company (Eugene, OR). Xanthohumol was a kind gift from Dr. Cristobal Miranda.

3.2 Caco-2 Cell Culture

3.2.1 Preparation of Culture Medium

The culture medium for the Caco-2 cells was prepared by mixing DMEM with 10 % FBS, 1% non-essential amino acids, and 1% antibiotic and antimycotic solution. The medium was prepared in a laminar hood under sterile. The culture medium was stored at 4 °C and was warmed to 37 °C prior to usage.

3.2.2 Procedure for Growing Caco-2 Cells in 162 cm² Flasks

The Caco-2 cells were grown in 162 cm² filter-vent flasks (Corning Inc., Corning, NY) with culture medium. The flasks were labeled, dated, passage number recorded, and were kept in the 37 °C incubator with an atmosphere of 5% CO₂ and 95% relative humidity. The culture medium was replaced every two days in a laminar hood. The cells were subcultured when they reach 95% confluency.

3.2.3 Subculturing Caco-2 Cells in 162 cm² Flasks

To subculture the cells, the culture media were removed by suction or pooling. Then the cells were rinsed with 37 °C calcium and magnesium-free phosphate buffer saline (PBS) three times to clean the remaining culture media. After the last PBS wash has been completed, 10 mL of trypsin-EDTA in calcium and magnesium-free PBS was added into the flask. The flask was rinsed thoroughly and discarded most liquid. Only approximately 3 mL of trypsin-EDTA was left in flask to cover the surface. The flask was placed in a 37°C incubator for 3 to 5 min until the cells started to detach from the flask. Then, 10 mL of culture media was added into the flask to stop the trypsin-EDTA reaction. Lastly, use a 10 mL pipet to suspend the trypsinized mixture to break apart possible clumping of cells.

A 50 µL aliquot of the cell suspension was loaded onto a hemacytometer (Hausser Scientific, Inc., Horsham, PA). The average from two sides of the hemacytometer were multiplied by 10,000 which is the estimated cell density of the suspension. Culture media is used to make the proper dilution to obtain the desirable density. To seed a T162 cm² flask, the required cell density needed is 2×10^4 cells/mL. Each of these subcultures results in an increase of the passage number. Because frequent subcultures are required, increasing passage numbers eventually change both morphology and function of Caco-2 cells as previously described. Thus, the passage number of the Caco-2 cells in our current studies was

limited from passage 25 to passage 30 in order to obtain consistent results by minimizing the possibility of altered function.

3.2.4 Plating and Maintaining Caco-2 Cells in Transwell® Plates

Transwell® plates (Corning Costar Co., Cambridge, MA) were the apparatuses used to study the transport of cimetidine in Caco-2 cells (Figure 3.1). Each Transwell® plate consisted of six Transwell® inserts as shown in Figure 3.2. The cell density of the cell suspension was adjusted to 2×10^5 cells/mL to seed 1.5 mL of this suspension into the Transwell® inserts for a total of 300,000 cells per insert in apical (AP) compartment. Then, 2.5 mL of culture medium was added to the basolateral (BL) compartment. The plates were gently shaken to allow cells to distribute uniformly. The plates were labeled with the date and passage number and were stored in a 37 °C incubator at 5% CO₂ and 95% relative humidity. The culture media were replaced every two days for the first two weeks and every day after two weeks. All procedures were performed in a laminar hood under sterile conditions.

3.3 Lactate Dehydrogenase (LDH) Assay

The release of LDH from the Caco-2 cell monolayers was examined with the various flavonoids and cimetidine in a dose and time response manner. This assay assessed the cytotoxicity of the various compounds so that proper

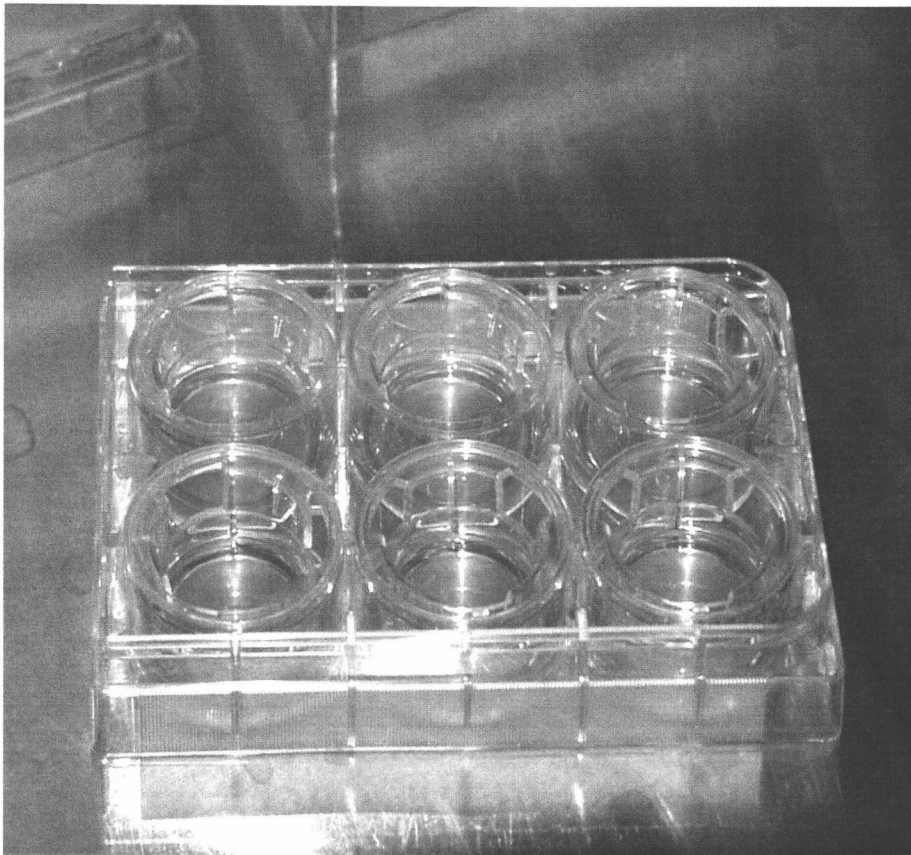


Figure 3.1 The Transwell[®] plate with inserts.

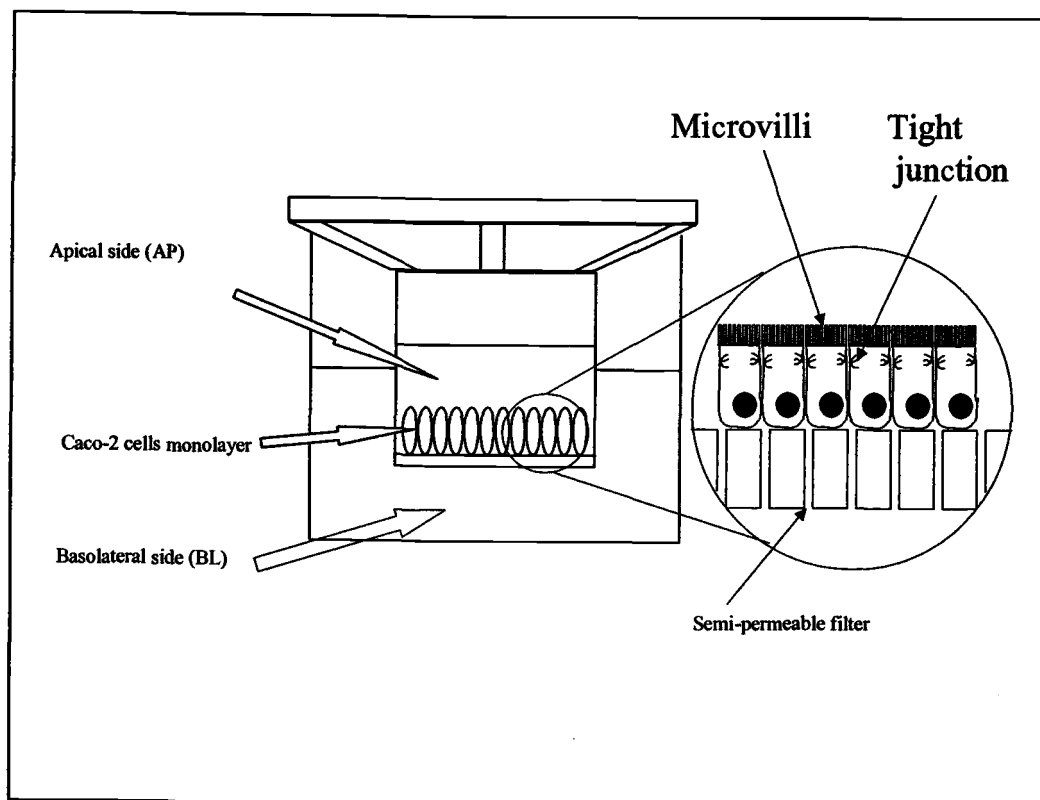


Figure 3.2 The cross-section of a transwell[®] insert with Caco-2 cell monolayer with a magnification of the cells on the polycarbonate membrane. The magnification shows the differentiation of the monolayer into absorptive cells containing microvilli and tight-junctions.

concentrations were used such that the integrity of the Caco-2 cell monolayers was not altered.

The Caco-2 cells were seeded in a 24-well tissue culture plates (Becton Dickinson Labware, Inc. Lincoln Park, NJ) at a density of 1×10^5 cells/well. The cells were grown for seven days with the media replaced every two days until experimentation.

On the day of the experiment, the culture media were replaced with serum-free DMEM that contained the various concentrations of the flavonoids. The concentrations used were 50 μ M, 100 μ M, 200 μ M, 500 μ M, as well as the appropriate vehicle controls (0.2 % DMSO and 0.5 % ethanol). Each treatment concentration was performed in triplicate. The treatment plates were kept at 37 °C in an incubator for 2 and 4 hr. At the end of the exposure period, the serum-free DMEM with various treatments was removed from the plate for LDH determination. LDH assay requires phosphate buffer (37 °C, pH 7.4) and freshly made stock solutions of NADH (2.5 mg/mL) and sodium pyruvate (1 mg/mL). The NADH and sodium pyruvate are kept on ice until needed. The buffers and solutions needed for the LDH assay were described in the Appendix 1 of this dissertation. The reagents were added in the following order to minimize variability, 312.5 μ L phosphate buffer, 12.5 μ L samples, 30 μ L NADH solution, and then 30 μ L sodium pyruvate solution for a total volume of 385 μ L in a glass tube. The mixtures were mixed on a vortex machine for 30 seconds and then an 200 μ L aliquot of the

reaction mixture was read at 340 nm in the Spectramax 190 spectrometer (Molecular Devices Co., Sunnyvale, CA). The absorbance is proportional to the content of LDH. If the LDH leakage of an experimental treatment is greater than five percent of the lysate of Caco-2 cells, the treatment is considered toxic to the Caco-2 cells.

3.4 Caco-2 Cell Monolayer Integrity

The integrity of the Caco-2 cell monolayers needs to be checked before any experiments can be performed. The studies in this thesis used two methods to evaluate the integrity. The first method is the use of mannitol to evaluate the paracellular transport. The second method measures the transepithelial electrical resistance (TEER) of the Caco-2 cell monolayers.

3.4.1 Mannitol Transport

The permeability coefficient (P_e) of ^3H -mannitol from AP to BL direction was determined to evaluate the integrity of Caco-2 cell monolayers. A transport rates of mannitol under 1% per hour indicated the integrity of the cell monolayers was not compromised during the experiments. The experiments were performed in duplicate at pH 7.4 in a 37 °C incubator (5% CO_2 and 95% relative humidity). A final concentration of 1×10^6 dpm/mL ^3H -mannitol was used in the experiment.

3.4.2 Measurement of Transepithelial Electrical Resistance (TEER)

The TEER values were always measured before the initiation of a transport experiment. The Transwell® inserts were washed three times with transport buffer (see Appendix 2). Then 1.5 mL and 2.5 mL pH 7.4 transport buffer were added to AP compartment and BL compartment, respectively. The Transwell® plates were incubated in a 37°C incubator with atmosphere of 5% CO₂ and 95% relative humidity for 30 min. An Evom Epithelial Voltohmmeter with a chopstick electrode, STX-2 (World Precision Instruments, Inc., New Haven, CT), was used to measure the TEER values. To measure a TEER value of an insert, the electrode is placed into the openings of the insert with the long arm of the electrode in the BL side and the short arm in the AP side (Figure 3.3). The reading represents the resistance of the Caco-2 cell monolayer plus the insert membrane in units of ohm, Ω . To obtain the net resistance of the Caco-2 cell monolayer, the gross resistance needs to be subtracted from the resistance of insert membrane (background blank), which is obtained from an empty insert filled with pH 7.4 transport buffer in both AP and BL compartments. After each insert was measured 3 times, the average resistance was multiplied by the surface area of the insert, 4.71 cm². The resulting values represents the TEER reading for a given insert in units of ohm*cm². A TEER reading below 500 ohm*cm² is considered to be leaky and that insert would not be suitable for an experiment thereby it is discarded.

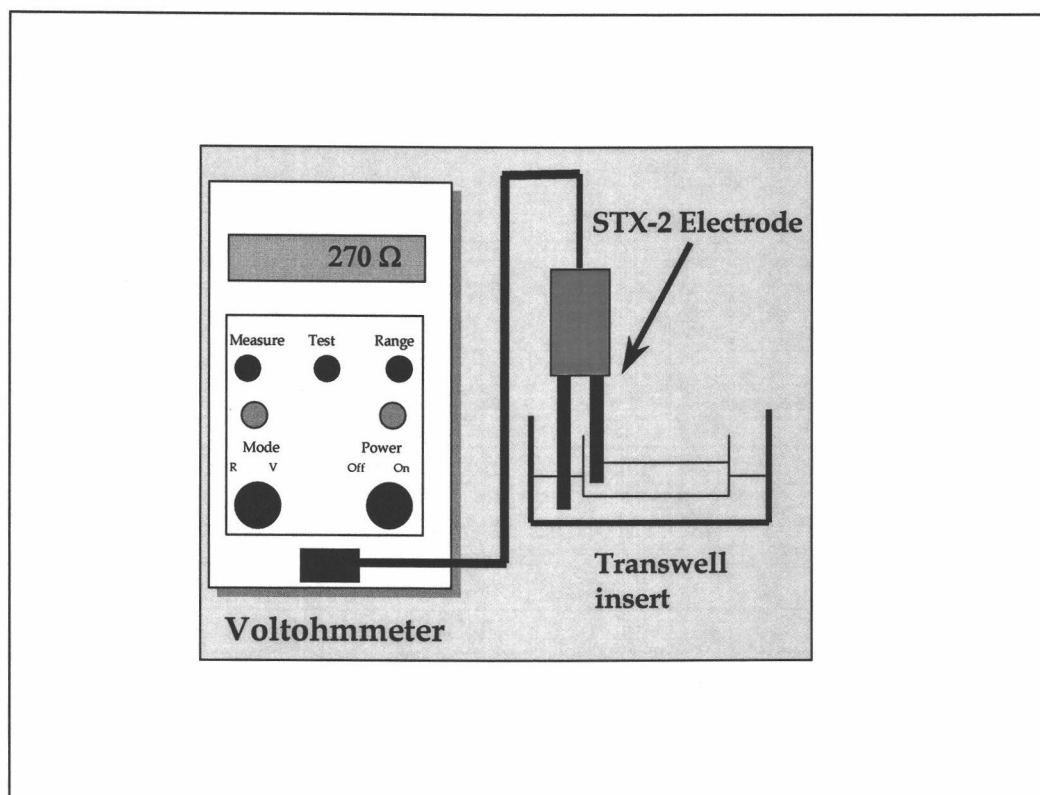


Figure 3.3 The diagram representing the measurement of resistance of the Caco-2 cell monolayer by a voltohmmeter with a STX-2 chopstick electrode.

3.5 Transport Experiments of Cimetidine

The Caco-2 cell monolayers used for experiments were 22 to 24 days old. All the treatments were performed in duplicate and repeated 2 to 3 times. The cimetidine solution for the transport experiments was prepared by mixing ^3H -cimetidine with cold cimetidine in transport buffer. The final concentration of radiolabel in the stock solution was adjusted to 1×10^6 dpm/mL. Prior to the experiment, the culture medium was aspirated from both compartments. The monolayers were washed three times with warm pH 7.4 transport buffer, 1.5 mL for AP compartment and 2.5 mL for BL compartment. Then, the monolayers were incubated in pH 7.4 transport buffer in a 37 °C incubator with 5% CO_2 and 95% relative humidity for 30 min.

The TEER reading measurement was performed immediately following the 30 min incubation. The procedure of measuring TEER reading was described in section 3.4.2. Then, the transport buffer was removed by aspiration and the radiolabeled drug solution was added into the inserts. For transport experiments from AP to BL direction, the ^3H -cimetidine solution ($1 \mu\text{M}$ Ci/mL) was added into apical compartment, 1.6 mL, and 2.6 mL pH 7.4 transport buffer was added to the BL compartment. For transport experiments from BL to AP direction, the ^3H -cimetidine solution ($1 \mu\text{M}$ Ci/mL) was added into BL compartment, 2.6 mL, and 1.6 mL pH 7.4 transport buffer was added to the AP compartment. If the experiments

involved co-treatment with other compounds such as flavonoids or 100 μ M verapamil, these were placed in both compartments to obtain the maximal effect. After experimental solutions were added, 100 μ L samples were drawn from both compartments and were placed into scintillation vials with 1 mL liquid scintillation cocktail. The final volumes for the experiment were 1.5 mL for AP compartments and 2.5 mL for BL compartments.

At various time intervals, 100 μ L samples were drawn from the receiver compartments, in other words, BL compartment for AP-to-BL transport and AP compartment for BL-to-AP transport. For each sample taken, another 100 μ L fresh transport buffer was added to the receiver compartment maintain consistent volume. The sampling intervals were 30 min, 1 hr, 1.5 hr, 2 hr, 3 hr, and 4 hr after the initiation of the experiments. Less than 10 % of cimetidine crossed the monolayers during the length of the experiment. Thus, all the cimetidine transport experiments can be carried out using 'non-sink' conditions. At the last sampling, 100 μ L samples were also drawn from donor compartments to calculate the mass balance. All the 100 μ L samples were mixed thoroughly with the liquid scintillation cocktail and placed into the scintillation counter (Beckman Coulter, Inc., Fullerton, CA) to obtain the radioactivity in the unit of disintegrations per minute (dpm). The estimation of permeability coefficient (P_e) was performed from this data (Section 3.8.1).

3.6 Rhodamine 123 Transport Experiments

Rhodamine 123 is a fluorescence dye that is a known P-gp substrate and was used as a positive control to confirm that the P-gp in the Caco-2 cells was functional. The Caco-2 cells were 22 to 24 days old and all the treatment conditions were performed in duplicate and repeated 2 or 3 times. The rhodamine 123 solution for the transport experiments was prepared by diluting the concentrated rhodamine 123 stock solution, 250 μM , in transport buffer. The resulting final concentration of rhodamine 123 used in the experiments was 2.5 μM . The rest of the procedure was previously described in section 2.4.2. All the samples were analyzed by the fluorescence photometer (Perkin Elmer Co., Norwalk, CT) using an excitation wavelength of 497 nm and an emission wavelength of 526 nm. The estimated permeability coefficient (P_e) was performed from the data (Section 3.8.1).

3.7 Uptake Experiments of Cimetidine

The uptake experiments were performed to determine the amount of cimetidine transported into the Caco-2 monolayers under different treatment conditions such as pH conditions and co-treatments of flavonoids. As in previous experiments, the Caco-2 cell monolayers used were 22 to 24 days old and were performed in triplicate. The cimetidine solution for the uptake experiments was prepared by mixing ^3H -cimetidine with 20 mM cold cimetidine in transport buffer. The final concentration of radiolabel in the stock solution was adjusted to 1.5×10^6

dpm/mL and the final concentration of cimetidine was 20 μ M. Prior to the experiment, the culture medium was aspirated from both compartments. The monolayers were washed three times with warm pH 7.4 transport buffer, 1.5 mL for AP compartment and 2.5 mL for BL compartment. Then, the monolayers were incubated in pH 7.4 transport buffer in a 37 °C incubator with 5% CO₂ and 95% relative humidity for 30 min. If the experiments involved co-treatment with other compounds such as flavonoids or verapamil, these were placed in both the AP and BL compartments to obtain the maximal effect.

For the AP uptake experiments, 1.5 mL radiolabeled cimetidine solution, 20 μ M and 1.5×10^6 dpm/mL, with or without co-treatment were added to the AP compartment. The incubation time for uptake was 3 min. Afterwards, the radiolabeled solution was removed and replaced with ice-cold pH 7.4 transport buffer to stop the uptake process. The insert was washed with ice-cold transport buffer 3 times to remove any radiolabeled drug binding to the surface of the cells. The insert membranes were excised and placed into a scintillation vial with 2 mL liquid scintillation cocktail for determination of the radioactivity.

For the BL uptake experiments, 2.5 mL radiolabeled cimetidine solution, 20 μ M and 1.5×10^6 dpm/mL, with or without co-treatment were added to an empty well of a 6 well cell culture plate (Becton Dickinson Labware, Inc. Lincoln Park, NJ). After a 30 min incubation, the Transwell[®] insert with the Caco-2 cells was placed into the well. After a 3 min incubation time, the insert was placed into a well

with ice-cold pH 7.4 transport buffer to stop the uptake process. The insert was washed with ice-cold transport buffer 3 times to remove any radiolabeled drug binding to the surface of the cells. The insert membrane was excised and placed into a scintillation vial with 2 mL liquid scintillation cocktail for determination of the radioactivity.

The radioactivity of all the samples was adjusted by the protein content of the Caco-2 cell monolayers. There was no significant difference in protein content of the Caco-2 cell monolayers among 22 to 24 days old. Therefore, it was assumed that the protein content of Caco-2 cell monolayers in the uptake experiments is identical among the inserts.

3.8 Data Analysis

3.8.1 Calculation of the Apparent Permeability Coefficient (Pe)

A specific example for the estimation for the apparent permeability coefficient (Pe) of cimetidine from the AP-to-BL and BL-to-AP directions is described in detail in the Appendix 3.

The percent mass transferred to the receiver at each time point can be estimated by using Equation 3.1:

$$\text{Percent mass transferred} = \frac{[R]_t}{[D]_0} \times 100 \% \quad \text{Eq 3.1}$$

where $[R]_t$ is the amount in the receiver compartment at time t , $[D]_0$ is the amount in the donor compartment at time zero. Because of the experimental conditions applied in these experiments, the amount of the radiolabeled compound in the donor compartment decreases as time increases. At time zero, the amount of radiolabeled compound in the donor compartment is presented as $[D]_0$. At the end of the time interval, the amount of radiolabeled compound in the donor compartment would be $[D]_0 - [R]_t$. It is assumed that the amount of radiolabeled compound in the donor compartment throughout the interval remains consistent at $[D]_0 - 0.5*[R]_t$. Therefore, the normalized percent mass transferred at each time interval is presented in Equation 3.2, which take into consideration the loss of the compound from the donor compartment during each time interval.

$$\text{Normal percent mass transferred} = \frac{[R]_t}{[D]_0 - 0.5*[R]_t} \times 100\% \quad \text{Eq 3.2}$$

Once the normal percent mass transferred is obtained, the effective permeability coefficient can be calculated by using Equation 3.3:

$$Pe = V/A \times \Delta\% / \Delta t \quad \text{Eq 3.3}$$

where Pe is the effective permeability coefficient in units of cm/sec ; V is the volume of the solution in the donor compartment (1.5 cm^3 for AP-to-BL direction and 2.5 cm^3 for BL-to-AP direction); A is the surface area of the monolayer, 4.71 cm^2 ; $\Delta\%$ is the normal percent mass transferred in a given time interval; and, Δt is the length of a given time interval in seconds.

3.8.2 Determination of the Michaelis-Menton Constant (K_m)

Previous study has suggested that P-gp follows Michaelis-Menten kinetics [215]. Thus, one can calculate the K_m of cimetidine and P-gp. Because the P_e of cimetidine from the BL-to-AP direction represents the combination of passive diffusion and active efflux, the P_e of cimetidine in BL-to-AP direction when co-treated with 100 μ M verapamil represents the P_e of passive diffusion and other possible efflux mechanisms other than P-gp efflux. By subtracting this P_e from the P_e of cimetidine alone, one can obtain the P_e of the active efflux of P-gp. This P-gp efflux's P_e can be transformed into an efflux rate using Equation 3.4:

$$V = 60 \times P_e \times C \times A \quad \text{Eq 3.4}$$

where V is the efflux rate in $\mu\text{mol}/\text{min}$; P_e is the efflux permeability coefficient in cm/sec ; C is the concentration of cimetidine in $\mu\text{mol}/\text{L}$; and, A is the surface area of the insert membrane. Then the K_m of P-gp can be obtained by using the following equation:

$$V = \frac{V_{\max} \times C}{K_m + C} \quad \text{Eq 3.5}$$

where V is the efflux rate in $\mu\text{mol}/\text{min}$; V_{\max} is the maximal efflux rate in $\mu\text{mol}/\text{min}$; K_m is the Michaelis-Menten constant in μM ; and, C is the concentration of cimetidine in μM . This nonlinear regression analysis was performed in SigmaPlot® 2001 (SPSS Inc., Chicago, IL) to obtain a good fit.

3.8.3 Inhibitory Concentration 50% (IC₅₀) Determination of Flavonoids

The inhibitory concentration 50% (IC₅₀) parameter was determined to estimate the inhibitory potency of various flavonoids on the efflux of cimetidine. In the beginning, several models were used to determine IC₅₀. all of the models provided similar values of IC₅₀ for a given flavonoid. Finally, a four-parameter sigmoid model was used to obtain the IC₅₀ of each flavonoid studied. By use this model, the precision of determining IC₅₀ was provided in term of 95% confidence interval, which is absent in other models. The four-parameter sigmoid model is given in Equation 3.6:

$$Pe = Pe_{\min} + \frac{Pe_{\text{range}}}{[1 + \exp((-C - IC_{50}) / b)]} \quad \text{Eq 3.6}$$

where Pe is the Pe of cimetidine in units of cm/sec; Pe_{min} is the estimated minimum Pe of cimetidine in units of cm/sec when the maximum inhibition of the flavonoid is applied; Pe_{range} is the estimated Pe range of cimetidine in units of cm/sec; C is the concentration of the flavonoid in unit of log(μM); b is the slope the curve with no unit; and, IC₅₀ is the inhibitory concentration 50% in unit of log(μM). Based on the selected four-parameter sigmoid model, the IC₅₀ represents the concentration of the flavonoid which corresponds to 50% of the efflux inhibition of cimetidine for that particular flavonoid. The model selection and the estimation of IC₅₀ were performed in SigmaPlot® 2001 (SPSS Inc., Chicago, IL).

3.8.4 Statistical Analysis

For the transport studies, the insert was considered the experimental unit. The P_e for a given insert was obtained by averaging the P_e from all time intervals studied. To test if the difference between control mean and treatment mean, the unpaired Welch approximate t-test was performed. In order to determine whether the mean of P_e for the treatments differed from that of control, a multi-way analysis of covariance (ANCOVA) was used as the initial model. The nominal factors included treatment effect, block effect, and date effect. The covariance was the TEER reading. The date and block effects were treated as random variable. The results came out that none of block effect, date effect, and TEER reading had significant impact on the permeability coefficient of cimetidine. So the final analysis was done by the one-way analysis of variance (ANOVA) followed by Dunnett's multiple comparison test were performed. A p-value less than 0.05 was considered statistically different. All statistical tests in this thesis were performed by SAS release 8.01 (SAS Institute Inc., Cary, NC).

4. RESULTS

4.1 Cytotoxicity of the Flavonoids in Caco-2 Cells

The cytotoxic effect of the compounds used in the Caco-2 cell transport experiments was evaluated by the LDH assay. LDH leakage is an indicator of membrane damage to the cells. When the membrane is damaged, LDH is released into the test media. The compounds are considered cytotoxic if the LDH release content exceeds 5 % of the Caco-2 cell lysate. The experimental treatments in the present studies included Caco-2 cells alone; Caco-2 cell lysate for total LDH content; 20 μ M and 2.5 mM cimetidine; 100 μ M and 500 μ M quercetin; 50 μ M and 100 μ M xanthohumol; and 200 μ M genistein. The results for the 2 hr and 4 hr incubations are shown in Figures 4.1 and 4.2, respectively. The LDH release patterns between the 2 hr and 4 hr incubations were similar. Concentrations of cimetidine up to 2.5 mM did not cause significant damage to the Caco-2 cell monolayers. Similar results were also seen in the flavonoid treatments of quercetin, xanthohumol, and genistein. However, 500 μ M quercetin caused greater than 8% of LDH released for both the 2 hr and 4 hr incubations. This suggests that a high concentration of quercetin (500 μ M) will produce cellular damage of the Caco-2 cells within 2 hr. Therefore, the highest concentration of each flavonoids used in experimentation was 100 μ M.

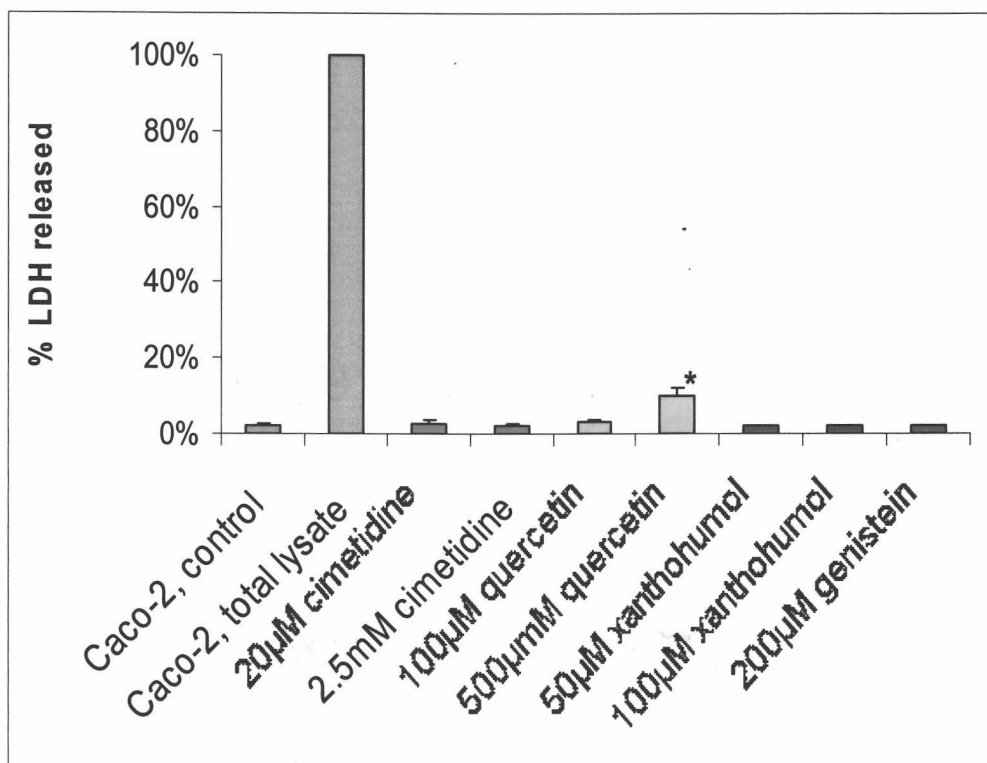


Figure 4.1 Two hour lactate dehydrogenase (LDH) release pattern of various experimental treatments from 7 day old Caco-2 cell monolayers, n=3. "*" means the LDH release content of the treatment was greater than five percent of Caco-2 cell lysate.

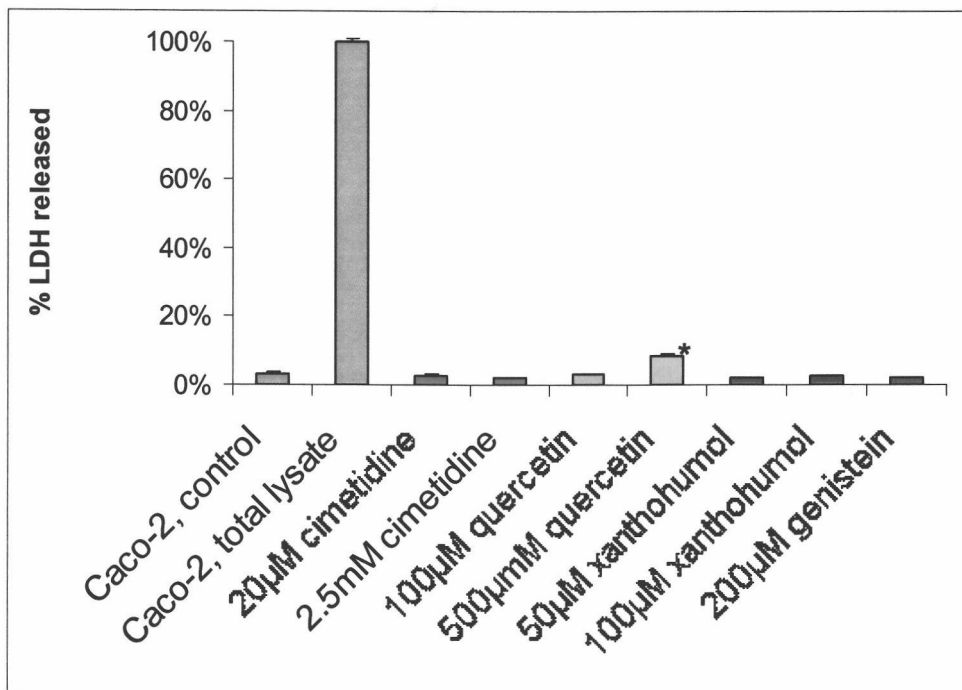


Figure 4.2 Four hour lactate dehydrogenase (LDH) release pattern of various experimental treatments from 7 day old Caco-2 cell monolayers, n=3. “*” means the LDH release content of the treatment was greater than five percent of Caco-2 cell lysate.

4.2 Integrity of the Caco-2 Cell Monolayers

The integrity of the Caco-2 cell monolayers was evaluated by monitoring the transport of ^3H -mannitol ($1\mu\text{M Ci/mL}$) and TEER from each insert. The AP-to-BL Pe of ^3H -mannitol was negatively associated with the culturing days (Figure 4.3). The mean Pe was 3.78×10^{-6} cm/sec at day seven down to 1.38×10^{-6} cm/sec at day twenty-eight, with a plateau reached at day twenty-one with a Pe value of 1.11×10^{-6} cm/sec. This suggests that the tight junctions were developing progressively as the culturing days increased. Twenty-one days after seeding, the mannitol transport rates did not exceed one percent per hour (Figure 4.4). This indicates that the integrity of the Caco-2 cell monolayers was maintained for the duration of the mannitol transport experiment. The Pe of mannitol from AP-to-BL direction across 21 day old cells ranged from 0.94×10^{-6} to 1.39×10^{-6} cm/sec with a mean of 1.11×10^{-6} cm/sec and standard deviation of 0.24×10^{-6} , $n=3$.

TEER values reflect the resistance across the tight junctions of the cell monolayers. The TEER reading was positively associated with the culturing days after seeding/plating (Figure 4.5). The mean TEER readings at day 10 and 32 were $541 \text{ ohm} \cdot \text{cm}^2$ and $1094 \text{ ohm} \cdot \text{cm}^2$, respectively. In general, the TEER readings were greater than $800 \text{ ohm} \cdot \text{cm}^2$ if the cell monolayers were greater than 21 days. The high TEER is reflective of an intact monolayer with no leaks because

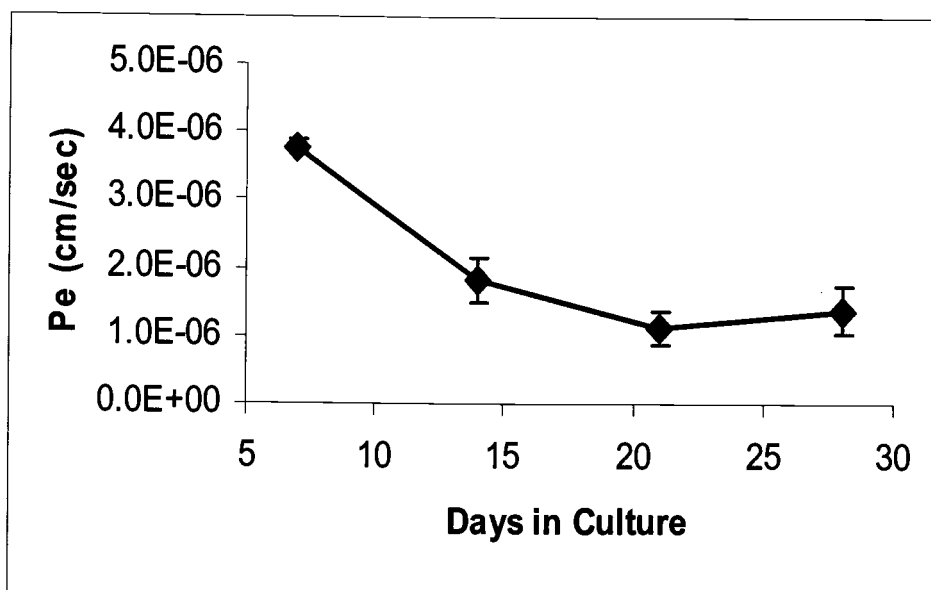


Figure 4.3 AP-to-BL permeability coefficient of ^3H -mannitol ($1\mu\text{M Ci/mL}$) as a function of days in culture in Caco-2 cells ($n=3$).

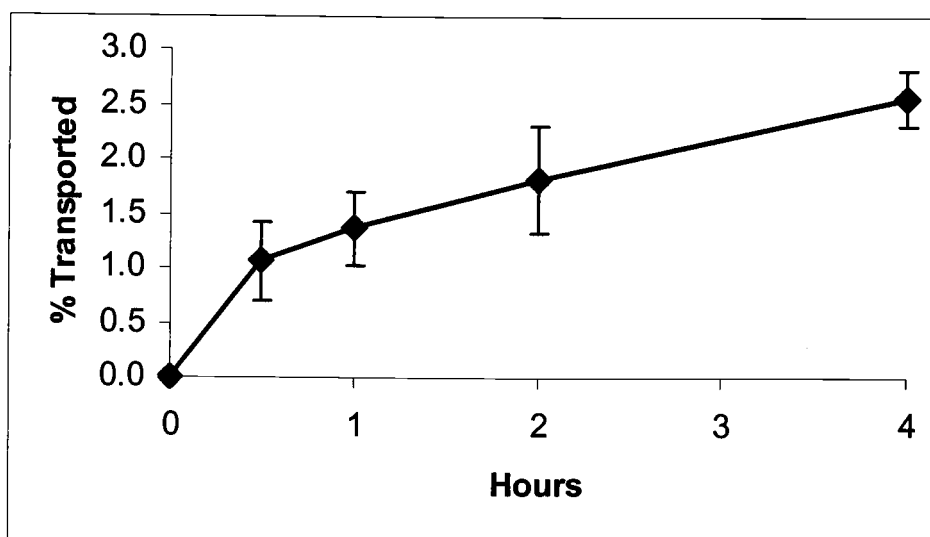


Figure 4.4 Percent transported of ^3H -mannitol ($1\mu\text{M Ci/mL}$) in twenty-one days old Caco-2 cell monolayers ($n=3$). The mean of P_e is $1.11 \times 10^{-6} \text{ cm/sec}$ at day 21.

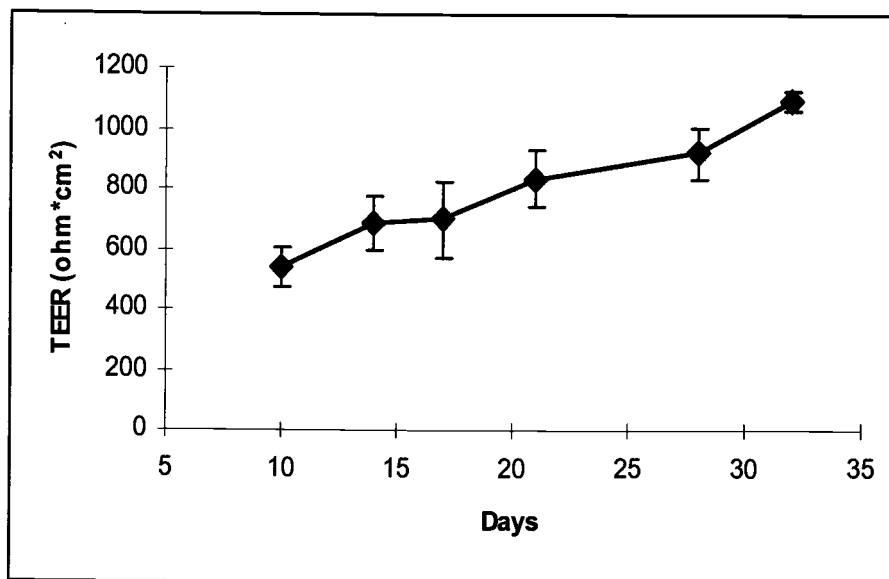


Figure 4.5 Transepithelial electrical resistance (TEER) readings of Caco-2 cell monolayers as a function of days in culture (post seeding) (n = 4 - 10).

tight junctions are adequately formed. TEER readings were performed on all inserts and only the inserts with TEER readings greater than $500 \text{ ohm} \cdot \text{cm}^2$ were used.

4.3 Transport of Rhodamine 123

Rhodamine 123 is a known P-gp substrate. Determination of the P_e for rhodamine 123 describes the function of P-gp in our Caco-2 cell monolayers. The results for the permeability of $2.5 \text{ } \mu\text{M}$ rhodamine 123 are shown in Figure 4.6. The mean P_e of rhodamine 123 from AB-to-BL, BL-to-AP, and BL-to-AP while co-treated with $100 \text{ } \mu\text{M}$ verapamil were $9.98 \times 10^{-7} \text{ cm/sec}$, $2.61 \times 10^{-6} \text{ cm/sec}$, and $6.34 \times 10^{-7} \text{ cm/sec}$, respectively. The sample sizes ranged from 4 to 7 inserts. The P_e of rhodamine 123 from the BL-to-AP direction was significantly greater than that of the AP-to-BL direction based on the unpaired Welch t-test. After co-treatment with $100 \text{ } \mu\text{M}$ verapamil, the P_e of rhodamine 123 from the BL-to-AP direction was greatly reduced. These results support that the efflux of rhodamine 123 was mediated by P-gp thereby verifying the function of P-gp in our Caco-2 cell transport model.

4.4 Transport of Cimetidine

The transport of cimetidine was characterized in our established Caco-2 cell transport model. Under physiological pH conditions (pH 7.4), about 80% of cimetidine is present in the ionized form. This may cause cimetidine to use the

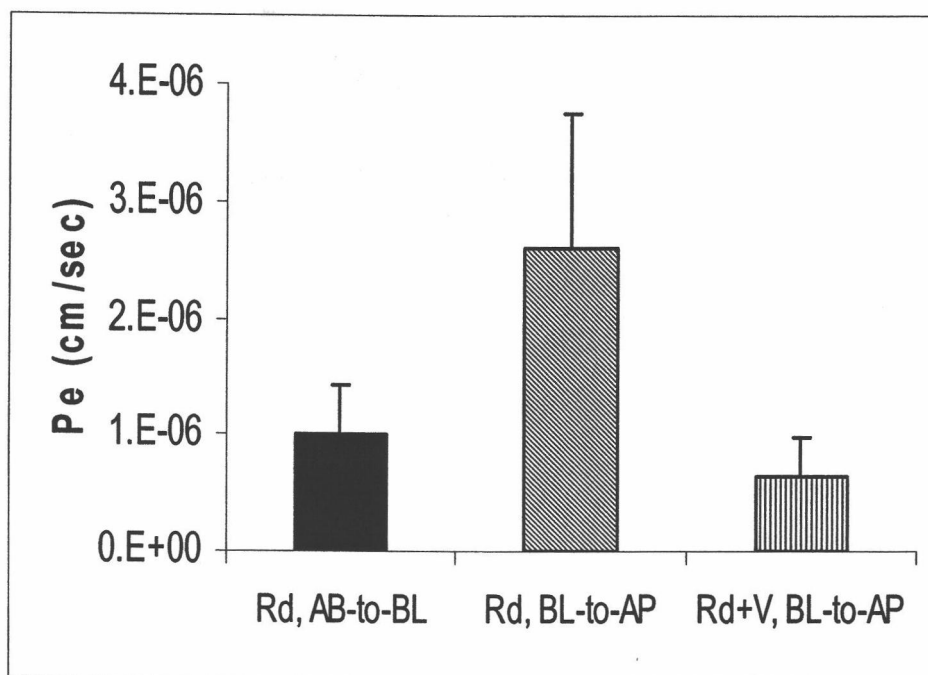


Figure 4.6 Effective permeability coefficient of 2.5 μ M rhodamine 123 from AB-to-BL and BL-to-AP directions in Caco-2 cell monolayers ($n = 4 - 7$). Rd: 2.5 μ M rhodamine 123; V: 100 μ M verapamil.

paracellular pathway instead of the transcellular pathway to pass through absorptive cells. To make sure that the transport of cimetidine did depend on ionization, the transport of cimetidine was evaluated under different pHs (pH 5.5, pH 6.5, and pH 7.4). The AP-to-BL P_e of cimetidine at the various pHs are shown in Figure 4.7. The mean P_e of cimetidine at pH 5.5, pH 6.5, and pH 7.4 were 2.19×10^{-6} cm/sec, 1.77×10^{-6} cm/sec, and 1.96×10^{-6} cm/sec, respectively. The sample size ranged from 2 to 11 inserts. Using Tukey pairwise multiple comparison test, there is no significant difference among these pH conditions. Therefore, one can assume that the ionization state of cimetidine does not play a significant role in the transport of cimetidine through the Caco-2 cell monolayers.

In the majority of the transport experiments, the permeability of cimetidine was measured with co-treatment with other compounds such as verapamil, and flavonoids. Verapamil, quercetin, genistein, and naringenin were dissolved in ethanol. Rutin, quercitrin, and genistin were dissolved in DMSO. Experiments using the transport vehicles alone (ethanol and DMSO) were conducted to establish that they do not significantly impact the transport of cimetidine. The permeability of cimetidine from the BL-to-AP direction with or without the co-treatment of ethanol or DMSO is shown in Figure 4.8. The final concentration of ethanol used was 0.5% (v/v) and 0.2% (v/v) for DMSO. These were the highest vehicle concentrations used during the 4 hr transport studies. The mean P_e for cimetidine, cimetidine with ethanol, and cimetidine with DMSO were 2.02×10^{-6} cm/sec, 1.95

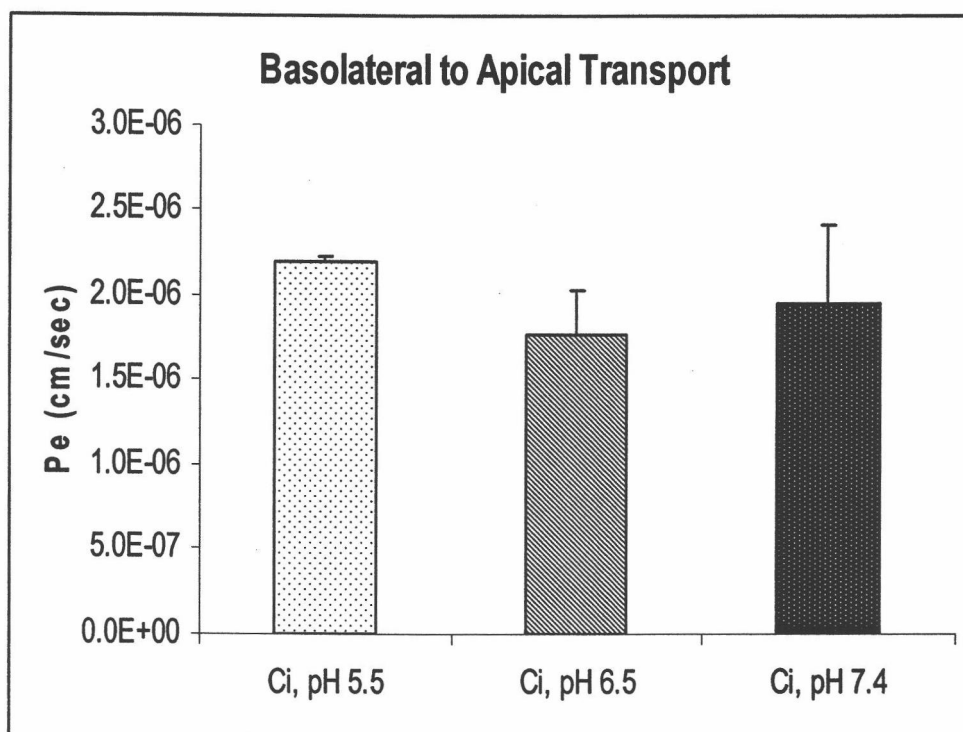


Figure 4.7 Basolateral (BL) to apical (AP) effective permeability coefficient (P_e) of 20 μ M cimetidine under different pH environments in Caco-2 cell monolayers ($n = 2 - 11$). Ci: cimetidine.

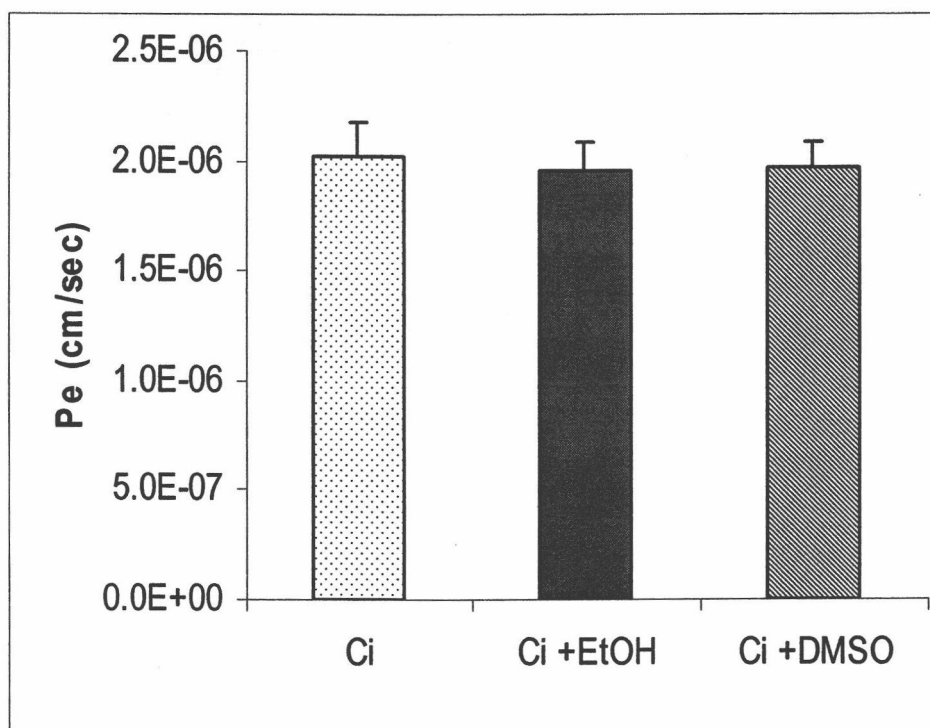


Figure 4.8 Basolateral-to-apical permeability coefficient of 20 μ M cimetidine (Ci) with or without co-treatment of 0.5% (v/v) ethanol (EtOH) or 0.2% (v/v) dimethyl sulfoxide (DMSO) in Caco-2 cell monolayers ($n = 4 - 6$).

$\times 10^{-6}$ cm/sec, and 1.97×10^{-6} cm/sec, respectively. Using the one-way ANOVA followed by Dunnett's multiple comparison test, neither ethanol nor DMSO caused a significant difference in the permeability of cimetidine. Thus, the vehicles used during the co-treatment experiments will not have a significant effect on the permeability of cimetidine.

The transports of cimetidine from different transport directions were investigated. The mean P_e of 20 μ M cimetidine from AP-to-BL and BL-to-AP directions were 0.67×10^{-6} cm/sec and 2.02×10^{-6} cm/sec, respectively (Figure 4.9). The P_e of cimetidine in BL-to-AP direction was almost twice more than that in AP-to-BL direction (p -value < 0.01). This indicates that there was an efflux mechanism(s) involved in the transport of cimetidine.

Once the efflux phenomenon in the transport of cimetidine was determined, efforts were now made to identify the efflux transporter involved. P-gp was initially considered because there are many substrates for P-gp and P-gp has been demonstrated to be functionally active in Caco-2 cells. The permeability of 20 μ M cimetidine while co-treated with 100 μ M verapamil was investigated because verapamil has been well established to be competitive inhibitor of P-gp. The mean P_e of 20 μ M cimetidine co-treated with 100 μ M verapamil from the AP-to-BL and BL-to-AP directions were 0.71×10^{-6} cm/sec and 1.53×10^{-6} cm/sec, respectively (Figure 4.10). The P_e of 20 μ M cimetidine alone in both directions were 0.67×10^{-6} cm/sec and 2.02×10^{-6} cm/sec, respectively. When co-treated with 100 μ M

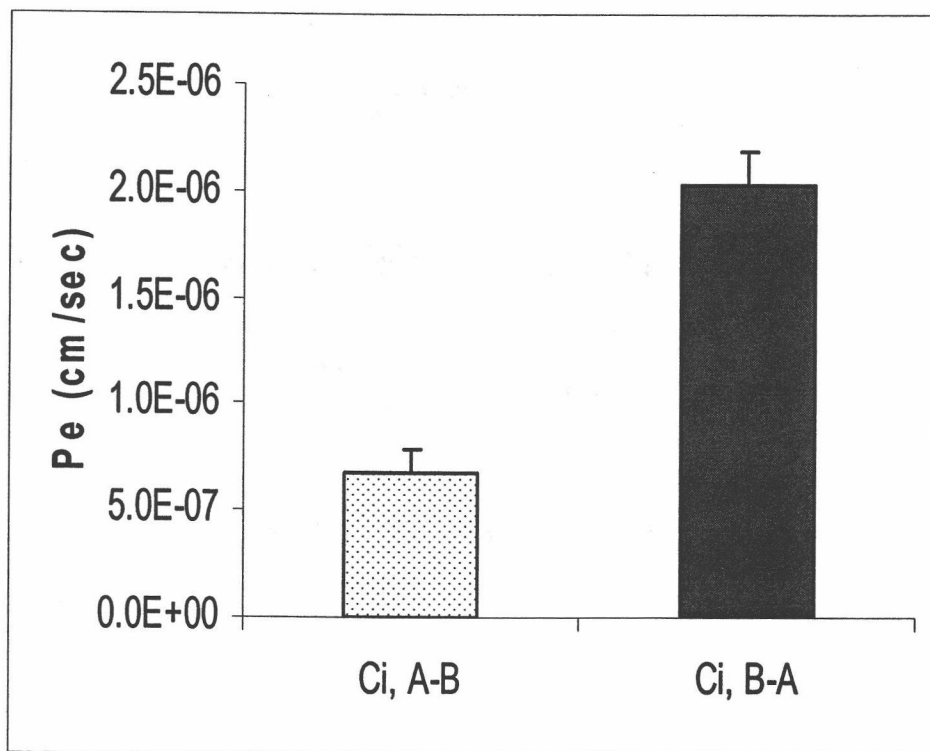


Figure 4.9 Permeability coefficient of 20 μ M cimetidine (Ci) in different transport directions from the Caco-2 cell monolayers ($n = 6$). A-B: apical to basolateral direction; and, B-A: basolateral to apical direction.

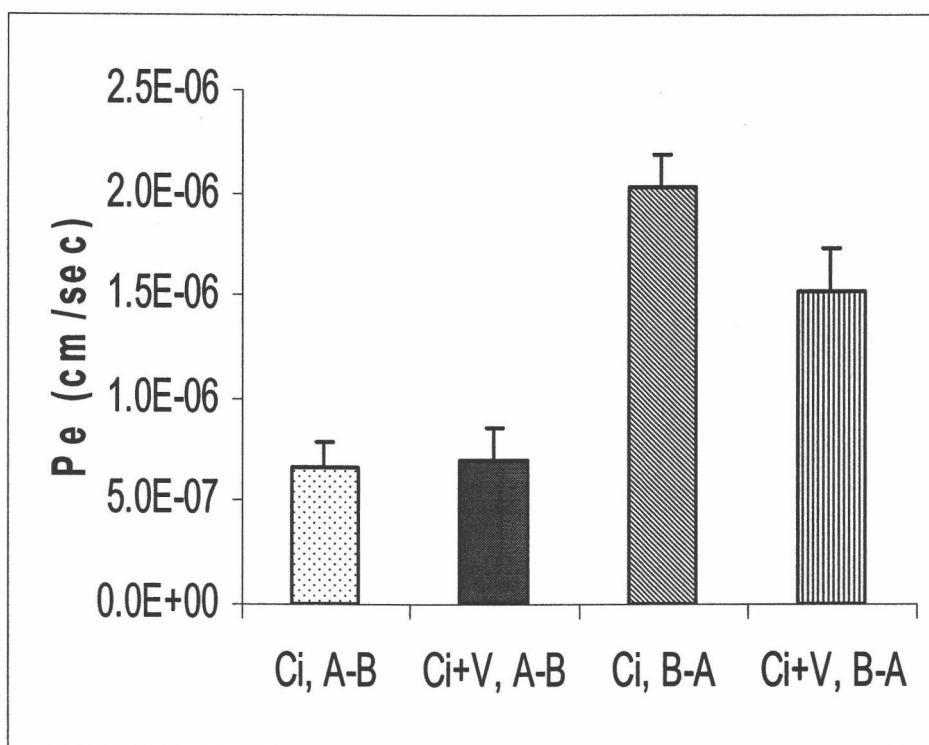


Figure 4.10 Permeability coefficient of 20 μ M cimetidine (Ci) with or without co-treatment of 100 μ M verapamil (V) in Caco-2 cell monolayers ($n = 4 - 8$). A-B: apical to basolateral direction; and, B-A: basolateral to apical direction.

verapamil, there was a statistically significant decrease in P_e of cimetidine from the BL-to-AP direction (p -value < 0.05) compared to cimetidine alone. These findings support that P-gp is involved in the efflux of cimetidine in the Caco-2 cells.

An analysis of the enzymatic kinetics was conducted after it was proven that P-gp was involved in the efflux of cimetidine. Because a previous study suggested that P-gp can fit into Michaelis-Menten enzymatic kinetics [215], Michaelis-Menten constant (K_m) of P-gp with cimetidine was determined. To obtain the K_m , the permeability of cimetidine from the BL-to-AP direction at various concentrations (2 μ M, 10 μ M, 50 μ M, 100 μ M, 200 μ M, 500 μ M, 800 μ M, 1000 μ M, 1200 μ M, 1500 μ M, 2000 μ M, and 2500 μ M,) was measured. Figure 4.11 depicts the BL-to-AP P_e of cimetidine decrease with increasing concentrations of cimetidine. This P_e of cimetidine represents the combination of P-gp efflux, passive diffusion, and other possible efflux. In order to obtain the permeability associated only with P-gp, the BL-to-AP P_e of cimetidine co-treated with 100 μ M verapamil (Figure 4.11) were determined. This resulting permeability coefficient represents the combination of passive diffusion and other efflux other than through P-gp. By subtracting this permeability coefficient, the permeability of P-gp efflux can be obtained.

Because the permeability coefficient cannot be directly applied into the Michaelis-Menten equation, the aforementioned permeability coefficients, P_e , were transformed into efflux rates as shown in Figure 4.12. The efflux rate of P-gp was

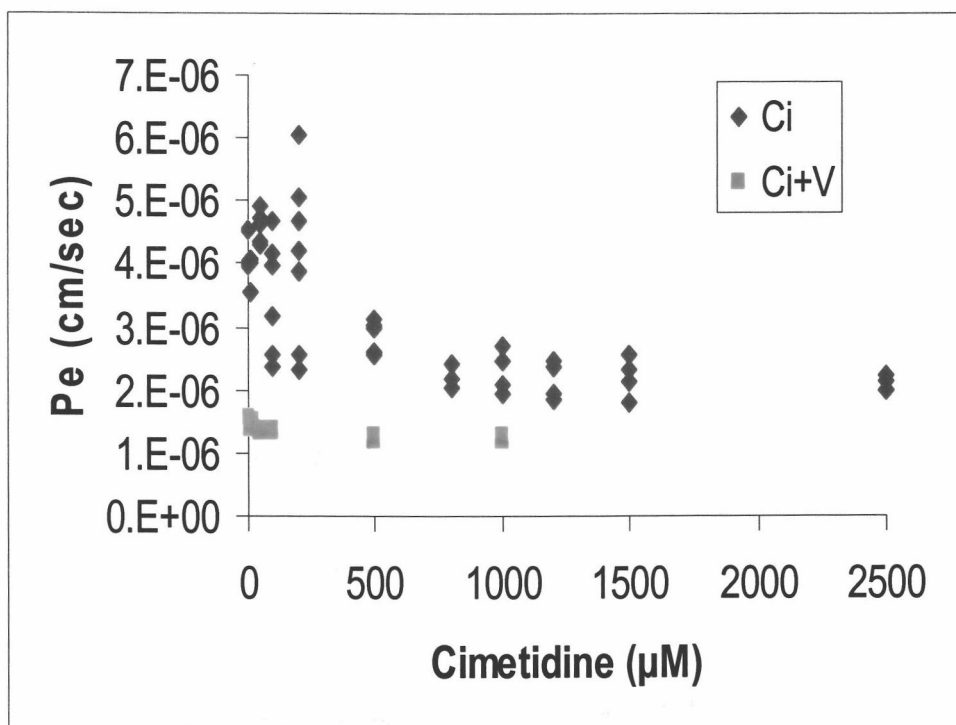


Figure 4.11 Scatter plot of BL-to-AP permeability coefficient versus the concentration of cimetidine (Ci) with or without the co-exposure of 100 μM verapamil (V). Each point represents the average Pe for a given insert.

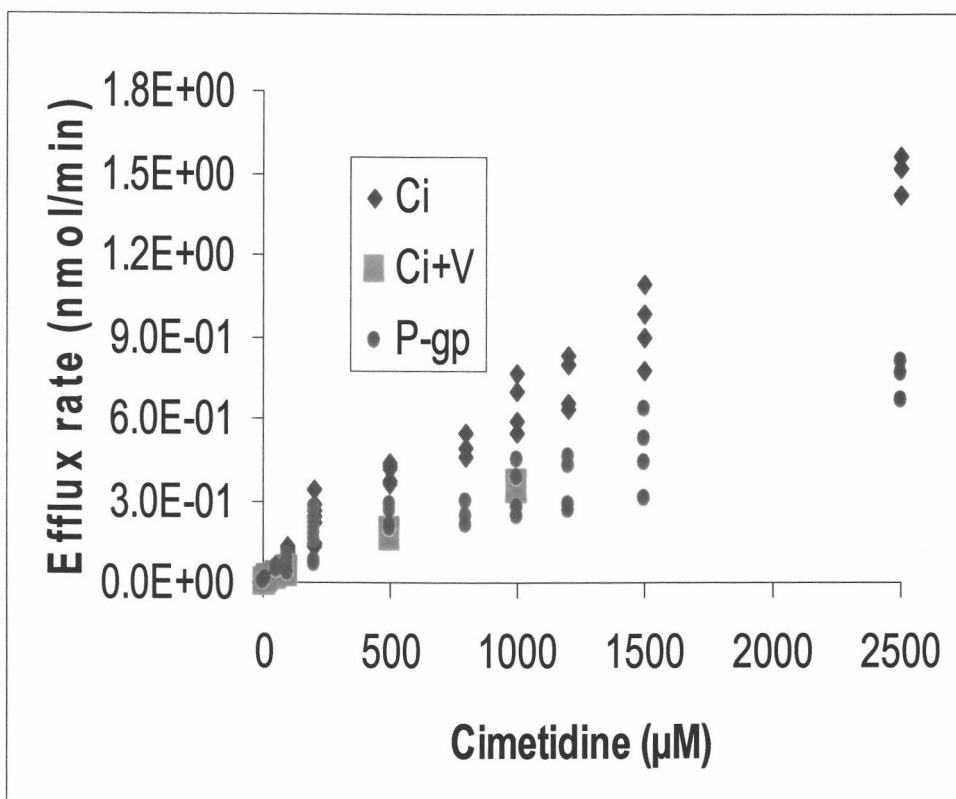


Figure 4.12 Scatter plot of efflux rate versus the concentration of cimetidine (Ci) with or without the co-treatment of 100 μM verapamil (V). Each dot represents the average P_e for a given insert. P-gp: P-gp efflux rate.

determined. The standard Michaelis-Menten equation, Eq 3.5, was applied to the data and the resulting K_m was estimated to be 5,600 μM (Figure 4.13). This suggests that cimetidine is not a good substrate for P-gp because it has a low affinity for the transport protein.

In addition to the P-gp efflux, other possible mechanisms which could be involved in the efflux of cimetidine were investigated. Because the concentration of certain ions such as Cl^- and Na^+ may regulate the transport of cimetidine, the permeability of cimetidine while co-treated with specific inhibitors of the aforementioned ion transporters was performed. Bumetanide is an inhibitor of the $\text{Na}^+ - \text{K}^+ - 2\text{Cl}^-$ transporter and DIDS is an inhibitor of the $\text{Cl}^-/\text{HCO}_3^-$ transporter. The BL-to-AP P_e of 20 μM cimetidine with or without co-treatment with 100 μM bumetanide or 100 μM diisothiocyanatostilbene-disulfonic acid (DIDS) are shown in Figure 4.14. The mean P_e of cimetidine from BL-to-AP and BL-to-AP while co-treated with bumetanide or DIDS were 2.02×10^{-6} cm/sec, 1.84×10^{-6} cm/sec, and 1.70×10^{-6} cm/sec, respectively. One-way ANOVA followed by Dunnett's test revealed that both co-treatments significantly reduce the BL-to-AP P_e of cimetidine. These results suggest that Cl^- ion transporters may be involved in the transport of cimetidine.

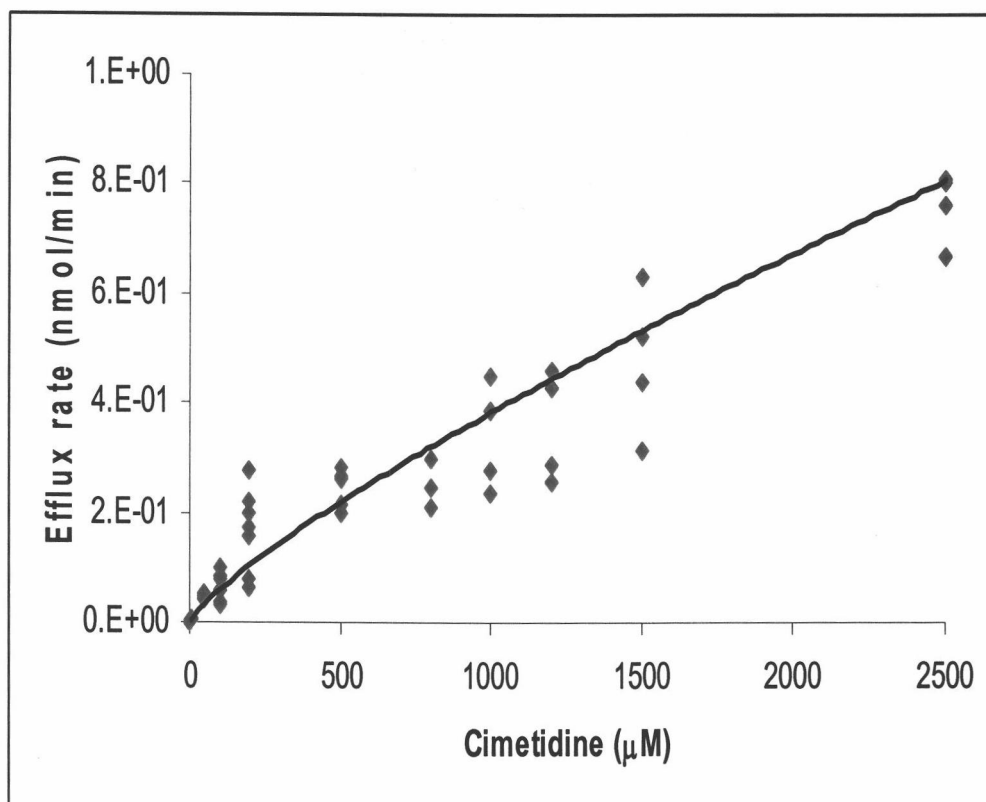


Figure 4.13 Scatter plot of P-gp efflux rate versus the concentration of cimetidine (Ci). The standard Michaelis-Menten equation was applied to the data to estimate K_m .

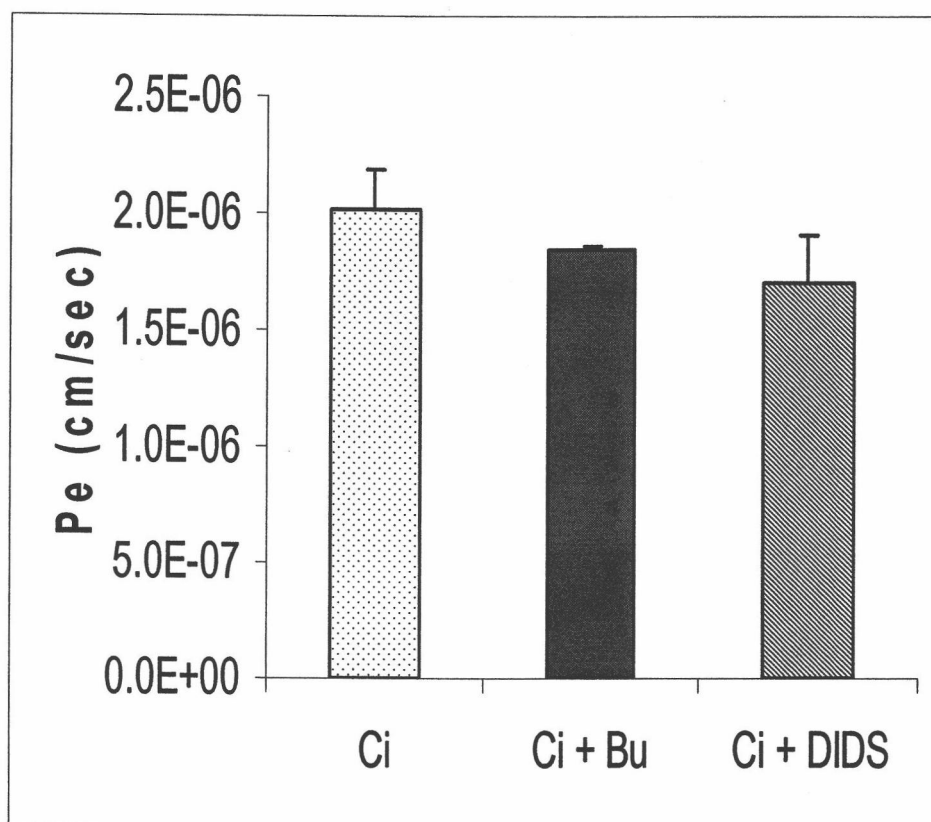


Figure 4.14 Basolateral-to-apical permeability coefficient of 20 μ M cimetidine (Ci) with or without co-treatment of 100 μ M bumetanide (Bu) or 100 μ M diisothiocyanatostilbene-disulfonic acid (DIDS) in Caco-2 cells ($n = 4 - 6$).

4.5 Effect of Flavonoids on the Transport of Cimetidine

The effect of flavonoids such as quercetin, genistein, naringenin, and xanthohumol, on the transport of cimetidine in Caco-2 cells was determined after the transport of cimetidine was characterized. The flavonoids studied were grouped into aglycones and glycosides based on their glycosylation. We proposed that the glycosylation of flavonoids might alter the transport of cimetidine.

To begin, the effects of flavonoid aglycones, quercetin, genistein, naringenin, and xanthohumol, on the permeability of cimetidine in the AP-to-BL direction were investigated. The AP-to-BL P_e of 20 μM cimetidine with or without co-treatment with 100 μM quercetin, genistein, naringenin, and xanthohumol is shown in Figure 4.15. The mean P_e of cimetidine from the AP-to-BL and AP-to-BL while co-treated with 100 μM quercetin, genistein, naringenin, or xanthohumol were 6.71×10^{-7} cm/sec, 6.96×10^{-7} cm/sec, 8.07×10^{-7} cm/sec, 7.85×10^{-7} cm/sec, and 8.03×10^{-7} cm/sec, respectively. One-way ANOVA followed by Dunnett's test revealed that none of these co-treatments were statistically different compared to the control, cimetidine alone.

Secondly, the effects of the flavonoid glycosides (rutin, quercitrin, genistin, and naringin) on the permeability of cimetidine in the AP-to-BL direction were evaluated. Quercitrin and rutin are the glycosides of quercetin, and genistin and naringin are the glycosides of genistein and naringenin, respectively. The AP-to-BL

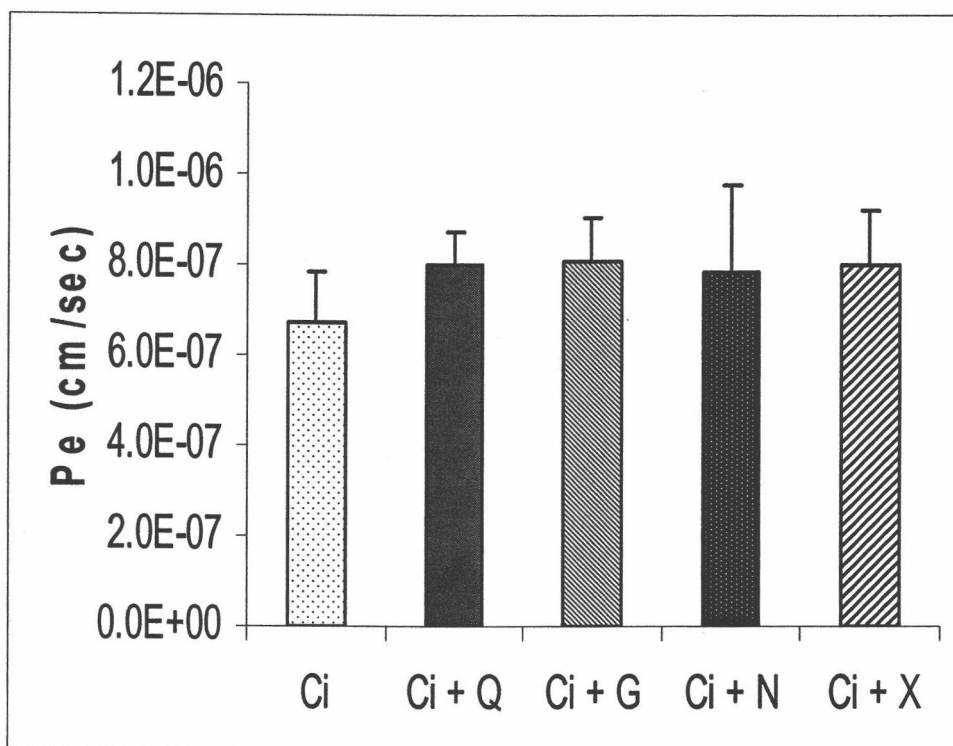


Figure 4.15 Apical-to-basolateral permeability coefficient of 20 μ M cimetidine (Ci) with or without co-treatment of 100 μ M flavonoid aglycones in Caco-2 cell monolayers ($n = 4 - 6$). Q: quercetin; G: genistein; N: naringenin; and, X: xanthohumol.

P_e of 20 μM cimetidine with or without co-treatment with 100 μM flavonoid glycosides is shown in Figure 4.16. The mean P_e of cimetidine from the AP-to-BL, and AP-to-BL while co-treated with 100 μM quercitrin, rutin, genistin, or naringin were 6.71×10^{-7} cm/sec, 8.06×10^{-7} cm/sec, 7.58×10^{-7} cm/sec, 8.24×10^{-7} cm/sec, and 8.03×10^{-7} cm/sec, respectively. No glycoside of xanthohumol has been identified to date. One-way ANOVA followed by Dunnett's test revealed that none of these co-treatments were statistically different compared to the control, cimetidine alone.

After investigating the effects of flavonoids on cimetidine transport in the AP-to-BL direction, experiments were performed to evaluate the effects of aglycones and glycosided flavonoids on cimetidine transport from the BL-to-AP direction in the Caco-2 cells. The BL-to-AP P_e of 20 μM cimetidine with or without co-treatment with 100 μM quercetin, genistein, naringenin, or xanthohumol is shown in Figure 4.17. The mean P_e of cimetidine from the BL-to-AP and BL-to-AP directions while co-treated with 100 μM quercetin, genistein, naringenin, or xanthohumol were 2.02×10^{-6} cm/sec, 1.24×10^{-6} cm/sec, 1.23×10^{-6} cm/sec, 1.06×10^{-6} cm/sec, and 9.55×10^{-7} cm/sec, respectively. One-way ANOVA followed by Dunnett's test showed that all these four co-treatments are statistically different compared to cimetidine alone. This demonstrates that co-treatment of these flavonoid aglycones can significantly reduce the permeability of cimetidine in the BL-to-AP direction.

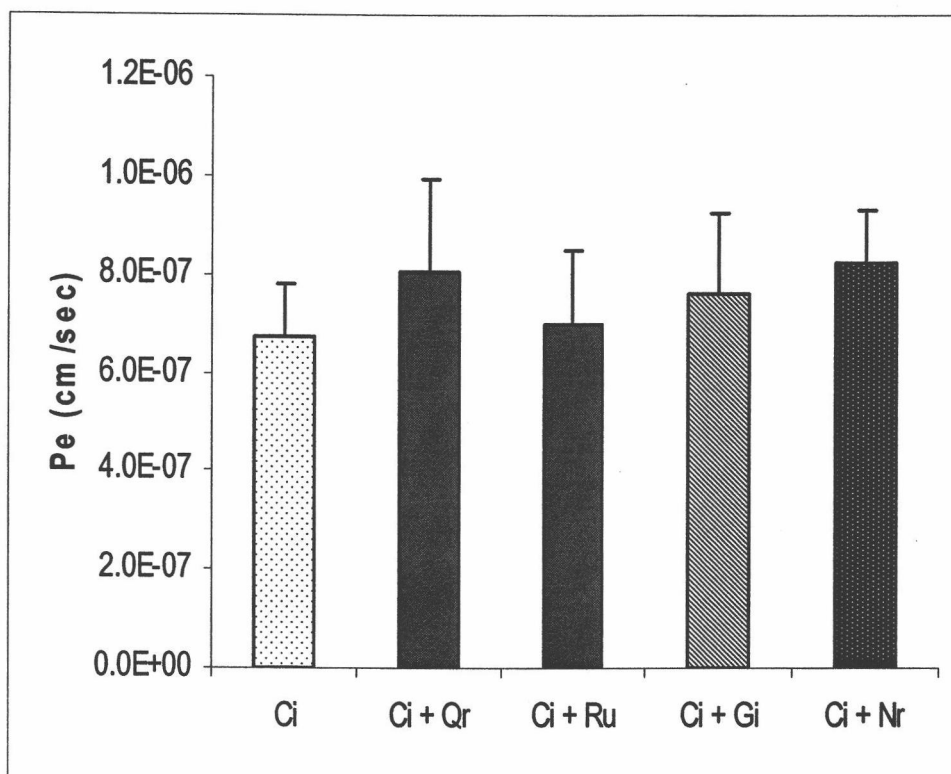


Figure 4.16 Apical-to-basolateral permeability coefficient of 20 μ M cimetidine (Ci) with or without co-treatment of 100 μ M flavonoid glycosides in Caco-2 cell monolayers ($n = 4 - 6$). Qr: quercitrin; Ru: rutin; Gi: genistin; and, Nr: naringin.

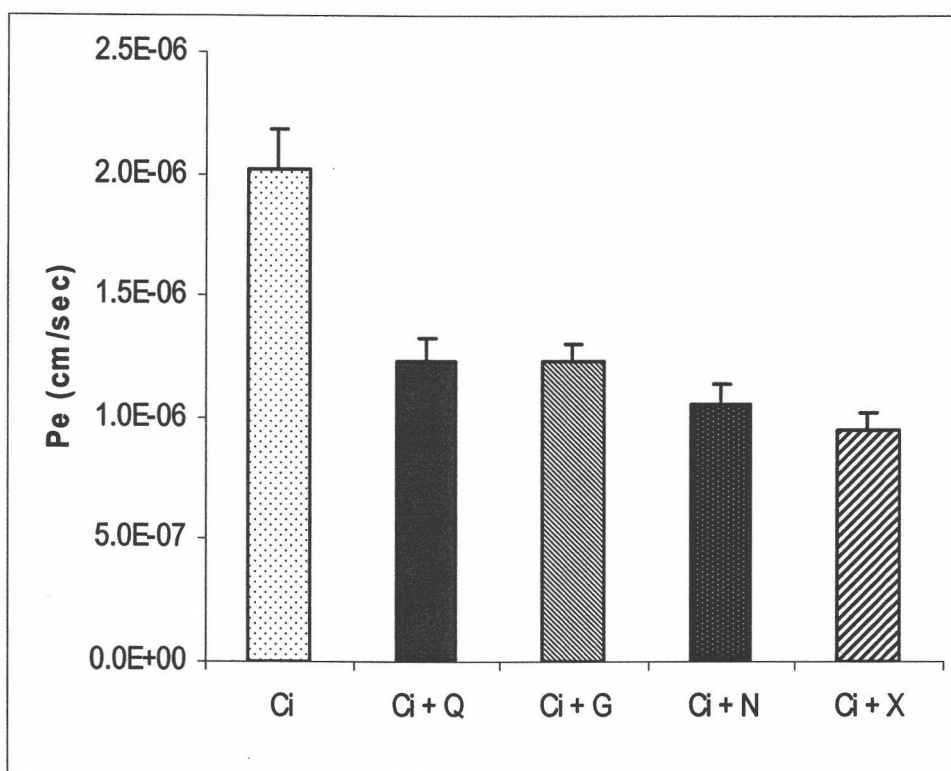


Figure 4.17 Basolateral-to-apical permeability coefficient of 20 μ M cimetidine (Ci) with or without co-treatment of 100 μ M flavonoid aglycones in Caco-2 cells ($n = 4 - 8$). Q: quercetin; G: genistein; N: naringenin; and, X: xanthohumol.

For the flavonoid glycosides, the BL-to-AP P_e of 20 μM cimetidine with or without co-treatment of 100 μM quercitrin, rutin, genistin, and naringin is shown in Figure 4.18. The mean P_e of cimetidine from the BL-to-AP and BL-to-AP directions while co-treated with 100 μM quercitrin, rutin, genistin, or naringin were 2.02×10^{-6} cm/sec, 1.78×10^{-6} cm/sec, 2.00×10^{-6} cm/sec, 1.24×10^{-6} cm/sec, and 1.79×10^{-6} cm/sec, respectively. Interestingly, unlike the results with the flavonoid aglycones, only genistin showed a significant difference. This suggests that the glycosylation of flavonoids attenuates their inhibition of the efflux of cimetidine. Thus, the inhibition potency of these effective flavonoids on the transport of cimetidine was evaluated.

To evaluate the inhibition potency of the effective flavonoids on the efflux of cimetidine, the inhibitory concentration 50% (IC_{50}) was the parameter which was determined. IC_{50} is defined as the concentration of flavonoid that reaches 50 % inhibition of the transport of cimetidine in the BL-to-AP direction. In order to obtain the IC_{50} of a given flavonoid, the BL-to-AP P_e of 20 μM cimetidine was evaluated under various concentrations (0.1 μM to 100 μM) of flavonoid. A four-parameter sigmoid model was applied to obtain the IC_{50} . A flavonoid with low IC_{50} is a more potent inhibitor than one with high IC_{50} in the inhibition of cimetidine efflux.

Figure 4.19 represents the scatter plot of BL-to-AP P_e of 20 μM cimetidine versus 0.01 μM , 0.02 μM , 0.05 μM , 0.1 μM , 0.5 μM , 1 μM , 3 μM , 5 μM , 10 μM ,

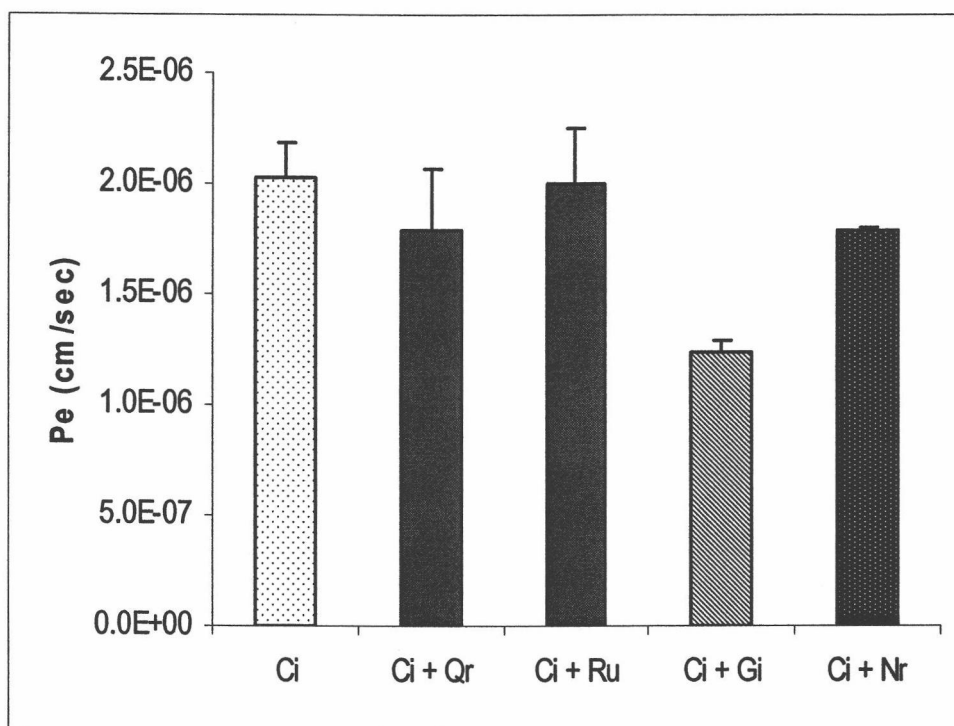


Figure 4.18 Basolateral-to-apical permeability coefficient of 20 μ M cimetidine (Ci) with or without co-treatment of 100 μ M flavonoid glycosides in Caco-2 cell monolayers ($n = 4 - 6$). Qr: quercitrin; Ru: rutin; Gi: genistin; and, Nr: naringin.

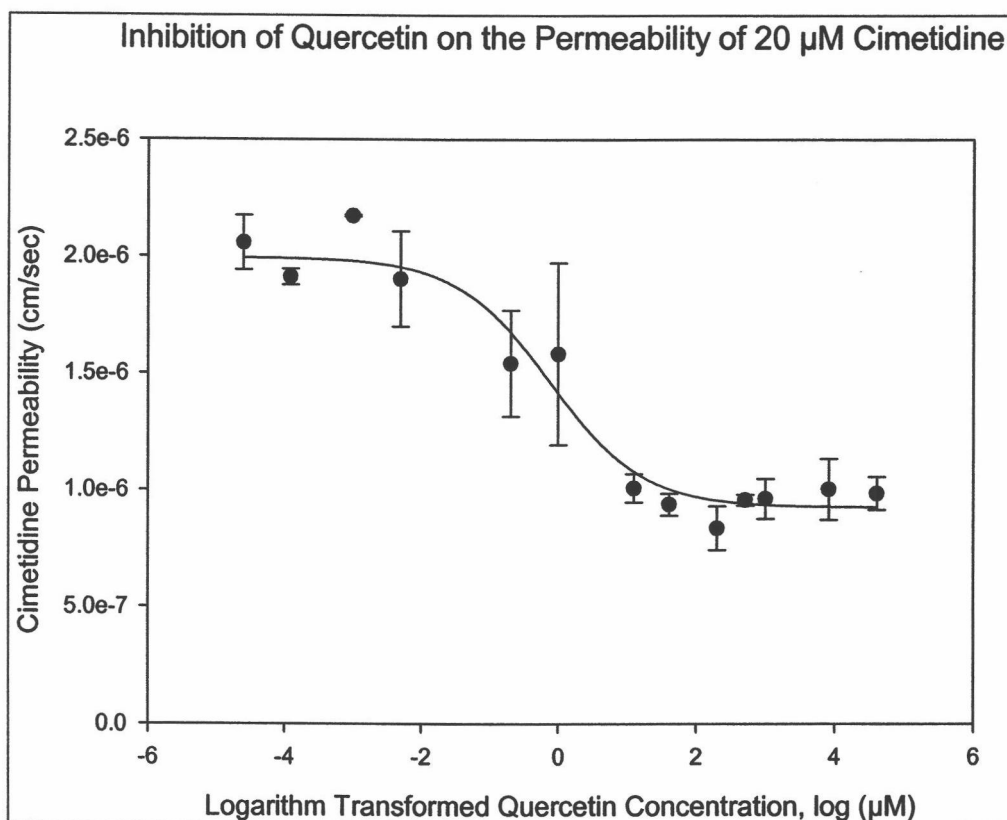


Figure 4.19 Basolateral-to-apical permeability of 20 μ M cimetidine versus various concentrations of quercetin (n = 2 - 8).

15 μM , 20 μM , 50 μM , and 100 μM quercetin. Each concentration was replicated 2 to 8 times. The IC_{50} of quercetin was estimated to be 0.89 μM with the 95% confidence interval between 0.58 μM and 1.37 μM .

Figure 4.20 represents the scatter plot of BL-to-AP P_e of 20 μM cimetidine versus 0.1 μM , 0.5 μM , 1 μM , 5 μM , 10 μM , 15 μM , 20 μM , 50 μM , and 100 μM naringenin. Each concentration was replicated 2 to 8 times. The IC_{50} of naringenin was estimated to be 0.65 μM with 95% confidence interval between 0.51 μM and 0.84 μM .

Figure 4.21 represents the scatter plot of BL-to-AP P_e of 20 μM cimetidine versus 0.1 μM , 0.2 μM , 0.5 μM , 0.8 μM , 1 μM , 5 μM , 10 μM , 20 μM , and 50 μM xanthohumol. Each concentration was performed in one to eight inserts. One data point for 50 μM treatment was discarded due to being an outlier. So the sample size for 50 μM was one. The IC_{50} of xanthohumol was estimated to be 0.36 μM with 95% confidence interval between 0.07 μM and 1.74 μM .

Figure 4.22 represents the scatter plot of BL-to-AP P_e of 20 μM cimetidine versus 0.05 μM , 0.5 μM , 0.8 μM , 1 μM , and 10 μM genistein. Each concentration was replicated six times. The IC_{50} of genistein was estimated to be 0.41 μM with 95% confidence interval between 0.23 μM and 0.72 μM . In figure 4.23, the scatter plot of BL-to-AP P_e of 20 μM cimetidine versus 0.1 μM , 0.5 μM , 1 μM , 3 μM , 5 μM , 10 μM , 20 μM , and 50 μM genistin. Genistin was the only flavonoid glycoside

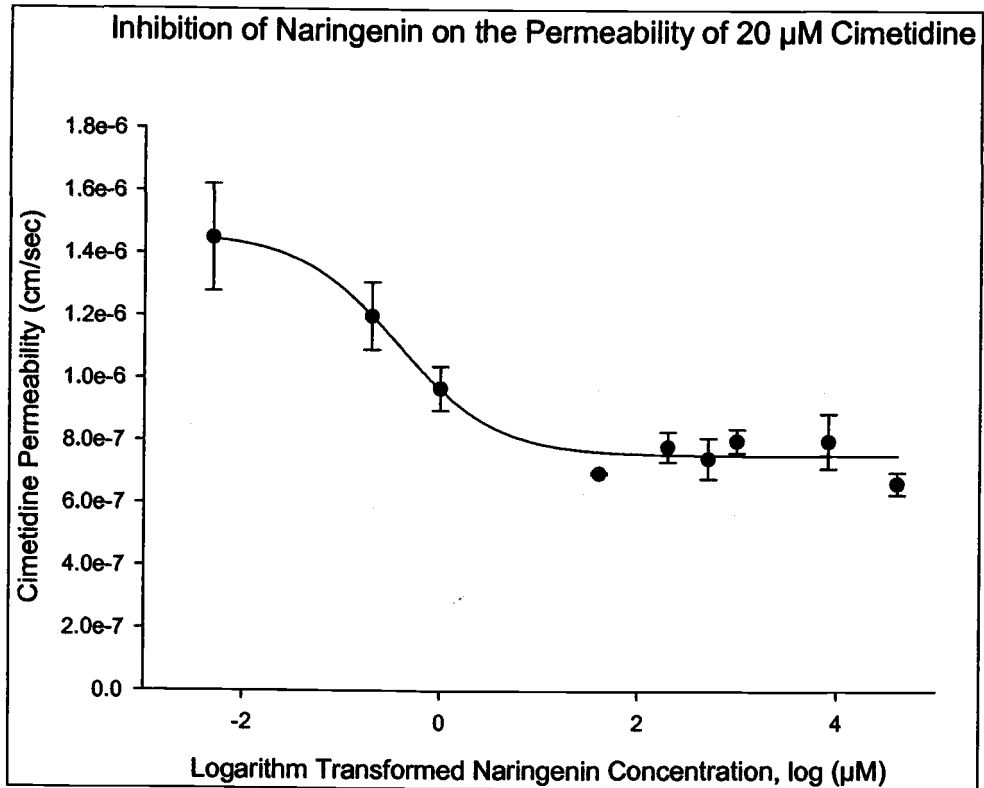


Figure 4.20 Basolateral-to-apical permeability of 20 μ M cimetidine versus various concentrations of naringenin (n = 2 - 8).

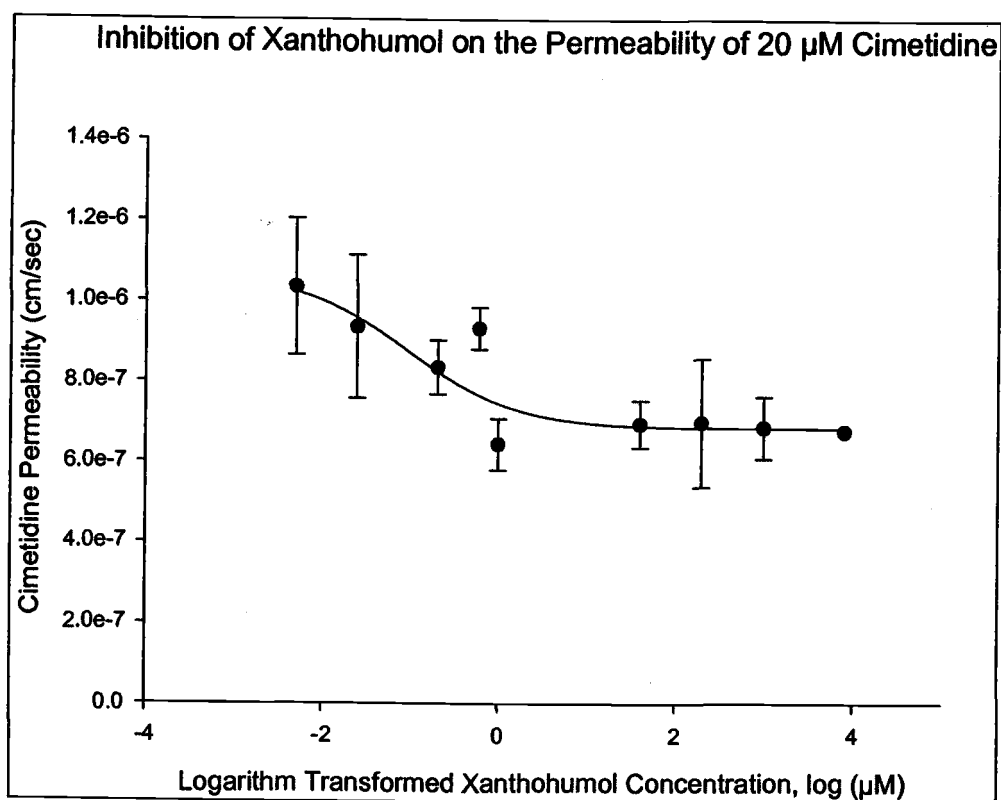


Figure 4.21 Basolateral-to-apical permeability of 20 μ M cimetidine versus various concentrations of xanthohumol ($n = 1 - 8$).

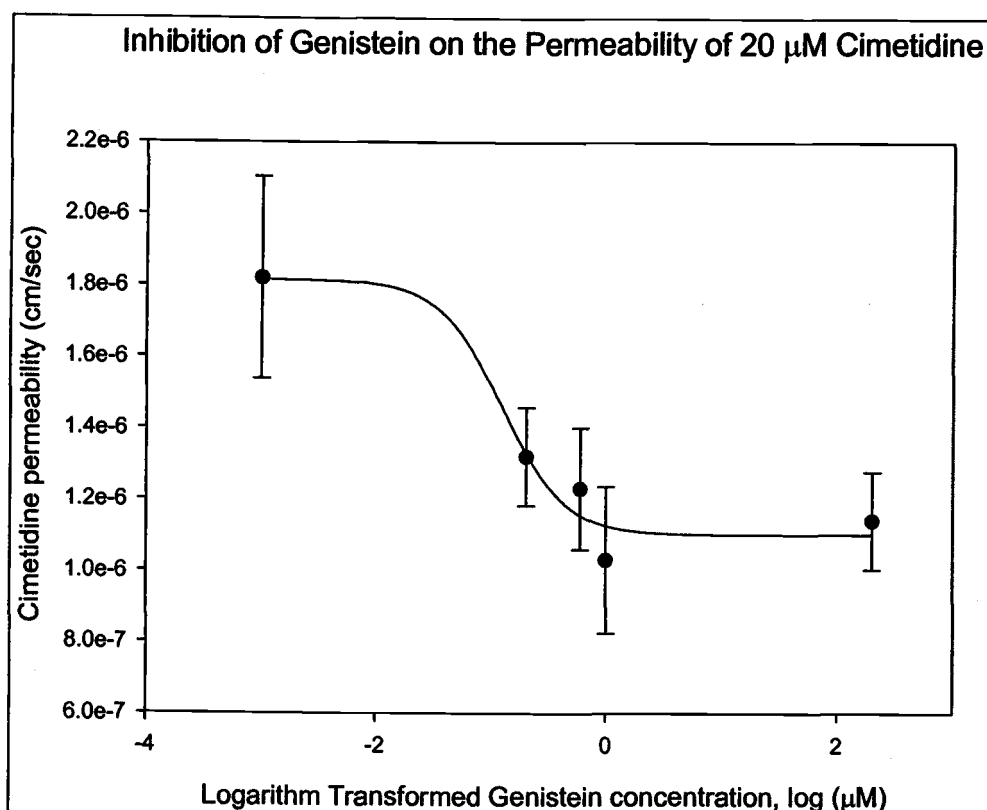


Figure 4.22 Basolateral-to-apical permeability of 20 μ M cimetidine versus various concentrations of genistein ($n = 6$).

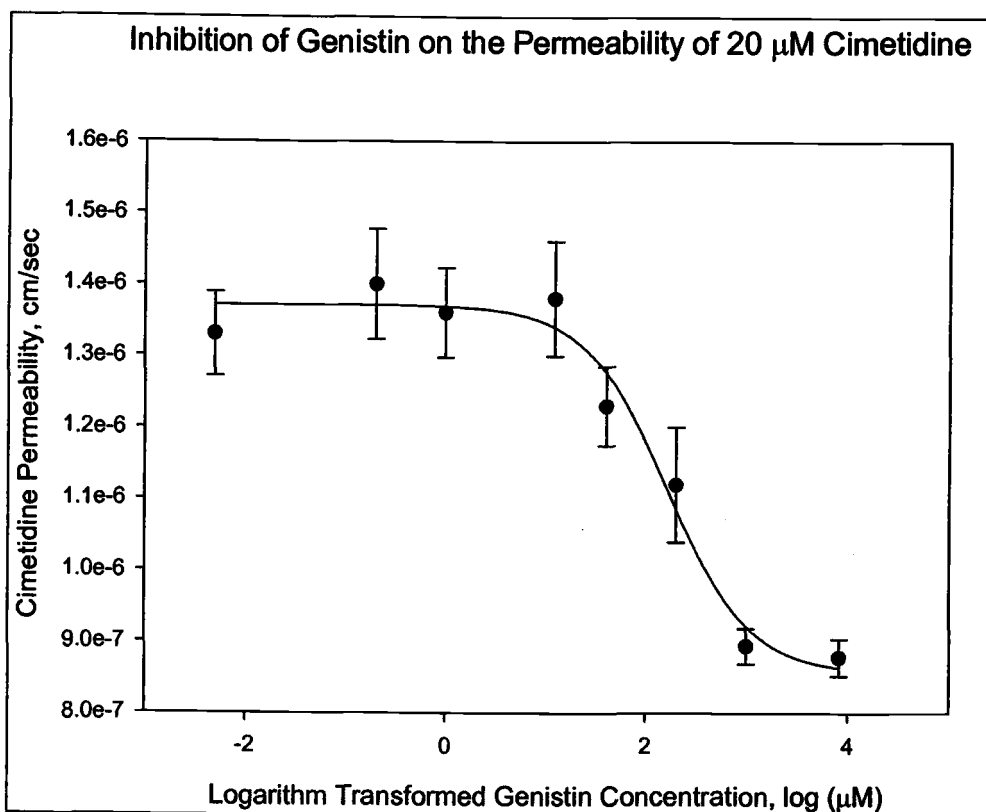


Figure 4.23 Basolateral-to-apical permeability of 20 μ M cimetidine versus various concentrations of genistin (n = 4).

to significantly inhibit the efflux of cimetidine. Each concentration was replicated four times. The IC_{50} of genistin was estimated to be $9.17\ \mu\text{M}$ with 95% confidence interval between $7.15\ \mu\text{M}$ and $11.76\ \mu\text{M}$.

Lastly, Table 4.1 summarizes the IC_{50} values of the effective flavonoids in the current studies and their respective 95% confidence interval. Aglycones, quercetin, naringenin, genistein, and xanthohumol had IC_{50} in high nanomolar range. This suggests that flavonoid aglycones are strong inhibitors of the efflux of cimetidine. On the other hand, only genistin, a flavonoid glycoside, showed significant inhibition in the efflux of cimetidine, with a IC_{50} twenty times greater compared to that of its aglycone, genistein. These results support that glycosylation of flavonoids can reduce their inhibition potency for efflux of cimetidine.

4.6 Effect of Quercetin on the Uptake of Cimetidine

The uptake of cimetidine in Caco-2 cell monolayers with or without the co-treatment of $100\ \mu\text{M}$ quercetin was investigated. The unit of uptake was picomole instead of picomole per mg protein because all the experiments were performed either on 23 or 24 day old cultures. There was no statistical difference in the protein mass from Caco-2 cell monolayers between 23 and 24 days. The time of uptake was 3 min to avoid possible saturation due an elongated incubation period.

In Figure 4.24, the uptake amount of cimetidine from either AP or BL side with or without the co-treatment of $100\ \mu\text{M}$ quercetin is shown. The experiment

Table 4.1 The inhibitory concentration 50% (IC₅₀) and 95% confidence interval (C.I.) of the effective flavonoids.

	IC ₅₀	95% C.I.
Quercetin	0.89 μM	0.58 – 1.37 μM
Naringenin	0.65 μM	0.51 – 0.84 μM
Xanthohumol	0.36 μM	0.07 – 1.74 μM
Genistein	0.41 μM	0.23 – 0.72 μM
Genistin	9.17 μM	7.15 – 11.76 μM

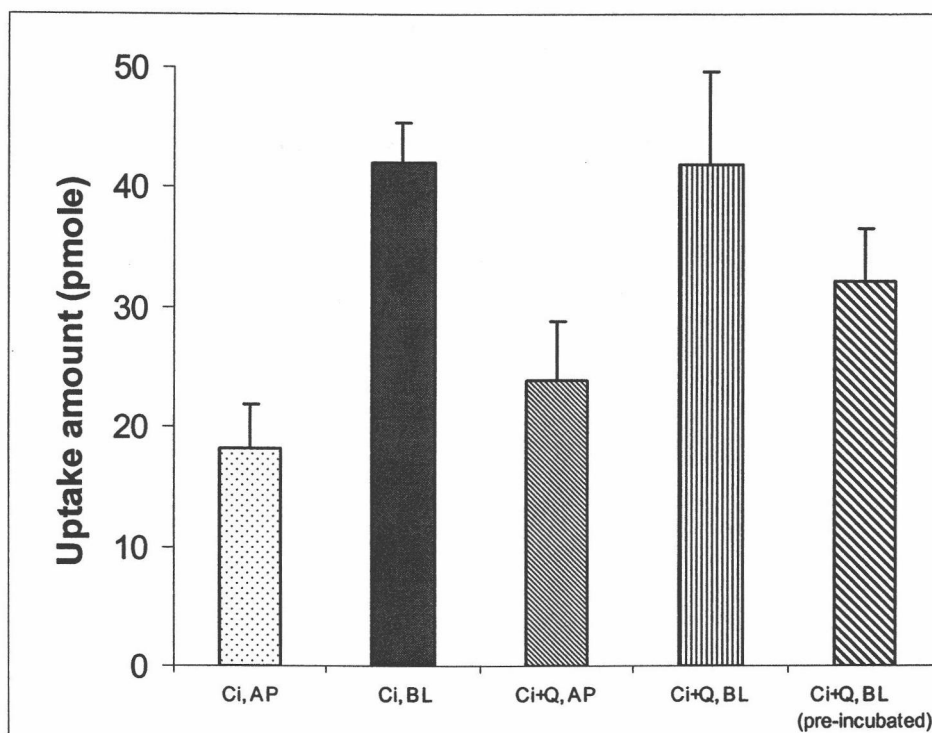


Figure 4.24 Uptake of 20 μM cimetidine (Ci) with or without co-treatment of 100 μM quercetin (Q) in Caco-2 cell monolayers ($n = 3 - 9$). AP: cimetidine was loaded from apical side; BL: cimetidine was loaded from apical side; Pre-incubated: quercetin was added 30 min before incubation.

was performed with 3 to 9 replicates. The mean uptake amounts of cimetidine from AP and BL sides were 18.28 pmole, 42.02 pmole, respectively. On the other hand, the mean uptake amounts of cimetidine from AP and BL sides with co-treatment of 100 μ M quercetin were 23.93 pmole, and 41.86 pmole, respectively. The mean cimetidine uptake from BL side was 32.12 pmole when quercetin was added 30 min before incubation. There was a significant difference in the uptake of cimetidine when cimetidine in the AP compartment compared to the BL compartment. Interestingly, the uptake amount of cimetidine was significantly lower than that of cimetidine alone when quercetin was added 30 min before the incubation.

The effect of pH was also evaluated during investigation of quercetin on the uptake of cimetidine in Caco-2 cells. Figure 4.25 represents the uptake amount of cimetidine from AP side under various pH environments (pH 5.5 and pH 7.4) with or without the co-treatment of 100 μ M quercetin. The mean uptake of cimetidine from AP side at pH 7.4 and pH 5.5 were 18.28 pmole and 14.85 pmole, respectively. On the other hand, the mean uptake of cimetidine from AP side at pH 7.4 and pH 5.5 with co-treatment of 100 μ M quercetin were 23.93 pmole and 21.19 pmole, respectively. The mean uptake of cimetidine at pH 5.5 was lower than that of pH 7.4 regardless if there was co-treatment of 100 μ M quercetin or not. Co-treatment of quercetin increased the uptake of cimetidine from AP side in both pH environments, however, only statistical difference was seen at pH 5.5.

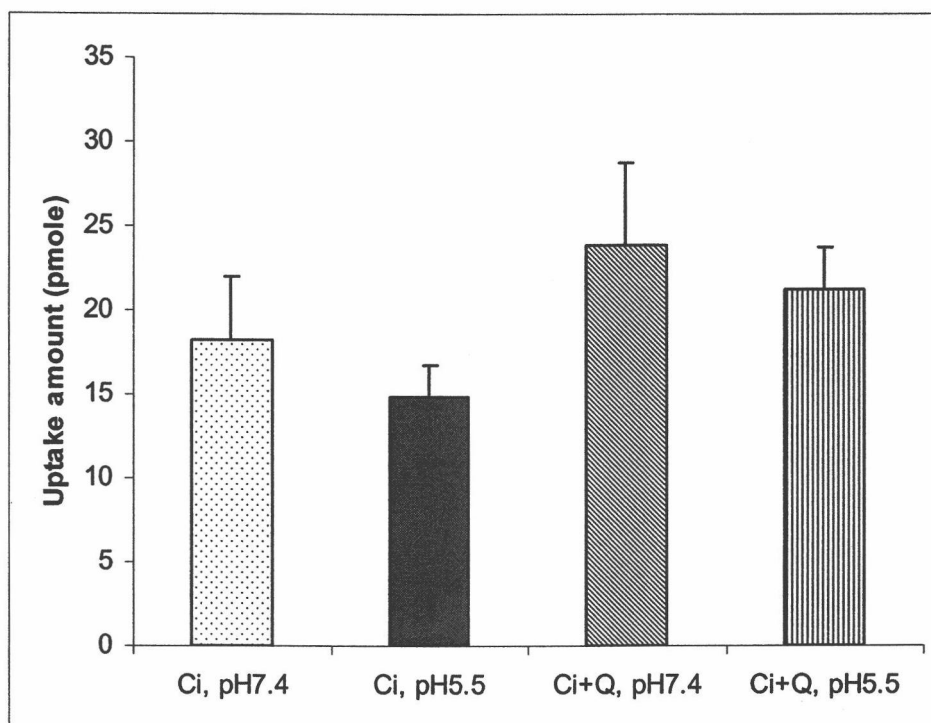


Figure 4.25 The uptake amount of 20 μM cimetidine (Ci) at pH 5.5 and pH 7.4 with or without co-treatment of 100 μM quercetin (Q) in Caco-2 cell monolayers ($n = 3 - 9$).

5. DISCUSSION

Flavonoids are polyphenolic compounds which exist abundantly in the human diet. It has been demonstrated they can cause various biological and pharmacological effects in both *in vivo* and *in vitro* systems. In these studies, the Caco-2 cells transportation model was used to investigate the effects of flavonoids on the transport of cimetidine. This model system was used to characterize the transport of cimetidine. These thesis results suggest that P-gp, an efflux pump, was involved in the absorption of cimetidine. Also, selected flavonoid such as quercetin, genistein, naringenin, xanthohumol, and genistin can significantly reduce the efflux of cimetidine. Therefore, some flavonoids may have the potential to enhance the bioavailability of cimetidine. These findings provide valuable knowledge about the interactions between flavonoids and efflux substrates.

We used the LDH assay to evaluate the cytotoxicity of the various treatment conditions such as cimetidine and flavonoids. LDH is a cytoplasmic enzyme which is released into culture supernatant upon damage of the cytoplasmic membrane. Within the 4 hr experiment period, concentrations of cimetidine up to 2.5 mM did not significantly damage the Caco-2 cell monolayers. As for the flavonoids, 500 μ M quercetin started to damage the cells at 2 hr incubation. This results agreed with a study by Canada *et al.* where 450 μ M quercetin caused significant LDH leakage following a 3-hr incubation using guinea pig enterocytes [216]. It produced

superoxide on autoxidation and damaged the cells [216]. Even though quercetin is probably the most abundant flavonoid in our diet, it is not likely to achieve 500 μM in intestinal lumen based on the average daily uptake of quercetin [49].

The cytotoxicity of flavonoid glycosides was not evaluated in the current LDH assay. Previous study suggested that flavonoid glycosides were less cytotoxic than their aglycones [217]. Moreover, the transport studies did not demonstrate a dramatic increase in permeability at the later time points which indicated the treatments were toxic to the Caco-2 cells.

Mannitol, a paracellular marker, was used to access the integrity of Caco-2 cell monolayers. The permeability of mannitol was gradually decreased as the culture day increases. After 21 culture days, the mean permeability of ^3H -mannitol was 1.11×10^{-6} cm/sec, which was less than 1 % per hr thereby meeting the primary criteria for the integrity of the cell monolayers being maintained. However, this permeability coefficient of mannitol was significantly higher than other published reports [218]. Possible reasons for this discrepancy include: the heterogeneity of Caco-2 cells; the difference between the Caco-2 cells passage numbers; the composition of the inserts; and, the differences in experimental conditions such as type of buffer, temperature, and pH. Because of these aforementioned differences, the mannitol transport experiments were performed every 4 to 6 months over the past 5 yrs to verify our Caco-2 cell system.

Also, measuring the electrical resistance of the Caco-2 cell monolayers was another approach to check the integrity of monolayers. The TEER values were

positively associated with the development of tight junctions. However, the range of TEER values were 377 to 2,400 ohm*cm² in previous studies [139, 152]. The TEER readings for these experiments after 21 culture days averaged 833 ohm*cm². However, the range of TEER readings in all the studies was 550 to 1,300 ohm*cm² (data not shown). The possible explanations for the variability include the heterogeneity of Caco-2 cells, and especially the difference in Caco-2 cells passage numbers. It has been demonstrated that the TEER readings of the Caco-2 cell monolayers from higher passages such as passages 87 was greater than those of lower passage numbers [126]. So using the Caco-2 cells with narrow passage numbers would be an effective alternative to obtain consistent TEER readings. Therefore, all studies were done with passages from 25 to 30.

The function of P-gp in the present Caco-2 cells was verified by the transportation of rhodamine 123, a known P-gp substrate and the permeability of rhodamine 123 in both AP-to-BL and BL-to-AP directions were similar to the published data [219]. The efflux of rhodamine 123 was 4 times greater than its absorption, and 100 μM verapamil, a known P-gp inhibitor, can effectively diminish the efflux of rhodamine 123. All these results indicated that P-gp in the present Caco-2 cell system was functional.

Cimetidine is a small molecule (MW 252.3) with a pKa of 6.8. At physiological pH condition (pH 7.4), most of the cimetidine exists in the unionized form. The permeability of cimetidine was measured at pH 5.5, 6.5, and 7.4, where the ionized fraction of cimetidine was 95%, 66%, and 20%, respectively. There was

no significant difference in the transport of cimetidine among the different pH environments. This suggests that neither pH nor the paracellular route play a major role in the absorption of cimetidine.

The effect of vehicle solvents on the efflux permeability of cimetidine was evaluated in the Caco-2 cell monolayers. Ethanol and DMSO were the vehicles used in the studies, and their highest concentrations were 0.5% (v/v) and 0.2%, respectively. Neither of these solvents had a significant impact on the permeability of cimetidine. Therefore, it was concluded that the vehicle solvents used in the present studies did not significantly affect the permeability of cimetidine.

The permeability coefficients of cimetidine in either the AP-to-BL or BL-to-AP directions were measured in the Caco-2 cell monolayers. The estimated permeability coefficients were similar to the published data with values of 0.67×10^{-6} cm/sec and 2.02×10^{-6} cm/sec [6, 9]. The results demonstrated that the efflux of cimetidine was significantly greater than its absorption. The efflux permeability of cimetidine was 3 times greater than that of absorption. The ratio between efflux and absorption is approximately 4. This ratio was not high compared to other P-gp substrates, which ratio can be more than 50 folds such as sulfasalazine and saquinavir [218, 220]. This raises the question whether cimetidine is a substrate of an efflux pump or not. Several lines of evidence tend to support that cimetidine is an efflux pump substrate. First, cimetidine is a hydrophobic molecule with a positive charge at physiological pH condition. Molecules with these characteristics are likely to be the substrates of P-gp, an efflux pump expressed in Caco-2 cells as

well as human intestinal epithelium [221]. Second, cimetidine is a substrate of the human organic cation transporter 1 (hOCT1), which is also expressed in Caco-2 cells [222, 223]. hOCT1 can facilitate the uptake of cimetidine and then compensate the effort of the efflux pump. The mixed effect of hOCT1 and the efflux pump may result in low efflux to absorption ratio of 4.

Once an efflux mechanism was determined in the absorption of cimetidine, then efforts were made to determine which efflux pump was involved. P-gp was our primary interest because cimetidine tends to be its substrate. The results presented in this thesis demonstrated that when cimetidine is co-treated with 100 μ M verapamil, the efflux permeability of cimetidine was significantly reduced (p -value < 0.05). This provides evidence that P-gp was at least partly involved in the efflux of cimetidine. Even when 100 μ M verapamil was applied, the permeability of cimetidine from the BL to AP direction could not be decreased to the same level as the AP to BL direction. This suggests that there are efflux transporters other than P-gp such as multidrug associated protein (MRP) that might be involved in the efflux of cimetidine.

Theoretically, when efflux inhibitors are applied, an increase in the absorption permeability of the efflux substrate should be observed as well as a decrease in its efflux. However, the absorption permeability of cimetidine was not reduced when co-treated with verapamil. This phenomenon was also observed in other studies and more investigation is still needed [218, 224].

The enzymatic parameter, K_m , of P-gp was calculated for the transport of cimetidine in Caco-2 cell monolayers, as the transportation characteristics of P-gp can be described by Michaelis-Menten kinetics [215]. In the present studies, we used nonlinear regression to fit the efflux rates into a simple Michaelis-Menten equation. The Michaelis-Menten constant, K_m , was estimated to be 5,600 μM . A high K_m constant indicates that cimetidine has low affinity for P-gp and therefore is not a good substrate. This may also explain why cimetidine has a relatively low ratio between efflux and absorption.

Previous studies suggested that not only P-gp but also other ion transporters might be involved in the transport of cimetidine [225]. In the present studies, we explored the possible involvement of $\text{Na}^+ - \text{K}^+ - 2\text{Cl}^-$ and $\text{Cl}^-/\text{HCO}_3^-$ transporters in the transport of cimetidine by using their specific inhibitors bumetanide and DIDS, respectively. The results showed that both of them could significantly reduce the efflux of cimetidine in the Caco-2 cell monolayers. These two compounds may also have the potential to enhance the bioavailability of cimetidine. However, their undesirable pharmacological effects such as diuresis may limit their application in further clinical trials.

The effects of flavonoids such as quercetin, genistein, naringenin, and xanthohumol on the permeability of cimetidine were investigated in the present Caco-2 cell system. The flavonoid aglycones studied can significantly reduce the efflux permeability of cimetidine. However, only the glycoside of genistein, genistin, can significantly reduce the efflux of cimetidine.

In the determination of inhibition potency for the effective flavonoids, we found the IC_{50} 's of the flavonoid aglycone such as quercetin, genistein, naringenin, and xanthohumol were in the high nanomolar range. On the other hand, most of the flavonoid glycosides such as rutin, quercitrin, and naringin did not have a significant effect on the efflux of cimetidine. Only genistin had a value of IC_{50} in the low micromolar range (9.17 μ M). If one was to make a comparison between genistein and genistin, the inhibition potency of genistein is about 20 times more potent than that of genistin. Other studies have indicated that genistein is more active than genistin and can cause more potent pharmacological effects such as antiproliferation [45, 217]. Based on these results, one can conclude that quercetin, genistein, and naringenin are more potent efflux inhibitors than their glycosides, rutin, quercitrin, genistin, and naringin. Because flavonoid glycosides undergo cleavage of their sugar moieties as soon as they are consumed, both flavonoid aglycones and glycosides may have similar effects on the inhibition of efflux from a clinical perspective.

The present absorption results indicated that the Caco-2 cell monolayers absorbed more cimetidine if the drug was applied from BL side instead of AP side. The possible explanation for this is because P-gp was expressed on the AP side of Caco-2 cells. If cimetidine was applied from AP side, it may either directly undergo uptake or be pumped out by P-gp. On the other hand, when cimetidine was applied from the BL side, the only mechanism involved was absorption because P-gp is not located in the BL side of Caco-2 cells. When cimetidine was co-treated with

quercetin, the uptake of cimetidine was not significantly different compared to cimetidine alone in both directions. This may be due to the short incubation period of 3 min which may not be sufficient for quercetin to inhibit the efflux pump. When the incubation period was extended to 30 min, there was a significant reduction of uptake of cimetidine from BL side.

The pH factor was also evaluated in the absorption of cimetidine in Caco-2 cell monolayers. The uptake of cimetidine from the AP side was less at pH 5.5 whether or not it was co-treated with quercetin. At pH 5.5, the ionized fraction of cimetidine was 5% in contrast to 80% at pH 7.4. This suggests that the efflux transporter prefers to pump unionized cimetidine than the ionized form. However, the difference of uptake amount between the two pH conditions was relatively small. The fraction of ionization may only play a minor role during the uptake studies.

What is the mechanism by which flavonoids inhibit the efflux of cimetidine? IC_{50} itself is a model-free parameter which means no presumption is needed to obtain IC_{50} . By using the Cheng-Prusoff equation, one can derive the inhibition constant, K_i , from IC_{50} and reveal the possible inhibition mechanism [226]. However, the sensitivity of the transport experiments in Caco-2 cell monolayers is not adequate to distinguish the different inhibition mechanisms by the Cheng-Prusoff equation. This problem also became apparent in other studies using the Caco-2 cell transport model [224]. From a structure perspective, flavonoids tend to be P-gp modulators instead of substrates [2]. Also, there is no

published research that indicates that flavonoids are substrates of P-gp. So, it is not likely that the flavonoids can inhibit the activity of P-gp by competitive inhibition. Previous studies have demonstrated that genistein and quercetin, but not genistin or quercitrin, could inhibit the activity of the mitochondrial proton F₀F₁-ATPase/ATP synthase in rat brain [217]. This provides an alternative explanation that flavonoids may inhibit the activity of P-gp by depleting its ATP source. Another possibility is that flavonoids may inhibit the activity of the organic cation transporter, which is also expressed in Caco-2 cells that can recognize cimetidine as substrate. However, there is no reported literature investigating the effect of flavonoids on organic cation transporters.

Another possibility is that there may be a structure-activity relationship among the different classes of flavonoids and their effects on the inhibition of cimetidine efflux. The flavonoids studied came from four different classes such as flavonol, flavanonane, isoflavone, and chalcone, respectively. Based on the results of inhibition potency, the IC₅₀ of quercetin, naringenin, genistein, and xanthohumol were in the high nanomolar range. If one considers the sensitivity of transport experiments, it is difficult to rank the inhibition potency among different classes of flavonoids because of the low sensitivity of transport experiments. Genistin, a glycoside of genistein and a member of the isoflavone family, was the only glycoside that showed significant inhibition in cimetidine efflux. Thus, these results suggested that isoflavones may have the most potent inhibition in the efflux of cimetidine compared to flavonols (quercetin) or flavonanes (naringenin). We did

not include the chalcone (xanthohumol) subfamily in our comparison because we did not have a glycoside of xanthohumol to study for comparison. In order to derive the structure-activity relationship (SAR) among the different classes of flavonoids, flavonoids other than the one studied such as apigenin, taxifolin, (+)-catechin, and cyanidin, etc... should be chosen to evaluate their inhibition potency in the efflux of cimetidine.

There are several approaches for the future studies of this thesis project. If one wants to determine the inhibition mechanism of flavonoids on P-gp through enzyme kinetics analysis, a model developed by Shapiro and Ling may be a good candidate [200]. In their system, P-gp-rich plasma membrane vesicle was prepared from CH^RB30 cells which allows one to focus on P-gp only and to avoid possible interference from other transporters. In addition, using a purified plasma membrane can prevent the confounding results from binding of compounds to their intracellular targets or concentration within organelles. To confirm that flavonoids can inhibit the efflux of P-gp substrates other than cimetidine, cyclosporine or vinblastine are good candidates for our Caco-2 cell model system. Also, additional flavonoid aglycones as well as their glycosides should be evaluated if one wants to extend these findings to other subfamilies of flavonoids. The present studies provide *in vitro* information about the interactions between flavonoids and cimetidine. To evaluate the effects of flavonoids *in vivo* or in clinical trials with P-gp substrates will be the long-term object once sufficient *in vitro* data are provided.

In summary, we provide evidence that flavonoids, especially aglycones, inhibit the efflux of cimetidine in the Caco-2 cell monolayers. Therefore, they may have the potential to enhance the bioavailability of cimetidine and possibly other P-glycoprotein substrates.

BIBLIOGRAPHY

1. Kuhnau, J., *The flavonoids. A class of semi-essential food components: their role in human nutrition.* World Rev Nutr Diet, 1976. **24**: p. 117-91.
2. Ferte, J., J.M. Kuhnel, G. Chapuis, Y. Rolland, G. Lewin, and M.A. Schwaller, *Flavonoid-related modulators of multidrug resistance: synthesis, pharmacological activity, and structure-activity relationships.* J Med Chem, 1999. **42**(3): p. 478-89.
3. Austin, C.A., S. Patel, K. Ono, H. Nakane, and L.M. Fisher, *Site-specific DNA cleavage by mammalian DNA topoisomerase II induced by novel flavone and catechin derivatives.* Biochem J, 1992. **282** (Pt 3): p. 883-9.
4. Bindoli, A., M. Valente, and L. Cavallini, *Inhibitory action of quercetin on xanthine oxidase and xanthine dehydrogenase activity.* Pharmacol Res Commun, 1985. **17**(9): p. 831-9.
5. Castro, A.F. and G.A. Altenberg, *Inhibition of drug transport by genistein in multidrug-resistant cells expressing P-glycoprotein.* Biochem Pharmacol, 1997. **53**(1): p. 89-93.
6. Collett, A., N.B. Higgs, E. Sims, M. Rowland, and G. Warhurst, *Modulation of the permeability of H₂ receptor antagonists cimetidine and ranitidine by P-glycoprotein in rat intestine and the human colonic cell line Caco-2.* J Pharmacol Exp Ther, 1999. **288**(1): p. 171-8.
7. Shapiro, A.B. and V. Ling, *Effect of quercetin on Hoechst 33342 transport by purified and reconstituted P-glycoprotein.* Biochem Pharmacol, 1997. **53**(4): p. 587-96.
8. Hidalgo, I.J., Raub, T.J., and Borchardt, R.T., *Characterization of the human colon carcinoma cell line (Caco-2) as a model system for intestinal epithelial permeability.* Gastroenterology, 1989. **96**: p. 736-749.

9. Pade, V. and S. Stavchansky, *Link between drug absorption solubility and permeability measurements in Caco-2 cells*. J Pharm Sci, 1998. **87**(12): p. 1604-7.
10. Chin, T.W., M. Loeb, and I.W. Fong, *Effects of an acidic beverage (Coca-Cola) on absorption of ketoconazole*. Antimicrob Agents Chemother, 1995. **39**(8): p. 1671-5.
11. Zimmerman, J.J., G.M. Ferron, H.K. Lim, and V. Parker, *The effect of a high-fat meal on the oral bioavailability of the immunosuppressant sirolimus (rapamycin)*. J Clin Pharmacol, 1999. **39**(11): p. 1155-61.
12. Conney, A.H., E.J. Pantuck, K.C. Hsiao, W.A. Garland, K.E. Anderson, A.P. Alvares, and A. Kappas, *Enhanced phenacetin metabolism in human subjects fed charcoal-broiled beef*. Clin Pharmacol Ther, 1976. **20**(6): p. 633-42.
13. Bailey, D.G., J.D. Spence, C. Munoz, and J.M. Arnold, *Interaction of citrus juices with felodipine and nifedipine*. Lancet, 1991. **337**(8736): p. 268-9.
14. Sigusch, H., M. Hippius, L. Henschel, K. Kaufmann, and A. Hoffmann, *Influence of grapefruit juice on the pharmacokinetics of a slow release nifedipine formulation*. Pharmazie, 1994. **49**(7): p. 522-4.
15. Fuhr, U., A. Maier-Bruggemann, H. Blume, W. Muck, S. Unger, J. Kuhlmann, C. Huschka, M. Zaigler, S. Rietbrock, and A.H. Staib, *Grapefruit juice increases oral nimodipine bioavailability*. Int J Clin Pharmacol Ther, 1998. **36**(3): p. 126-32.
16. Kupferschmidt, H.H., H.R. Ha, W.H. Ziegler, P.J. Meier, and S. Krahenbuhl, *Interaction between grapefruit juice and midazolam in humans*. Clin Pharmacol Ther, 1995. **58**(1): p. 20-8.
17. Hukkinen, S.K., A. Varhe, K.T. Olkkola, and P.J. Neuvonen, *Plasma concentrations of triazolam are increased by concomitant ingestion of grapefruit juice*. Clin Pharmacol Ther, 1995. **58**(2): p. 127-31.

18. Benton, R.E., P.K. Honig, K. Zamani, L.R. Cantilena, and R.L. Woosley, *Grapefruit juice alters terfenadine pharmacokinetics, resulting in prolongation of repolarization on the electrocardiogram*. Clin Pharmacol Ther, 1996. 59(4): p. 383-8.
19. Weber, A., R. Jager, A. Borner, G. Klinger, R. Vollanth, K. Matthey, and A. Balogh, *Can grapefruit juice influence ethinylestradiol bioavailability?* Contraception, 1996. 53(1): p. 41-7.
20. Kupferschmidt, H.H., K.E. Fattinger, H.R. Ha, F. Follath, and S. Krahenbuhl, *Grapefruit juice enhances the bioavailability of the HIV protease inhibitor saquinavir in man*. Br J Clin Pharmacol, 1998. 45(4): p. 355-9.
21. Kantola, T., K.T. Kivisto, and P.J. Neuvonen, *Grapefruit juice greatly increases serum concentrations of lovastatin and lovastatin acid*. Clin Pharmacol Ther, 1998. 63(4): p. 397-402.
22. Ku, Y.M., D.I. Min, and M. Flanigan, *Effect of grapefruit juice on the pharmacokinetics of microemulsion cyclosporine and its metabolite in healthy volunteers: does the formulation difference matter?* J Clin Pharmacol, 1998. 38(10): p. 959-65.
23. Lilja, J.J., K.T. Kivisto, J.T. Backman, T.S. Lamberg, and P.J. Neuvonen, *Grapefruit juice substantially increases plasma concentrations of buspirone*. Clin Pharmacol Ther, 1998. 64(6): p. 655-60.
24. Gross, A.S., Y.D. Goh, R.S. Addison, and G.M. Shenfield, *Influence of grapefruit juice on cisapride pharmacokinetics*. Clin Pharmacol Ther, 1999. 65(4): p. 395-401.
25. van Agtmael, M.A., V. Gupta, T.H. van der Wosten, J.P. Rutten, and C.J. van Boxtel, *Grapefruit juice increases the bioavailability of artemether*. Eur J Clin Pharmacol, 1999. 55(5): p. 405-10.

26. Lilja, J.J., K.T. Kivisto, and P.J. Neuvonen, *Grapefruit juice increases serum concentrations of atorvastatin and has no effect on pravastatin*. Clin Pharmacol Ther, 1999. 66(2): p. 118-27.
27. Ebert, U., R. Oertel, and W. Kirch, *Influence of grapefruit juice on scopolamine pharmacokinetics and pharmacodynamics in healthy male and female subjects*. Int J Clin Pharmacol Ther, 2000. 38(11): p. 523-31.
28. Jetter, A., M. Kinzig-Schippers, M. Walchner-Bonjean, U. Hering, J. Bulitta, P. Schreiner, F. Sorgel, and U. Fuhr, *Effects of grapefruit juice on the pharmacokinetics of sildenafil*. Clin Pharmacol Ther, 2002. 71(1): p. 21-9.
29. Charbit, B., L. Becquemont, B. Lepere, G. Peytavin, and C. Funck-Brentano, *Pharmacokinetic and pharmacodynamic interaction between grapefruit juice and halofantrine*. Clin Pharmacol Ther, 2002. 72(5): p. 514-23.
30. Lown, K.S., D.G. Bailey, R.J. Fontana, S.K. Janardan, C.H. Adair, L.A. Fortlage, M.B. Brown, W. Guo, and P.B. Watkins, *Grapefruit juice increases felodipine oral availability in humans by decreasing intestinal CYP3A protein expression*. J Clin Invest, 1997. 99(10): p. 2545-53.
31. Miniscalco, A., J. Lundahl, C.G. Regardh, B. Edgar, and U.G. Eriksson, *Inhibition of dihydropyridine metabolism in rat and human liver microsomes by flavonoids found in grapefruit juice*. J Pharmacol Exp Ther, 1992. 261(3): p. 1195-9.
32. Harborne, J.B. and H. Baxter, *Handbook of Natural Flavonoids*. 1999, Chichester: Wiley.
33. Middleton, E.M. and A.H. Teramura, *The Role of Flavonol Glycosides and Carotenoids in Protecting Soybean from Ultraviolet-B Damage*. Plant Physiol, 1993. 103(3): p. 741-752.

34. Morimoto, M., S. Kumeda, and K. Komai, *Insect antifeedant flavonoids from Gnaphalium affine D. Don*. J Agric Food Chem, 2000. **48**(5): p. 1888-91.
35. Tereschuk, M.L., M.V. Riera, G.R. Castro, and L.R. Abdala, *Antimicrobial activity of flavonoids from leaves of Tagetes minuta*. J Ethnopharmacol, 1997. **56**(3): p. 227-32.
36. Harborne, J.B., *In plant Flavonoids in biology and Medicine*, ed. J.B. Harborne. 1986, New York: Alan R. Liss. 15-24.
37. Bokkenheuser, V.D., C.H. Shackleton, and J. Winter, *Hydrolysis of dietary flavonoid glycosides by strains of intestinal Bacteroides from humans*. Biochem J, 1987. **248**(3): p. 953-6.
38. Hollman, P.C., J.M. van Trijp, M.N. Buysman, M.S. van der Gaag, M.J. Mengelers, J.H. de Vries, and M.B. Katan, *Relative bioavailability of the antioxidant flavonoid quercetin from various foods in man*. FEBS Lett, 1997. **418**(1-2): p. 152-6.
39. Griffiths, L.A. and G.E. Smith, *Metabolism of apigenin and related compounds in the rat. Metabolite formation in vivo and by the intestinal microflora in vitro*. Biochem J, 1972. **128**(4): p. 901-11.
40. Griffiths, L.A. and G.E. Smith, *Metabolism of myricetin and related compounds in the rat. Metabolite formation in vivo and by the intestinal microflora in vitro*. Biochem J, 1972. **130**(1): p. 141-51.
41. Nielsen, S.E., V. Breinholt, U. Justesen, C. Cornett, and L.O. Dragsted, *In vitro biotransformation of flavonoids by rat liver microsomes*. Xenobiotica, 1998. **28**(4): p. 389-401.
42. Ader, P., A. Wessmann, and S. Wolffram, *Bioavailability and metabolism of the flavonol quercetin in the pig*. Free Radic Biol Med, 2000. **28**(7): p. 1056-67.

43. Crespy, V., O. Aprikian, C. Morand, C. Besson, C. Manach, C. Demigne, and C. Remesy, *Bioavailability of phloretin and phloridzin in rats*. J Nutr, 2001. 131(12): p. 3227-30.
44. Prior, R.L. and G. Cao, *Antioxidant capacity and polyphenolic components of teas: implications for altering in vivo antioxidant status*. Proc Soc Exp Biol Med, 1999. 220(4): p. 255-61.
45. Yanagihara, K., A. Ito, T. Toge, and M. Numoto, *Antiproliferative effects of isoflavones on human cancer cell lines established from the gastrointestinal tract*. Cancer Res, 1993. 53(23): p. 5815-21.
46. Komori, A., J. Yatsunami, S. Okabe, S. Abe, K. Hara, M. Suganuma, S.J. Kim, and H. Fujiki, *Anticarcinogenic activity of green tea polyphenols*. Jpn J Clin Oncol, 1993. 23(3): p. 186-90.
47. Akiyama, T., J. Ishida, S. Nakagawa, H. Ogawara, S. Watanabe, N. Itoh, M. Shibuya, and Y. Fukami, *Genistein, a specific inhibitor of tyrosine-specific protein kinases*. J Biol Chem, 1987. 262(12): p. 5592-5.
48. Critchfield, J.W., C.J. Welsh, J.M. Phang, and G.C. Yeh, *Modulation of adriamycin accumulation and efflux by flavonoids in HCT-15 colon cells. Activation of P-glycoprotein as a putative mechanism*. Biochem Pharmacol, 1994. 48(7): p. 1437-45.
49. *NTP Technical Report on the toxicology and carcinogenesis studies of quercetin in F344/N rats*. 1991, U.S. Department of Health and Human Services, Public Health Service, National Toxicology Program: Research Triangle Park, NC.
50. Gugler, R., M. Leschik, and H.J. Dengler, *Disposition of quercetin in man after single oral and intravenous doses*. Eur J Clin Pharmacol, 1975. 9(2-3): p. 229-34.
51. Hollman, P.C., J.H. de Vries, S.D. van Leeuwen, M.J. Mengelers, and M.B. Katan, *Absorption of dietary quercetin glycosides and quercetin in healthy ileostomy volunteers*. Am J Clin Nutr, 1995. 62(6): p. 1276-82.

52. Hollman, P.C., M. vd Gaag, M.J. Mengelers, J.M. van Trijp, J.H. de Vries, and M.B. Katan, *Absorption and disposition kinetics of the dietary antioxidant quercetin in man*. Free Radic Biol Med, 1996. 21(5): p. 703-7.
53. Morand, C., V. Crespy, C. Manach, C. Besson, C. Demigne, and C. Remesy, *Plasma metabolites of quercetin and their antioxidant properties*. Am J Physiol, 1998. 275(1 Pt 2): p. R212-9.
54. Graefe, E.U., J. Wittig, S. Mueller, A.K. Riethling, B. Uehleke, B. Drewelow, H. Pforte, G. Jacobasch, H. Derendorf, and M. Veit, *Pharmacokinetics and bioavailability of quercetin glycosides in humans*. J Clin Pharmacol, 2001. 41(5): p. 492-9.
55. Ferry, D.R., A. Smith, J. Malkhandi, D.W. Fyfe, P.G. deTakats, D. Anderson, J. Baker, and D.J. Kerr, *Phase I clinical trial of the flavonoid quercetin: pharmacokinetics and evidence for in vivo tyrosine kinase inhibition*. Clin Cancer Res, 1996. 2(4): p. 659-68.
56. MacGregor, J.T. and L. Jurd, *Mutagenicity of plant flavonoids: structural requirements for mutagenic activity in Salmonella typhimurium*. Mutat Res, 1978. 54(3): p. 297-309.
57. Bjeldanes, L.F. and G.W. Chang, *Mutagenic activity of quercetin and related compounds*. Science, 1977. 197(4303): p. 577-8.
58. Saito, D., A. Shirai, T. Matsushima, T. Sugimura, and I. Hirono, *Test of carcinogenicity of quercetin, a widely distributed mutagen in food*. Teratog Carcinog Mutagen, 1980. 1(2): p. 213-21.
59. Morino, K., N. Matsukara, T. Kawachi, H. Ohgaki, T. Sugimura, and I. Hirono, *Carcinogenicity test of quercetin and rutin in golden hamsters by oral administration*. Carcinogenesis, 1982. 3(1): p. 93-7.
60. Hirono, I., I. Ueno, S. Hosaka, H. Takanashi, T. Matsushima, T. Sugimura, and S. Natori, *Carcinogenicity examination of quercetin and rutin in ACI rats*. Cancer Lett, 1981. 13(1): p. 15-21.

61. Dunnick, J.K. and J.R. Hailey, *Toxicity and carcinogenicity studies of quercetin, a natural component of foods*. Fundam Appl Toxicol, 1992. 19(3): p. 423-31.
62. de Whalley, C.V., S.M. Rankin, J.R. Hoult, W. Jessup, and D.S. Leake, *Flavonoids inhibit the oxidative modification of low density lipoproteins by macrophages*. Biochem Pharmacol, 1990. 39(11): p. 1743-50.
63. Avila, M.A., J.A. Velasco, J. Cansado, and V. Notario, *Quercetin mediates the down-regulation of mutant p53 in the human breast cancer cell line MDA-MB468*. Cancer Res, 1994. 54(9): p. 2424-8.
64. Srivastava, A.K., *Inhibition of phosphorylase kinase, and tyrosine protein kinase activities by quercetin*. Biochem Biophys Res Commun, 1985. 131(1): p. 1-5.
65. Ranelletti, F.O., N. Maggiano, F.G. Serra, R. Ricci, L.M. Larocca, P. Lanza, G. Scambia, A. Fattorossi, A. Capelli, and M. Piantelli, *Quercetin inhibits p21-RAS expression in human colon cancer cell lines and in primary colorectal tumors*. Int J Cancer, 2000. 85(3): p. 438-45.
66. Singhal, R.L., Y.A. Yeh, N. Praja, E. Olah, G.W. Sledge, Jr., and G. Weber, *Quercetin down-regulates signal transduction in human breast carcinoma cells*. Biochem Biophys Res Commun, 1995. 208(1): p. 425-31.
67. Agullo, G., L. Gamet, C. Besson, C. Demigne, and C. Remesy, *Quercetin exerts a preferential cytotoxic effect on active dividing colon carcinoma HT29 and Caco-2 cells*. Cancer Lett, 1994. 87(1): p. 55-63.
68. Larocca, L.M., L. Teofili, G. Leone, S. Sica, L. Pierelli, G. Menichella, G. Scambia, P. Benedetti Panici, R. Ricci, M. Piantelli, and et al., *Antiproliferative activity of quercetin on normal bone marrow and leukaemic progenitors*. Br J Haematol, 1991. 79(4): p. 562-6.
69. Piantelli, M., N. Maggiano, R. Ricci, L.M. Larocca, A. Capelli, G. Scambia, G. Isola, P.G. Natali, and F.O. Ranelletti, *Tamoxifen and quercetin interact*

- with type II estrogen binding sites and inhibit the growth of human melanoma cells.* J Invest Dermatol, 1995. **105**(2): p. 248-53.
70. Hackl, L.P., G. Cuttle, S.S. Dovichi, M.T. Lima-Landman, and M. Nicolau, *Inhibition of angiotensin-converting enzyme by quercetin alters the vascular response to bradykinin and angiotensin I.* Pharmacology, 2002. **65**(4): p. 182-6.
 71. Keli, S.O., M.G. Hertog, E.J. Feskens, and D. Kromhout, *Dietary flavonoids, antioxidant vitamins, and incidence of stroke: the Zutphen study.* Arch Intern Med, 1996. **156**(6): p. 637-42.
 72. Hertog, M.G., E.J. Feskens, P.C. Hollman, M.B. Katan, and D. Kromhout, *Dietary antioxidant flavonoids and risk of coronary heart disease: the Zutphen Elderly Study.* Lancet, 1993. **342**(8878): p. 1007-11.
 73. Rodgers, E.H. and M.H. Grant, *The effect of the flavonoids, quercetin, myricetin and epicatechin on the growth and enzyme activities of MCF7 human breast cancer cells.* Chem Biol Interact, 1998. **116**(3): p. 213-28.
 74. Barnes, S., T.G. Peterson, and L. Coward, *Rationale for the use of genistein-containing soy matrices in chemoprevention trials for breast and prostate cancer.* J Cell Biochem Suppl, 1995. **22**: p. 181-7.
 75. Watanabe, S., M. Yamaguchi, T. Sobue, T. Takahashi, T. Miura, Y. Arai, W. Mazur, K. Wahala, and H. Adlercreutz, *Pharmacokinetics of soybean isoflavones in plasma, urine and feces of men after ingestion of 60 g baked soybean powder (kinako).* J Nutr, 1998. **128**(10): p. 1710-5.
 76. Xu, X., K.S. Harris, H.J. Wang, P.A. Murphy, and S. Hendrich, *Bioavailability of soybean isoflavones depends upon gut microflora in women.* J Nutr, 1995. **125**(9): p. 2307-15.
 77. Martin, P.M., K.B. Horwitz, D.S. Ryan, and W.L. McGuire, *Phytoestrogen interaction with estrogen receptors in human breast cancer cells.* Endocrinology, 1978. **103**(5): p. 1860-7.

78. Lamartiniere, C.A., *Protection against breast cancer with genistein: a component of soy*. Am J Clin Nutr, 2000. **71**(6 Suppl): p. 1705S-7S; discussion 1708S-9S.
79. Okura, A., H. Arakawa, H. Oka, T. Yoshinari, and Y. Monden, *Effect of genistein on topoisomerase activity and on the growth of [Val 12]Ha-ras-transformed NIH 3T3 cells*. Biochem Biophys Res Commun, 1988. **157**(1): p. 183-9.
80. Carlo-Stella, C., E. Regazzi, D. Garau, L. Mangoni, M.T. Rizzo, A. Bonati, G. Dotti, C. Almici, and V. Rizzoli, *Effect of the protein tyrosine kinase inhibitor genistein on normal and leukaemic haemopoietic progenitor cells*. Br J Haematol, 1996. **93**(3): p. 551-7.
81. Kiguchi, K., A.I. Constantinou, and E. Huberman, *Genistein-induced cell differentiation and protein-linked DNA strand breakage in human melanoma cells*. Cancer Commun, 1990. **2**(8): p. 271-7.
82. Constantinou, A. and E. Huberman, *Genistein as an inducer of tumor cell differentiation: possible mechanisms of action*. Proc Soc Exp Biol Med, 1995. **208**(1): p. 109-15.
83. Dunn, J.E., *Cancer epidemiology in populations of the United States—with emphasis on Hawaii and California—and Japan*. Cancer Res, 1975. **35**(11 Pt. 2): p. 3240-5.
84. Helsby, N.A., J.K. Chipman, A. Gescher, and D. Kerr, *Inhibition of mouse and human CYP 1A- and 2E1-dependent substrate metabolism by the isoflavonoids genistein and equol*. Food Chem Toxicol, 1998. **36**(5): p. 375-82.
85. Versantvoort, C.H., H.J. Broxterman, J. Lankelma, N. Feller, and H.M. Pinedo, *Competitive inhibition by genistein and ATP dependence of daunorubicin transport in intact MRP overexpressing human small cell lung cancer cells*. Biochem Pharmacol, 1994. **48**(6): p. 1129-36.

86. Mouly, P., E.M. Gaydou, and J. Estienne, *Column liquid chromatographic determination of flavanone glycosides in Citrus. Application to grapefruit and sour orange juice adulterations*. J Chromatogr, 1993. **634**(1): p. 129-34.
87. Paganga, G., N. Miller, and C.A. Rice-Evans, *The polyphenolic content of fruit and vegetables and their antioxidant activities. What does a serving constitute?* Free Radic Res, 1999. **30**(2): p. 153-62.
88. Fuhr, U. and A.L. Kummert, *The fate of naringin in humans: a key to grapefruit juice-drug interactions?* Clin Pharmacol Ther, 1995. **58**(4): p. 365-73.
89. Bugianesi, R., G. Catasta, P. Spigno, A. D'Uva, and G. Maiani, *Naringenin from cooked tomato paste is bioavailable in men*. J Nutr, 2002. **132**(11): p. 3349-52.
90. Ruh, M.F., T. Zacharewski, K. Connor, J. Howell, I. Chen, and S. Safe, *Naringenin: a weakly estrogenic bioflavonoid that exhibits antiestrogenic activity*. Biochem Pharmacol, 1995. **50**(9): p. 1485-93.
91. Erlund, I., E. Meririnne, G. Alfthan, and A. Aro, *Plasma kinetics and urinary excretion of the flavanones naringenin and hesperetin in humans after ingestion of orange juice and grapefruit juice*. J Nutr, 2001. **131**(2): p. 235-41.
92. So, F.V., N. Guthrie, A.F. Chambers, M. Moussa, and K.K. Carroll, *Inhibition of human breast cancer cell proliferation and delay of mammary tumorigenesis by flavonoids and citrus juices*. Nutr Cancer, 1996. **26**(2): p. 167-81.
93. van Acker, F.A., O. Schouten, G.R. Haenen, W.J. van der Vijgh, and A. Bast, *Flavonoids can replace alpha-tocopherol as an antioxidant*. FEBS Lett, 2000. **473**(2): p. 145-8.
94. Shin, Y.W., S.H. Bok, T.S. Jeong, K.H. Bae, N.H. Jeoung, M.S. Choi, S.H. Lee, and Y.B. Park, *Hypocholesterolemic effect of naringin associated with*

- hepatic cholesterol regulating enzyme changes in rats.* Int J Vitam Nutr Res, 1999. **69**(5): p. 341-7.
95. Ho, P.C., D.J. Saville, and S. Wanwimolruk, *Inhibition of human CYP3A4 activity by grapefruit flavonoids, furanocoumarins and related compounds.* J Pharm Pharm Sci, 2001. **4**(3): p. 217-27.
 96. Edwards, D.J. and S.M. Bernier, *Naringin and naringenin are not the primary CYP3A inhibitors in grapefruit juice.* Life Sci, 1996. **59**(13): p. 1025-30.
 97. Ghosal, A., H. Satoh, P.E. Thomas, E. Bush, and D. Moore, *Inhibition and kinetics of cytochrome P4503A activity in microsomes from rat, human, and cDNA-expressed human cytochrome P450.* Drug Metab Dispos, 1996. **24**(9): p. 940-7.
 98. Bear, W.L. and R.W. Teel, *Effects of citrus flavonoids on the mutagenicity of heterocyclic amines and on cytochrome P450 1A2 activity.* Anticancer Res, 2000. **20**(5B): p. 3609-14.
 99. Takanaga, H., A. Ohnishi, H. Matsuo, and Y. Sawada, *Inhibition of vinblastine efflux mediated by P-glycoprotein by grapefruit juice components in caco-2 cells.* Biol Pharm Bull, 1998. **21**(10): p. 1062-6.
 100. Stevens, J.F., A.W. Taylor, and M.L. Deinzer, *Quantitative analysis of xanthohumol and related prenylflavonoids in hops and beer by liquid chromatography-tandem mass spectrometry.* J Chromatogr A, 1999. **832**(1-2): p. 97-107.
 101. Miranda, C.L., J.F. Stevens, V. Ivanov, M. McCall, B. Frei, M.L. Deinzer, and D.R. Buhler, *Antioxidant and prooxidant actions of prenylated and nonprenylated chalcones and flavanones in vitro.* J Agric Food Chem, 2000. **48**(9): p. 3876-84.
 102. Tabata, N., M. Ito, H. Tomoda, and S. Omura, *Xanthohumols, diacylglycerol acyltransferase inhibitors, from Humulus lupulus.* Phytochemistry, 1997. **46**(4): p. 683-7.

103. Miranda, C.L., J.F. Stevens, A. Helmrich, M.C. Henderson, R.J. Rodriguez, Y.H. Yang, M.L. Deinzer, D.W. Barnes, and D.R. Buhler, *Antiproliferative and cytotoxic effects of prenylated flavonoids from hops (Humulus lupulus) in human cancer cell lines*. Food Chem Toxicol, 1999. 37(4): p. 271-85.
104. Henderson, M.C., C.L. Miranda, J.F. Stevens, M.L. Deinzer, and D.R. Buhler, *In vitro inhibition of human P450 enzymes by prenylated flavonoids from hops, Humulus lupulus*. Xenobiotica, 2000. 30(3): p. 235-51.
105. Miranda, C.L., G.L. Aponso, J.F. Stevens, M.L. Deinzer, and D.R. Buhler, *Prenylated chalcones and flavanones as inducers of quinone reductase in mouse Hepa 1c1c7 cells*. Cancer Lett, 2000. 149(1-2): p. 21-9.
106. Fogh, J., J.M. Fogh, and T. Orfeo, *One hundred and twenty-seven cultured human tumor cell lines producing tumors in nude mice*. J Natl Cancer Inst, 1977. 59(1): p. 221-6.
107. Chantret, I., Barbat, A., Dussaulx, E., Brattain, M. G., and Zweibaum, A., *Epithelial polarity, villin expression, and enterocytic differentiation of cultured human colon carcinoma cells: A survey of twenty cell lines*. Cancer Res, 1988. 48: p. 1936.
108. Pinto, M., Robine-Leon, S., Appay, M.-D., Kedinger, M., Triadou, N., Dussaulx, E., Lacroix, B., Simon-Assmann, P., Haffen, K., Fogh, J., and Zweinbaum, A., *Enterocyte-like differentiation and polarization of the human colon carcinoma cell line Caco-2 in culture*. Biol. Cell, 1983. 47: p. 323.
109. Vachon, P.H.a.B., J.F., *Transient mosaic patterns of morphological and functional differentiation in the Caco-2 cell line*. Gastroenterology, 1992. 103: p. 414.
110. Anderson, J.M., and Van Itallie, C.M., *Tight junction and the molecular basis for regulation of paracellular permeability*. Am. J. Physiol., 1995. 269: p. G467.

111. Prueksaritanont, T., L.M. Gorham, J.H. Hochman, L.O. Tran, and K.P. Vyas, *Comparative studies of drug-metabolizing enzymes in dog, monkey, and human small intestines, and in Caco-2 cells*. Drug Metab Dispos, 1996. **24**(6): p. 634-42.
112. Raeissi, S.D., Z. Guo, G.L. Dobson, P. Artursson, and I.J. Hidalgo, *Comparison of CYP3A activities in a subclone of Caco-2 cells (TC7) and human intestine*. Pharm Res, 1997. **14**(8): p. 1019-25.
113. Baker, S.S. and R.D. Baker, Jr., *Antioxidant enzymes in the differentiated Caco-2 cell line*. In Vitro Cell Dev Biol, 1992. **28A**(9-10): p. 643-7.
114. Beaulieu, J.F. and A. Quaroni, *Clonal analysis of sucrase-isomaltase expression in the human colon adenocarcinoma Caco-2 cells*. Biochem J, 1991. **280** (Pt 3): p. 599-608.
115. Hauri, H.P., B. Sander, and H. Naim, *Induction of lactase biosynthesis in the human intestinal epithelial cell line Caco-2*. Eur J Biochem, 1994. **219**(1-2): p. 539-46.
116. Howell, S., A.J. Kenny, and A.J. Turner, *A survey of membrane peptidases in two human colonic cell lines, Caco-2 and HT-29*. Biochem J, 1992. **284** (Pt 2): p. 595-601.
117. Darmoul, D., M. Lacasa, L. Baricault, D. Marguet, C. Sapin, P. Trotot, A. Barbat, and G. Trugnan, *Dipeptidyl peptidase IV (CD 26) gene expression in enterocyte-like colon cancer cell lines HT-29 and Caco-2. Cloning of the complete human coding sequence and changes of dipeptidyl peptidase IV mRNA levels during cell differentiation*. J Biol Chem, 1992. **267**(7): p. 4824-33.
118. Buur, A. and N. Mork, *Metabolism of testosterone during in vitro transport across CACO-2 cell monolayers: evidence for beta-hydroxysteroid dehydrogenase activity in differentiated CACO-2 cells*. Pharm Res, 1992. **9**(10): p. 1290-4.

119. Kamitani, H., M. Geller, and T. Eling, *Expression of 15-lipoxygenase by human colorectal carcinoma Caco-2 cells during apoptosis and cell differentiation*. J Biol Chem, 1998. **273**(34): p. 21569-77.
120. Boulenc, X., M. Bourrie, I. Fabre, C. Roque, H. Joyeux, Y. Berger, and G. Fabre, *Regulation of cytochrome P450IA1 gene expression in a human intestinal cell line, Caco-2*. J Pharmacol Exp Ther, 1992. **263**(3): p. 1471-8.
121. D'Agostino, L., B. Daniele, S. Pignata, R. Gentile, P. Tagliaferri, A. Contegiacomo, G. Silvestro, C. Polistina, A.R. Bianco, and G. Mazzacca, *Ornithine decarboxylase and diamine oxidase in human colon carcinoma cell line CaCo-2 in culture*. Gastroenterology, 1989. **97**(4): p. 888-94.
122. Buckholz, C., *Acute bioactivation and hepatotoxicity of ketoconazole in rat and the determinant presence of flavin-containing monooxygenase isoforms in human duodenum, jejunum, ileum, and Caco-2 cell model system*, in *Department of Pharmaceutical Sciences*. 2003, Oregon State University: Corvallis.
123. Peters, W.H. and H.M. Roelofs, *Time-dependent activity and expression of glutathione S-transferases in the human colon adenocarcinoma cell line Caco-2*. Biochem J, 1989. **264**(2): p. 613-6.
124. Baranczyk-Kuzma, A., J.A. Garren, I.J. Hidalgo, and R.T. Borchardt, *Substrate specificity and some properties of phenol sulfotransferase from human intestinal Caco-2 cells*. Life Sci, 1991. **49**(16): p. 1197-206.
125. Yu, H., T.J. Cook, and P.J. Sinko, *Evidence for diminished functional expression of intestinal transporters in Caco-2 cell monolayers at high passages*. Pharm Res, 1997. **14**(6): p. 757-62.
126. Lu, S., A.W. Gough, W.F. Bobrowski, and B.H. Stewart, *Transport properties are not altered across Caco-2 cells with heightened TEER despite underlying physiological and ultrastructural changes*. J Pharm Sci, 1996. **85**(3): p. 270-3.

127. Briske-Anderson, M.J., J.W. Finley, and S.M. Newman, *The influence of culture time and passage number on the morphological and physiological development of Caco-2 cells*. Proc Soc Exp Biol Med, 1997. **214**(3): p. 248-57.
128. Mesonero, J., L. Mahraoui, M. Matosin, A. Rodolosse, M. Rousset, and E. Brot-Laroche, *Expression of the hexose transporters GLUT1-GLUT5 and SGLT1 in clones of Caco-2 cells*. Biochem Soc Trans, 1994. **22**(3): p. 681-4.
129. Tsuji, A., H. Takanaga, I. Tamai, and T. Terasaki, *Transcellular transport of benzoic acid across Caco-2 cells by a pH-dependent and carrier-mediated transport mechanism*. Pharm Res, 1994. **11**(1): p. 30-7.
130. Takanaga, H., I. Tamai, and A. Tsuji, *pH-dependent and carrier-mediated transport of salicylic acid across Caco-2 cells*. J Pharm Pharmacol, 1994. **46**(7): p. 567-70.
131. Osypiw, J.C., D. Gleeson, R.W. Loble, P.W. Pemberton, and R.F. McMahon, *Acid-base transport systems in a polarized human intestinal cell monolayer: Caco-2*. Exp Physiol, 1994. **79**(5): p. 723-39.
132. Janecki, A.J., M.H. Montrose, C.M. Tse, F.S. de Medina, A. Zweibaum, and M. Donowitz, *Development of an endogenous epithelial Na(+)/H(+) exchanger (NHE3) in three clones of caco-2 cells*. Am J Physiol, 1999. **277**(2 Pt 1): p. G292-305.
133. Nicklin, P.L., W.J. Irwin, I.F. Hassan, M. Mackay, and H.B. Dixon, *The transport of acidic amino acids and their analogues across monolayers of human intestinal absorptive (Caco-2) cells in vitro*. Biochim Biophys Acta, 1995. **1269**(2): p. 176-86.
134. Smith, T.K., C.L. Gibson, B.J. Howlin, and J.M. Pratt, *Active transport of amino acids by gamma-glutamyl transpeptidase through Caco-2 cell monolayers*. Biochem Biophys Res Commun, 1991. **178**(3): p. 1028-35.

135. Thwaites, D.T., G.T. McEwan, C.D. Brown, B.H. Hirst, and N.L. Simmons, *Na(+)-independent, H(+)-coupled transepithelial beta-alanine absorption by human intestinal Caco-2 cell monolayers*. J Biol Chem, 1993. **268**(25): p. 18438-41.
136. Hidalgo, I.J. and R.T. Borchardt, *Transport of bile acids in a human intestinal epithelial cell line, Caco-2*. Biochim Biophys Acta, 1990. **1035**(1): p. 97-103.
137. Hirohashi, T., H. Suzuki, X.Y. Chu, I. Tamai, A. Tsuji, and Y. Sugiyama, *Function and expression of multidrug resistance-associated protein family in human colon adenocarcinoma cells (Caco-2)*. J Pharmacol Exp Ther, 2000. **292**(1): p. 265-70.
138. Hunter, J., M.A. Jepson, T. Tsuruo, N.L. Simmons, and B.H. Hirst, *Functional expression of P-glycoprotein in apical membranes of human intestinal Caco-2 cells. Kinetics of vinblastine secretion and interaction with modulators*. J Biol Chem, 1993. **268**(20): p. 14991-7.
139. Hilgendorf, C., H. Spahn-Langguth, C.G. Regardh, E. Lipka, G.L. Amidon, and P. Langguth, *Caco-2 versus Caco-2/HT29-MTX co-cultured cell lines: permeabilities via diffusion, inside- and outside-directed carrier-mediated transport*. J Pharm Sci, 2000. **89**(1): p. 63-75.
140. Ward, J.L. and C.M. Tse, *Nucleoside transport in human colonic epithelial cell lines: evidence for two Na+-independent transport systems in T84 and Caco-2 cells*. Biochim Biophys Acta, 1999. **1419**(1): p. 15-22.
141. Saito, H. and K. Inui, *Dipeptide transporters in apical and basolateral membranes of the human intestinal cell line Caco-2*. Am J Physiol, 1993. **265**(2 Pt 1): p. G289-94.
142. Thwaites, D.T., C.D. Brown, B.H. Hirst, and N.L. Simmons, *Transepithelial glycylsarcosine transport in intestinal Caco-2 cells mediated by expression of H(+)-coupled carriers at both apical and basal membranes*. J Biol Chem, 1993. **268**(11): p. 7640-2.

143. Hu, M., J. Chen, Y. Zhu, A.H. Dantzig, R.E. Stratford, Jr., and M.T. Kuhfeld, *Mechanism and kinetics of transcellular transport of a new beta-lactam antibiotic loracarbef across an intestinal epithelial membrane model system (Caco-2)*. Pharm Res, 1994. 11(10): p. 1405-13.
144. Ng, K.Y. and R.T. Borchardt, *Biotin transport in a human intestinal epithelial cell line (Caco-2)*. Life Sci, 1993. 53(14): p. 1121-7.
145. Vincent, M.L., R.M. Russell, and V. Sasak, *Folic acid uptake characteristics of a human colon carcinoma cell line, Caco-2. A newly-described cellular model for small intestinal epithelium*. Hum Nutr Clin Nutr, 1985. 39(5): p. 355-60.
146. Lacey, S.W., J.M. Sanders, K.G. Rothberg, R.G. Anderson, and B.A. Kamen, *Complementary DNA for the folate binding protein correctly predicts anchoring to the membrane by glycosyl-phosphatidylinositol*. J Clin Invest, 1989. 84(2): p. 715-20.
147. Mahraoui, L., M. Rousset, E. Dussaulx, D. Darmoul, A. Zweibaum, and E. Brot-Laroche, *Expression and localization of GLUT-5 in Caco-2 cells, human small intestine, and colon*. Am J Physiol, 1992. 263(3 Pt 1): p. G312-8.
148. MacDonald, R.S., W.H. Thornton, Jr., and T.L. Bean, *Insulin and IGE-1 receptors in a human intestinal adenocarcinoma cell line (CACO-2): regulation of Na⁺ glucose transport across the brush border*. J Recept Res, 1993. 13(7): p. 1093-113.
149. Said, H.M. and T.Y. Ma, *Mechanism of riboflavine uptake by Caco-2 human intestinal epithelial cells*. Am J Physiol, 1994. 266(1 Pt 1): p. G15-21.
150. Dix, C.J., I.F. Hassan, H.Y. Obray, R. Shah, and G. Wilson, *The transport of vitamin B12 through polarized monolayers of Caco-2 cells*. Gastroenterology, 1990. 98(5 Pt 1): p. 1272-9.

151. Grasset, E., M. Pinto, E. Dussaulx, A. Zweibaum, and J.F. Desjeux, *Epithelial properties of human colonic carcinoma cell line Caco-2: electrical parameters*. Am J Physiol, 1984. **247**(3 Pt 1): p. C260-7.
152. Gres, M.C., B. Julian, M. Bourrie, V. Meunier, C. Roques, M. Berger, X. Boulenc, Y. Berger, and G. Fabre, *Correlation between oral drug absorption in humans, and apparent drug permeability in TC-7 cells, a human epithelial intestinal cell line: comparison with the parental Caco-2 cell line*. Pharm Res, 1998. **15**(5): p. 726-33.
153. Wils, P., A. Warnery, V. Phung-Ba, S. Legrain, and D. Scherman, *High lipophilicity decreases drug transport across intestinal epithelial cells*. J Pharmacol Exp Ther, 1994. **269**(2): p. 654-8.
154. Strocchi, A. and M.D. Levitt, *A reappraisal of the magnitude and implications of the intestinal unstirred layer*. Gastroenterology, 1991. **101**(3): p. 843-7.
155. Hidalgo, I.J., K.M. Hillgren, G.M. Grass, and R.T. Borchardt, *Characterization of the unstirred water layer in Caco-2 cell monolayers using a novel diffusion apparatus*. Pharm Res, 1991. **8**(2): p. 222-7.
156. Karlsson, J. and P. Artursson, *A new diffusion chamber system for the determination of drug permeability coefficients across the human intestinal epithelium that are independent of the unstirred water layer*. Biochim Biophys Acta, 1992. **1111**(2): p. 204-10.
157. Artursson, P. and J. Karlsson, *Correlation between oral drug absorption in humans and apparent drug permeability coefficients in human intestinal epithelial (Caco-2) cells*. Biochem Biophys Res Commun, 1991. **175**(3): p. 880-5.
158. Ren, S. and E.J. Lien, *Caco-2 cell permeability vs human gastrointestinal absorption: QSPR analysis*. Prog Drug Res, 2000. **54**: p. 1-23.

159. Yee, S., *In vitro* permeability across Caco-2 cells (colonic) can predict in vivo (small intestinal) absorption in man--fact or myth. *Pharm Res*, 1997. 14(6): p. 763-6.
160. CDER, F.a.D.A., USA, *Guidance for Industry. Waiver of In Vivo Bioavailability and Bioequivalence Studies for Immediate-Release Solid Oral Dosage Forms Based on a Biopharmaceutics Classification System*. 2000.
161. Brimblecombe, R.W., W.A. Duncan, G.J. Durant, C.R. Ganellin, M.E. Parsons, and J.W. Black, *Proceedings: The pharmacology of cimetidine, a new histamine H2-receptor antagonist*. *Br J Pharmacol*, 1975. 53(3): p. 435-36.
162. Pounder, R.E., J.G. Williams, R.C. Russell, G.J. Milton-Thompson, and J.J. Misiewicz, *Inhibition of food-stimulated gastric acid secretion by cimetidine*. *Gut*, 1976. 17(3): p. 161-8.
163. The United States Pharmacopeial Convention, I., ed. *USP DI*. 16 ed. Drug Information for the Health Care Professional. Vol. 1. 1996, Rand McNally: Rockville, MD. 1611.
164. Walkenstein, S.S., J.W. Dubb, W.C. Randolph, W.J. Westlake, R.M. Stote, and A.P. Intoccia, *Bioavailability of cimetidine in man*. *Gastroenterology*, 1978. 74(2 Pt 2): p. 360-5.
165. Rowley-Jones, D.a.G. *Cimetidine by intramuscular administration: Efficacy and safety*. in *World Conference on Clinical Pharmacology and Therapeutics*. 1980. London.
166. Somogyi, A. and R. Gugler, *Clinical pharmacokinetics of cimetidine*. *Clin Pharmacokinet*, 1983. 8(6): p. 463-95.
167. Somogyi, A., H.G. Rohner, and R. Gugler, *Pharmacokinetics and bioavailability of cimetidine in gastric and duodenal ulcer patients*. *Clin Pharmacokinet*, 1980. 5(1): p. 84-94.

168. Bodemar, G., B. Norlander, and A. Walan, *Pharmacokinetics of cimetidine after single doses and during continuous treatment*. Clin Pharmacokinet, 1981. 6(4): p. 306-15.
169. Taylor, D.C., P.R. Cresswell, and D.C. Bartlett, *The metabolism and elimination of cimetidine, a histamine H₂-receptor antagonist, in the rat, dog, and man*. Drug Metab Dispos, 1978. 6(1): p. 21-30.
170. Lu, X., C. Li, and D. Fleisher, *Cimetidine sulfoxidation in small intestinal microsomes*. Drug Metab Dispos, 1998. 26(9): p. 940-2.
171. Mitchell, S.C., J.R. Idle, and R.L. Smith, *The metabolism of [14C]cimetidine in man*. Xenobiotica, 1982. 12(5): p. 283-92.
172. Chang, T., M. Levine, and G.D. Bellward, *Selective inhibition of rat hepatic microsomal cytochrome P-450. II. Effect of the in vitro administration of cimetidine*. J Pharmacol Exp Ther, 1992. 260(3): p. 1450-5.
173. Levine, M. and G.D. Bellward, *Effect of cimetidine on hepatic cytochrome P450: evidence for formation of a metabolite-intermediate complex*. Drug Metab Dispos, 1995. 23(12): p. 1407-11.
174. Levine, M., E.Y. Law, S.M. Bandiera, T.K. Chang, and G.D. Bellward, *In vivo cimetidine inhibits hepatic CYP2C6 and CYP2C11 but not CYP1A1 in adult male rats*. J Pharmacol Exp Ther, 1998. 284(2): p. 493-9.
175. Rennick, B., J. Ziemniak, I. Smith, M. Taylor, and M. Acara, *Tubular transport and metabolism of cimetidine in chicken kidneys*. J Pharmacol Exp Ther, 1984. 228(2): p. 387-92.
176. Brandle, E. and J. Greven, *Transport of cimetidine across the basolateral membrane of rabbit kidney S2 proximal tubules*. Arch Int Pharmacodyn Ther, 1991. 314: p. 169-85.

177. Pan, B.F., A. Dutt, and J.A. Nelson, *Enhanced transepithelial flux of cimetidine by Madin-Darby canine kidney cells overexpressing human P-glycoprotein*. J Pharmacol Exp Ther, 1994. **270**(1): p. 1-7.
178. Biedler, J.L. and H. Riehm, *Cellular resistance to actinomycin D in Chinese hamster cells in vitro: cross-resistance, radioautographic, and cytogenetic studies*. Cancer Res, 1970. **30**(4): p. 1174-84.
179. Kessel, D. and H.B. Bosmann, *On the characteristics of actinomycin D resistance in L5178Y cells*. Cancer Res, 1970. **30**(11): p. 2695-701.
180. Dano, K., *Cross resistance between vinca alkaloids and anthracyclines in Ehrlich ascites tumor in vivo*. Cancer Chemother Rep, 1972. **56**(6): p. 701-8.
181. Juliano, R.L. and V. Ling, *A surface glycoprotein modulating drug permeability in Chinese hamster ovary cell mutants*. Biochim Biophys Acta, 1976. **455**(1): p. 152-62.
182. Roninson, I.B., H.T. Abelson, D.E. Housman, N. Howell, and A. Varshavsky, *Amplification of specific DNA sequences correlates with multidrug resistance in Chinese hamster cells*. Nature, 1984. **309**(5969): p. 626-8.
183. Roninson, I.B., J.E. Chin, K.G. Choi, P. Gros, D.E. Housman, A. Fojo, D.W. Shen, M.M. Gottesman, and I. Pastan, *Isolation of human mdrl DNA sequences amplified in multidrug-resistant KB carcinoma cells*. Proc Natl Acad Sci U S A, 1986. **83**(12): p. 4538-42.
184. Ueda, K., M.M. Cornwell, M.M. Gottesman, I. Pastan, I.B. Roninson, V. Ling, and J.R. Riordan, *The mdrl gene, responsible for multidrug-resistance, codes for P-glycoprotein*. Biochem Biophys Res Commun, 1986. **141**(3): p. 956-62.
185. Rosenberg, M.F., R. Callaghan, R.C. Ford, and C.F. Higgins, *Structure of the multidrug resistance P-glycoprotein to 2.5 nm resolution determined by*

- electron microscopy and image analysis*. J Biol Chem, 1997. **272**(16): p. 10685-94.
186. Goldstein, L.J., H. Galski, A. Fojo, M. Willingham, S.L. Lai, A. Gazdar, R. Pirker, A. Green, W. Crist, G.M. Brodeur, and et al., *Expression of a multidrug resistance gene in human cancers*. J Natl Cancer Inst, 1989. **81**(2): p. 116-24.
 187. Benard, J., J. Bourhis, F. de Vathaire, E. Ferrandis, M.J. Terrier-Lacombe, J. Lemerle, G. Riou, and O. Hartmann, *Prognostic value of MDR1 gene expression in neuroblastoma: results of a multivariate analysis*. Prog Clin Biol Res, 1994. **385**: p. 111-6.
 188. te Boekhorst, P.A., K. de Leeuw, M. Schoester, S. Wittebol, K. Nooter, A. Hagemerijer, B. Lowenberg, and P. Sonneveld, *Predominance of functional multidrug resistance (MDR-1) phenotype in CD34+ acute myeloid leukemia cells*. Blood, 1993. **82**(10): p. 3157-62.
 189. Carulli, G., M. Petrini, A. Marini, F. Vaglini, F. Caracciolo, and B. Grassi, *P-glycoprotein and drug resistance in acute leukemias and in the blastic crisis of chronic myeloid leukemia*. Haematologica, 1990. **75**(6): p. 516-21.
 190. Schneider, J., M. Bak, T. Efferth, M. Kaufmann, J. Mattern, and M. Volm, *P-glycoprotein expression in treated and untreated human breast cancer*. Br J Cancer, 1989. **60**(6): p. 815-8.
 191. Cheng, A.L., I.J. Su, Y.C. Chen, T.C. Lee, and C.H. Wang, *Expression of P-glycoprotein and glutathione-S-transferase in recurrent lymphomas: the possible role of Epstein-Barr virus, immunophenotypes, and other predisposing factors*. J Clin Oncol, 1993. **11**(1): p. 109-15.
 192. Petrini, M., D. Di Simone, A. Favati, L. Mattii, P. Valentini, and B. Grassi, *GST-pi and P-170 co-expression in multiple myeloma*. Br J Haematol, 1995. **90**(2): p. 393-7.
 193. Thiebaut, F., T. Tsuruo, H. Hamada, M.M. Gottesman, I. Pastan, and M.C. Willingham, *Cellular localization of the multidrug-resistance gene product*

- P-glycoprotein in normal human tissues*. Proc Natl Acad Sci U S A, 1987. 84(21): p. 7735-8.
194. Thiebaut, F., T. Tsuruo, H. Hamada, M.M. Gottesman, I. Pastan, and M.C. Willingham, *Immunohistochemical localization in normal tissues of different epitopes in the multidrug transport protein P170: evidence for localization in brain capillaries and crossreactivity of one antibody with a muscle protein*. J Histochem Cytochem, 1989. 37(2): p. 159-64.
 195. Gottesman, M.M. and I. Pastan, *Biochemistry of multidrug resistance mediated by the multidrug transporter*. Annu Rev Biochem, 1993. 62: p. 385-427.
 196. Horio, M., M.M. Gottesman, and I. Pastan, *ATP-dependent transport of vinblastine in vesicles from human multidrug-resistant cells*. Proc Natl Acad Sci U S A, 1988. 85(10): p. 3580-4.
 197. Higgins, C.F. and M.M. Gottesman, *Is the multidrug transporter a flippase?* Trends Biochem Sci, 1992. 17(1): p. 18-21.
 198. Kerb, R., S. Hoffmeyer, and U. Brinkmann, *ABC drug transporters: hereditary polymorphisms and pharmacological impact in MDR1, MRP1 and MRP2*. Pharmacogenomics, 2001. 2(1): p. 51-64.
 199. Roepe, P.D., L.Y. Wei, J. Cruz, and D. Carlson, *Lower electrical membrane potential and altered pHi homeostasis in multidrug-resistant (MDR) cells: further characterization of a series of MDR cell lines expressing different levels of P-glycoprotein*. Biochemistry, 1993. 32(41): p. 11042-56.
 200. Shapiro, A.B. and V. Ling, *Reconstitution of drug transport by purified P-glycoprotein*. J Biol Chem, 1995. 270(27): p. 16167-75.
 201. Safa, A.R., R.K. Stern, K. Choi, M. Agresti, I. Tamai, N.D. Mehta, and I.B. Roninson, *Molecular basis of preferential resistance to colchicine in multidrug-resistant human cells conferred by Gly-185----Val-185 substitution in P-glycoprotein*. Proc Natl Acad Sci U S A, 1990. 87(18): p. 7225-9.

202. Chaudhary, P.M. and I.B. Roninson, *Induction of multidrug resistance in human cells by transient exposure to different chemotherapeutic drugs*. J Natl Cancer Inst, 1993. **85**(8): p. 632-9.
203. Kohno, K., S. Sato, H. Takano, K. Matsuo, and M. Kuwano, *The direct activation of human multidrug resistance gene (MDR1) by anticancer agents*. Biochem Biophys Res Commun, 1989. **165**(3): p. 1415-21.
204. Chin, K.V., S. Tanaka, G. Darlington, I. Pastan, and M.M. Gottesman, *Heat shock and arsenite increase expression of the multidrug resistance (MDR1) gene in human renal carcinoma cells*. J Biol Chem, 1990. **265**(1): p. 221-6.
205. Wei, L.Y. and P.D. Roepe, *Low external pH and osmotic shock increase the expression of human MDR protein*. Biochemistry, 1994. **33**(23): p. 7229-38.
206. Mickley, L.A., S.E. Bates, N.D. Richert, S. Currier, S. Tanaka, F. Foss, N. Rosen, and A.T. Fojo, *Modulation of the expression of a multidrug resistance gene (mdr-1/P-glycoprotein) by differentiating agents*. J Biol Chem, 1989. **264**(30): p. 18031-40.
207. Jancis, E.M., R. Carbone, K.J. Loechner, and P.S. Dannies, *Estradiol induction of rhodamine 123 efflux and the multidrug resistance pump in rat pituitary tumor cells*. Mol Pharmacol, 1993. **43**(1): p. 51-6.
208. Zhao, J.Y., M. Ikeguchi, T. Eckersberg, and M.T. Kuo, *Modulation of multidrug resistance gene expression by dexamethasone in cultured hepatoma cells*. Endocrinology, 1993. **133**(2): p. 521-8.
209. Tsuruo, T., H. Iida, S. Tsukagoshi, and Y. Sakurai, *Overcoming of vincristine resistance in P388 leukemia in vivo and in vitro through enhanced cytotoxicity of vincristine and vinblastine by verapamil*. Cancer Res, 1981. **41**(5): p. 1967-72.
210. Safa, A.R., C.J. Glover, J.L. Sewell, M.B. Meyers, J.L. Biedler, and R.L. Felsted, *Identification of the multidrug resistance-related membrane glycoprotein as an acceptor for calcium channel blockers*. J Biol Chem, 1987. **262**(16): p. 7884-8.

211. Yusa, K. and T. Tsuruo, *Reversal mechanism of multidrug resistance by verapamil: direct binding of verapamil to P-glycoprotein on specific sites and transport of verapamil outward across the plasma membrane of K562/ADM cells*. *Cancer Res*, 1989. **49**(18): p. 5002-6.
212. Shapiro, A.B. and V. Ling, *The mechanism of ATP-dependent multidrug transport by P-glycoprotein*. *Acta Physiol Scand Suppl*, 1998. **643**: p. 227-34.
213. Lum, B.L., G.A. Fisher, N.A. Brophy, A.M. Yahanda, K.M. Adler, S. Kaubisch, J. Halsey, and B.I. Sikic, *Clinical trials of modulation of multidrug resistance. Pharmacokinetic and pharmacodynamic considerations*. *Cancer*, 1993. **72**(11 Suppl): p. 3502-14.
214. Jachez, B., R. Nordmann, and F. Loor, *Restoration of taxol sensitivity of multidrug-resistant cells by the cyclosporine SDZ PSC 833 and the cyclopeptolide SDZ 280-446*. *J Natl Cancer Inst*, 1993. **85**(6): p. 478-83.
215. Michelson, S. and D. Slate, *A mathematical model of the P-glycoprotein pump as a mediator of multidrug resistance*. *Bull Math Biol*, 1992. **54**(6): p. 1023-38.
216. Canada, A.T., W.D. Watkins, and T.D. Nguyen, *The toxicity of flavonoids to guinea pig enterocytes*. *Toxicol Appl Pharmacol*, 1989. **99**(2): p. 357-61.
217. Zheng, J. and V.D. Ramirez, *Inhibition of mitochondrial proton F₀F₁-ATPase/ATP synthase by polyphenolic phytochemicals*. *Br J Pharmacol*, 2000. **130**(5): p. 1115-23.
218. Liang, E., J. Proudfoot, and M. Yazdanian, *Mechanisms of transport and structure-permeability relationship of sulfasalazine and its analogs in Caco-2 cell monolayers*. *Pharm Res*, 2000. **17**(10): p. 1168-74.
219. Yumoto, R., T. Murakami, Y. Nakamoto, R. Hasegawa, J. Nagai, and M. Takano, *Transport of rhodamine 123, a P-glycoprotein substrate, across rat intestine and Caco-2 cell monolayers in the presence of cytochrome P-450 3A-related compounds*. *J Pharmacol Exp Ther*, 1999. **289**(1): p. 149-55.

220. Alsenz, J., H. Steffen, and R. Alex, *Active apical secretory efflux of the HIV protease inhibitors saquinavir and ritonavir in Caco-2 cell monolayers*. Pharm Res, 1998. 15(3): p. 423-8.
221. Fardel, O., V. Lecureur, and A. Guillouzo, *The P-glycoprotein multidrug transporter*. Gen Pharmacol, 1996. 27(8): p. 1283-91.
222. Nair, C.N., *Proton gradient independent organic cation transport by HeLa cells*. J Pharmacol Exp Ther, 1988. 246(1): p. 121-4.
223. Martel, F., D. Grundemann, C. Calhau, and E. Schomig, *Apical uptake of organic cations by human intestinal Caco-2 cells: putative involvement of ASF transporters*. Naunyn Schmiedebergs Arch Pharmacol, 2001. 363(1): p. 40-9.
224. Bhardwaj, R.K., H. Glaeser, L. Becquemont, U. Klotz, S.K. Gupta, and M.F. Fromm, *Piperine, a major constituent of black pepper, inhibits human P-glycoprotein and CYP3A4*. J Pharmacol Exp Ther, 2002. 302(2): p. 645-50.
225. Dudley, A.J. and C.D. Brown, *Mediation of cimetidine secretion by P-glycoprotein and a novel H(+)-coupled mechanism in cultured renal epithelial monolayers of LLC-PK1 cells*. Br J Pharmacol, 1996. 117(6): p. 1139-44.
226. Cheng, Y. and W.H. Prusoff, *Relationship between the inhibition constant (K_i) and the concentration of inhibitor which causes 50 per cent inhibition (I₅₀) of an enzymatic reaction*. Biochem Pharmacol, 1973. 22(23): p. 3099-108.

APPENDICES

Appendix 1. The Preparation of Buffers and Solutions for LDH Assay

Phosphate buffer: 2.17 g potassium phosphate monobasic and 22.46 g sodium phosphate were dissolved in 700 to 800 mL double distilled water (DDW). Use 1 M hydrochloride acid or 1 M sodium hydroxide to adjust pH to 7.4. Transfer to volumetric flask and make up to one liter. Phosphate buffer can be stored in room temperature.

NADH solution: NADH (β -nicotinamide adenine dinucleotide, reduced form, Sigma #N-8129) was dissolved in phosphate buffer to make up to 2.5 mg/mL. The NADH solution needs to be prepared right before experiment and stored in amber bottles on ice.

Sodium pyruvate solution: Sodium pyruvate (Sigma#P-2256) was dissolved in phosphate buffer to make up to 1 mg/mL. The sodium pyruvate solution needs to be prepared right before experiment and stored in amber bottles on ice.

Appendix 2. The Preparation of Transport Buffer

In order to prepare one liter of transport buffer, 0.28 g calcium chloride in the form of hexahydrate, 0.4 g potassium chloride, 0.06 g potassium dihydrogen phosphate, 0.1 g magnesium chloride in the form of crystal, 0.1 g magnesium sulfate in the form of heptahydrate, 8 g sodium chloride, 0.35 g sodium bicarbonate, 4.5 g D-glucose, and 2.603 g (N-[2-Hydroxyethyl] piperazine-N'-[2-ethanesulfonic acid]) (HEPES) in form of sodium salt. The buffer was adjusted to pH 7.4 by 1 M hydrochloride acid or 1 M sodium hydroxide. Then the buffer was filtrated by 3.0 mM pore size filter in a laminar hood with regular sterile conditions. The filtered buffer was stored in room temperature.